QUANTIFICATION OF IRON TRANSFER FROM DIET TO THE BRAIN IN THE RAT MODEL USING STABLE ISOTOPE TECHNIQUES

CHEN JIEHUA
(*Bachelor of Science*)
Sun Yat-Sen University, China

A THESIS SUBMITTED

FOR THE DEGREE OF

DOCTOR OF PHILOSOPHY

DEPARTMENT OF CHEMISTRY

NATIONAL UNIVERSITY OF SINGAPORE

2013

DECLARATION

I hereby declare that this thesis is my original work and it has been written by me in its entirety, under the supervision of A/P Thomas Walczyk, (in the laboratory NutriTrace@NUS), Chemistry Department, National University of Singapore, between 03/08/2009 to 30/09/2013.

I have duly acknowledged all the sources of information which have been used in the thesis.

This thesis has also not been submitted for any degree in any university previously.

The content of the thesis has been partly published in:

1) Metallomics (Chen J-H, Shahnavas S, Singh N, Ong W-Y, & Walczyk T (2013) Stable iron isotope tracing reveals significant brain iron uptake in adult rats. *Metallomics* 5(2):167-173)

Name	Signature	Date

ACKNOWLEDGEMENTS

I would like to express my gratitude to my supervisor, A/P Thomas Walczyk, for his valuable guidance and great patience throughout my PhD project. He nurtured the ignorant me to become a girl who starts to think critically. I also like to thank Dr. Patrick Galler, for his guidance in the establishment of the analytical methods for the project. In addition, I am grateful to receive the valuable advice and technical support from A/P Ong Wei Yi and Dr. Patrick Reilly.

I truly appreciate the help and support from my fellow colleagues. Especially Ms Nadia Singh, without whom I could have quitted my PhD. I appreciate her contributions to all the studies in the project as our research assistant and her endless mental support as my friend. In addition, I would like to express my gratitude to Ms Shahreena Shahnavas, for her contribution to Study I; Ms Tay Huimin for her contribution to Study II; Mr. Neo Aik Xin and Mr. Li Bin, for their contributions to Study III as colleagues and their support as friends; Ms Fransiska Dewi, for her committed assistance in the sacrifice of the rats and her kindness for proofreading my thesis; Ms. Ren Yao and Ms. Gina Chew, for their technical contributions to the project; Ms Soumiya Srinivasan and Ms Chia Yi Peng for proofreading of the thesis.

I would like to thank my family for their endless love and support that are always accompanying me, constantly encouraging me to overcome the difficulties in life.

TABLE OF CONTENTS

DECLARATION ..... **ii**

ACKNOWLEDGEMENTS ..... **iii**

TABLE OF CONTENTS ..... **iv**

ADDENDUM ..... **x**

SUMMARY ..... **xi**

List of Tables ..... **xiii**

List of Figures ..... **xiv**

List of Abbreviations ..... **xvi**

1 Chapter 1 Literature review **1**

1.1 Introduction **1**

1.2 Iron – a double edged sword **2**

1.2.1 The biological role of iron 2

1.2.2 Iron and oxidative stress 6

1.3 Body iron metabolism **9**

1.3.1 Dietary iron sources 9

1.3.2 Intestinal iron absorption 10

1.3.3 Iron transport and cellular iron uptake 13

1.3.3.1 Plasma iron pool 13

1.3.3.2 Transferrin 14

1.3.3.3 Transferrin-dependent iron uptake mechanisms 16

1.3.4 Body iron storage 20
1.3.4.1 Body iron distribution 20
1.3.4.2 Ferritin 21
1.3.4.3 Hemosiderin 23
1.3.5 Cellular iron metabolism 23
1.3.6 Iron excretion 26
1.3.7 Regulation of body iron 28
1.3.7.1 Cellular iron regulation – IRP/IRE system 29
1.3.7.2 Systemic iron regulation - Hepcidin 30
1.4 Brain iron homeostasis 33
1.4.1 Brain barriers 33
1.4.1.1 The blood-brain barrier 33
1.4.1.2 The blood-cerebrospinal fluid barrier 33
1.4.2 Brain iron distribution 34
1.4.2.1 Brain regional iron distribution 34
1.4.2.2 Cellular iron distribution 35
1.4.3 Brain iron uptake and export 37
1.4.3.1 Brain iron uptake 37
1.4.3.1.1 The blood-brain barrier pathway 37
1.4.3.1.2 The blood cerebrospinal fluid barrier pathway 39
1.4.3.2 Brain iron efflux 39
1.4.3.3 Cellular iron uptake and export in brain 40
1.4.4 Brain iron regulation 42

1.5 Iron and neurodegeneration 44

1.5.1 Age-related iron accumulation in brain 44

1.5.2 Iron and neurodegeneration 45

1.5.2.1 The free radical theory of aging 45

1.5.2.2 The roles of iron in Alzheimer's and Parkinson's diseases 47

1.5.2.2.1 The role of iron in Alzheimer's diseases 48

1.5.2.2.2 The role of iron in Parkinson's diseases 51

1.5.3 Dietary iron and neurodegeneration 53

1.5.3.1 The effect of high dietary iron intake on brain iron homeostasis . 55

1.5.3.2 The effect of systemic iron deficiency on brain iron homeostasis 56

1.5.3.3 Dietary iron and risks of Alzheimer's and Parkinson's diseases .. 58

1.5.3.4 Strategies for reducing brain iron content 60

2 Chapter 2 Methodology 62

2.1 The application of isotope tracing techniques in nutritional studies 63

2.1.1 Stable isotopes versus radioactive isotopes 63

2.1.2 The application of radioisotopes to assess brain iron metabolism 65

2.2 The use of stable isotopes as tracers 71

2.2.1 Study Design 72

2.2.2 Isotope Dilution Mass Spectrometry (IDMS) 72

2.2.2.1 Quantification of iron content in tissues using IDMS 72

2.2.3 Instrumentations for iron isotope ratio measurement 74

2.2.3.1 Thermal Ionization Mass Spectrometry (TIMS) 75

2.2.3.1.1 Filament arrangement 75

2.2.3.1.2 Principles of TIMS 76

2.2.3.2 Multi-Collector Inductively Coupled Plasma Mass Spectrometry (MC-ICP-MS) ……...77

2.2.3.3 TIMS versus MC-ICP-MS 80

Bibliography 82

3 Chapter 3 101

3.1 Abstract 102

3.2 Introduction 103

3.3 Methods and materials 106

3.3.1 Animals 106

3.3.2 Stable isotope labels 107

3.3.3 Tissue sampling 108

3.3.4 Preparation of blood/tissue samples for iron isotopic analysis 109

3.3.5 Iron analysis of blood 110

3.3.6 Mass spectrometry 110

3.3.7 Data analysis 112

3.4 Results 113

3.5 Discussion 116

3.6 Conclusion 120

3.7 Bibliography 122

4 Chapter 4 127

4.1 Abstract 128

4.2 Introduction 129

4.3 Methodology 131

4.3.1 Study design 131

4.3.2 Animals 133

4.3.3 Stable isotope labels 134

4.3.4 Blood and tissue sampling 135

4.3.5 Iron elemental and isotopic analysis 136

4.3.6 Data analysis 137

4.3.6.1 Efflux Rate Index 138

4.3.6.2 Tissue iron uptake (*DI* group) 139

4.3.6.3 Evaluation of kinetics of iron efflux (*TI* group) 139

4.3.7 Statistical analysis 140

4.4 Results 140

4.4.1 Tracer analysis of blood samples 141

4.4.2 Tissue iron uptake for the *DI* group 142

4.4.3 Iron turnover in tissue 143

4.4.3.1 Qualitative assessment (*DI* group) 143

4.4.3.2 Quantitative assessment (*TI* group) 144

4.5 Discussion 146

4.6 Conclusion 152

4.7 Bibliography 153

5 Chapter 5 157

5.1 Abstract 158

5.2 Introduction 159

5.3 Methodology 161

5.3.1 Study design 161

5.3.2 Stable isotope labels 162

5.3.3 Animals 162

5.3.3.1 Study design 163

5.3.4 Iron isotopic analysis 165

5.3.5 Data analysis 165

5.3.6 Statistical analysis 168

5.4 Results 168

5.5 Discussion 176

5.6 Conclusion 182

5.7 Bibliography 184

ADDENDUM

Chapter 3, 4 and 5 in this thesis were prepared as manuscripts for submission to scientific journals. Chapter 3 has been published in Metallomics. Chapter 4 will be submitted to Brain Structure and Function. Chapter 5 will be submitted to Journal of Nutrition.

SUMMARY

Iron deposits in brain are a common hallmark of Alzheimer's disease (AD) and Parkinson's disease (PD). This has led to the hypothesis that iron may play a functional role in the pathogenesis of AD/PD through free radical damage. Recent epidemiological findings point to a possible relationship between dietary iron and AD/PD. It remains, however, unclear how dietary iron affects brain iron. In this project, we have developed a novel methodological approach using stable iron isotopes to trace dietary iron and investigate the relationship between dietary iron and brain iron in an adult rat model in 3 studies.

Previous short-term studies using radiotracers suggested that brain iron uptake is in minute quantity as compared to other tissues in adult rodents, leading to the assumption that brain iron uptake must be marginal in humans after brain development is complete. In Study I, a known amount of an enriched stable iron isotope (^{57}Fe) was added to drinking water given to adult rats for a period of 4 months to directly determine the fraction of iron that was transferred over time from diet to the brain. Uptake of tracer iron and final iron content in tissues were assessed by Isotope Dilution Mass Spectrometry (IDMS). In consistent with previous findings, we found that a minute amount of iron was taken up by the rat brain from diet (~0.000054%). But this amount is considerable when compared to the total amount of brain iron. About 9% of brain iron could be traced back to the diet in a period of four months, a time span that compares to 7-10 human years.

To further investigate the brain iron dynamics, a dual-stable-isotope and a triple-stable-isotope feeding approaches were adopted in Study II, to assess whether the process of brain iron deposition is uni-directional or bi-directional. Our result confirmed the hypothesis that iron deposition in brain is bi-directional. In addition, the half-life of dietary iron in the adult rat brain was estimated to be about 9 months, which could serve as an indicator for the turnover rate of dietary iron in the brain. The understanding of dietary iron trafficking in the brain will shed light on the possible role of dietary iron intake in iron-implicated neurodegenerative diseases.

In Study III, the established dual-stable-isotope feeding technique was applied to investigate the changes in brain iron homeostasis in response to different levels of dietary iron intake in adult rats. IDMS was adopted to assess dietary iron recovery in brain as well as the relative iron efflux rate from brain. The most remarkable finding of this study was that uptake efficiency of dietary iron by the brain is determined by systemic iron influx. Accordingly, dietary iron recovery in brain was the lowest for the low dietary iron regimen. However, administration of high amounts of dietary iron resulted in down-regulation of intestinal iron absorption which, in response, resulted in a lower systemic iron influx as compared to the control group. Brain iron uptake and, thus, brain iron accumulation could therefore be lowered by giving either high and low amounts of iron to the rats. This finding points to brain iron uptake being determined by systemic iron influx and not by active regulation in response to body iron status in adult rats.

List of Tables

Table 2-1 Merits and limitations of the use of radioisotopes and stable isotopes as metabolic tracers 64

Table 2-2 Summary of studies on brain iron uptake using radioactive isotope techniques on animal models*. 67

Table 2-3 Interferences encountered in iron analysis by ICP-MS* 79

Table 3-1 Iron concentration and iron isotopic enrichment of analyzed tissue samples. 114

Table 4-1 Total amount of consumed feed, water and iron tracers for the *DI* group (4 month of feeding) and the *TI* group (5 month of feeding) 141

Table 4-2 Efflux rates and half-lives of dietary iron in the rat tissues in *TI* group* 145

Table 5-1 Iron composition of the drinking water 164

Table 5-2 The summary of the total amount of consumed feed, water and iron tracers of the feeding groups 169

Table 5-3 Systemic iron changes in the rat body in response to dietary iron availability 174

List of Figures

Fig. 1-1 Schematic representation of the reduction of oxygen to water 8

Fig. 1-2 Intestinal iron absorption..... 11

Fig. 1-3 Transferrin receptor mediated endocytosis for cellular iron uptake 19

Fig. 1-4 Iron distribution in the body and exchange pools. 27

Fig. 1-5 The effect of cytoplasmic iron levels on IRE/IRP system. 30

Fig. 1-6 Relation between the non-haemin iron and the age in different cortical fields..... 45

Fig. 2-1 The illustration of the principle of IDMS..... 74

Fig. 2-2 Ion source configuration used in thermal ionization mass spectrometry 76

Fig. 2-3 Analyzer system of the TRITON 77

Fig. 2-4 Schematic of a Neptune MC-ICP-MS..... 78

Fig. 3-1 Iron transfer efficiency from diet to organs 114

Fig. 3-2 Fraction of iron in the organ coming from feed. 115

Fig. 4-1 Dual-isotope tracing for studying brain iron import and export 132

Fig. 4-2 Triple-isotope tracing for modeling kinetics of iron release from brain132

Fig. 4-3 Amount ratios of tracer to total iron (mol/mol) in blood against time for the DI group (n=3 rats). 142

Fig. 4-4 Amount ratios of tracer to total iron (mol/mol) in blood against time for the TI group (n=5 rats)..... 142

Fig. 4-5 Tissue iron uptake 143

Fig. 4-6 Efflux rate index of different tissues for the DI group (n=3 rats) 144

Fig. 4-7 Changes in Efflux Rate Indices over two months in the TI group (n=5 rats) 146

Fig. 5-1 Dual-isotope tracing scheme for studying brain iron import and export in animal models 162

Fig. 5-2 Changes of systemic iron influx in response to different dietary iron levels 170

Fig. 5-3 Systemic changes of brain iron in response to dietary iron supply. 171

Fig. 5-4 Efflux rate indices of different tissues of the three feeding groups 176

List of Abbreviations

6-OHDA	6-hydrooxydopamine
AD	Alzheimer's diseases
Aβ	Amyloid-β peptide
APP	Amyloid-β protein precursor
AAS	Atomic absorption spectrometry
BBB	Blood-brain barrier
BCB	Blood-cerebrospinal fluid barrier
BMP	Bone morphogenic proteins
CNS	Central nervous system
CSF	Cerebrospinal fluid
DMT1	Divalent metal ion transporter 1
Dcytb	Duodenal cytochrome b
FPN	Ferroportin
HCP1	Heme Carrier Protein 1
HO-1	Heme oxygenase-1
HJV	Hemojuvelin
HH	Hereditary hemochromatosis
HP	Hypertransferrinemic
ICP-AES	Inductively coupled plasma atomic emission spectroscopy
ICP-MS	Inductively coupled plasma mass spectrometry
ICP	Inductively coupled plasma
IF	Interstitial fluid
IP	Intraperitoneal
IV	Intravenous
ID	Iron deficient
IDA	Iron deficiency anemia
IL	Iron loaded
IRE	Iron regulatory element
IRP	Iron regulatory protein
IDMS	Isotope dilution mass spectrometry
LIP	Labile iron pool
Mr	Molecular weight
MPTP	Methyl-4-phenyl-1,2,3,6-tetrapyridine
MC-ICP-MS	Multi-collector inductively coupled plasma mass spectrometry
NDD	Neurodegenerative diseases
NFT	Neurofibrillary tangles
NTBI	Non-transferrin-bound-iron
PD	Parkinson's diseases

PUFA	Polyunsaturated fatty acid
ROS	Reactive oxygen species
RDA	Recommended dietary allowances
STEAP3	Six-transmembrane epithelial antigen of the prostate 3
SD	Sprague Dawley
SEM	Secondary Electronic Multipliers
SFT	Stimulator of Fe transport
SNpc	Substantia nigra pars compacta
SN	Substantia nigra
Tf-Fe^{3+}	Tf-bound iron
TIMS	Thermal ionization mass spectrometry
TfR	Transferrin receptor
Tf	Transferrin
UTRs	Untranslated regions
WT	Wild type

Chapter 1 Literature review

1.1 Introduction

As a result of successful socioeconomic development and, consequently, progress in scientific research, public health, nutrition and education, populations are ageing worldwide at an unprecedented scale. However, the concomitant morbidity with increasing longevity counteracts, to certain extent, the benefits of living longer. An ever-increasing number of people, especially in industrialized countries, are afflicted with age-related neurodegenerative diseases (NDD), including Alzheimer's disease (AD), Parkinson's disease (PD). The worldwide prevalence of AD is predicted to increase by 4 times (~100 million people) in the next four decades whereas that of PD is projected to double (9 million people) in the next 25 years (1, 2). In addition to the high public health costs, these diseases pose immense economic and emotional burden on patients and caregivers (3). The current situation necessitates a better understanding of the etiology of these diseases for the development of effective preventive and therapeutic interventions.

The pathogenesis of AD/PD remains largely unknown, but many lines of evident suggest that iron deposition in the brain with age might play a role in the development of these diseases with the associated oxidative stress as the underlying mechanism (4, 5). Iron is essential for life. Excess free iron, however, can participate in Fenton and Haber-Weiss chemistry, generating free radicals that can impose oxidative stress to cellular components which may ultimately lead to

cell death. Iron accumulation in the brain with age might result in over-exposure of brain to oxidative stress, enhancing the risks of AD/PD development.

Surprisingly, the increasing trend of the prevalence of AD and PD still persists after age correction (6, 7), pointing to a possible role of diet on the development of these diseases. Worldwide affluence has led to increased consumption of high-iron food products in the population, e.g. red meat, iron-fortified food and iron supplements (8). As the body has no active excretion mechanism for iron, high influx of dietary iron into the body may lead to high body iron, potentially increasing the brain iron uptake. Most epidemiological studies showed that high dietary intake was associated with higher risks of AD/PD whereas others found the opposite or no connection (9-15). This hypothesis was further evaluated by testing the efficacies of iron chelators/iron absorption inhibitors on neuroprotection *in vitro* and *in vivo* (16-23). Results of some of these studies are promising though others raise doubts on the effect of dietary iron supply on brain iron accumulation. These inconclusive findings demand for further research to explore if risks of contracting AD and PD can be mitigated through diet and translation into preventive strategies.

1.2 Iron – a double edged sword

1.2.1 The biological role of iron

As the second most abundant metal and the fourth most abundant element of the earth's crust, iron is a virtually indispensable micronutrient to all life-forms, from

mammals and lower vertebrates to unicellular organisms. It is involved in a plethora of metabolic processes ranging from oxygen transport and storage, electron transport, oxidation-reduction reactions to cell division and DNA synthesis (24).

Iron, a transition metal, exists in several oxidation states ranging from Fe^{6+} to Fe^{2-}, depending on its chemical environment (25). Among all the oxidation states, ferric (Fe^{3+}) and ferrous (Fe^{2+}) iron are the most stable both, in the aqueous environment of the body and in food. The reversible interchange between these states is the basis of many biological redox reactions (26). Consequently, the ease of donating and accepting electrons renders iron the required capability to carry out redox reactions that are essential for cellular metabolic processes occurring within the biological systems.

Being the most abundant trace element present in the human body, iron constitutes ~38 mg/kg of body weight in an average adult female and ~50 mg iron/kg in an average male. Over 65% of body iron exists primarily in hemoglobin in circulating erythrocytes, up to about 10% is present in the muscle as myoglobin, about 1% to 5% is found as part of enzymes, and the remaining surplus body iron is stored mostly in the liver as ferritin and hemosiderin (25).

As reflected in the body iron distribution, the most essential role of iron in the body is to participate in O_2 transport in the forms of hemoglobin and myoglobin

molecules. Hemoglobin consists of four globular protein subunits and each of the subunit contains a heme group in which iron is embedded at the center of a protoporphyrin IX ring (27). As only ferrous iron can bind to O_2, when hemoglobin is not loaded, hemoglobin iron is in the form of Fe (II). In binding, Fe (II) is temporarily and reversely oxidized to Fe (III) by O_2, resulting in subsequent structural change at the iron site of hemoglobin. The structure of hemoglobin facilitates O_2 transport from lungs to tissues and carries CO_2 back to the lungs. Myoglobin, also a heme-containing protein, is the primary O_2 carrier in muscle tissues. In contrast to hemoglobin, myoglobin is composed of only one globin chain and one heme unit (28). The affinity of myoglobin to oxygen is higher than that of hemoglobin, allowing O_2 carried by hemoglobin to diffuse into muscle cells.

Cytochromes, as iron-containing enzymes, also carry a heme group. Cytochromes are capable of performing reduction and oxidation due to the redox properties of iron, thus can be actively involved in the production of cellular energy production as electron carriers (28). Iron sulfur enzymes that contain no heme group (e.g. nicotinamide adenine dinucleotide dehydrogenase (NADH)), are also involved in electron transport (29). In other iron-dependent enzymes, iron is required as a cofactor or activator but is not part of the molecule.

In light of the biological role of iron in the body, iron is essential for body development and for maintaining physiological functions. Either conditions of

iron depletion or overload can potentially result in iron-related disorders that remain one of the most common disorders worldwide.

Too little iron in the body might lead to iron deficiency (ID), a condition that can compromise an array of normal body functions. Notwithstanding that iron is the most common metal on our planet and the increased food availability with socioeconomic development, ID is still the most widespread nutrient deficiency worldwide, affecting 1.6 million people globally (30). Half of the population with ID suffers from a more severe disorder – Iron Deficiency Anemia (IDA). IDA mainly affects children and women of childbearing age in developing countries, but its prevalence in industrialized countries are not of negligence (31). Pregnant women with IDA are at greater risks of poor pregnancy outcome, i.e. increased mortality around childbirth. In addition, IDA adversely affects immune function, delays physical and mental development in childhood, and impairs work capacity and productivity of manual workers (24, 32)

Despite the crucial role of iron in metabolic processes in the body, it can be highly toxic at the moment that iron scavenging capacities of the body, e.g. by transferrin as the major iron transport protein in the body, are exceeded (33).

Pathological iron overload can be classified as primary iron overload and secondary iron overload. The former refers to hereditary hemochromatosis (HH) whereas the latter represents iron overload resulting from transfusion. HH is an

autosomal recessive disorder characterized by disregulated intestinal iron absorption that leads to pathological rise in body iron (34). The excess iron is mainly deposited in parenchymal cells of the liver, leading to tissue damage and fibrosis. Mutations in the *HFE* gene (*C282Y*) leading to disease have a higher prevalence in populations of northern European descent (1/200). Homozygotes for this mutation usually develop iron overload whereas the carriers are genetically predisposed to HH. As 1/10 white Americans are *C282Y* allele carriers, HFE-associated HH is probably the most common monoallelic genetic disease in Caucasians (35). Transfusional iron overload is prevalent in anemic patients requiring transfusion of erythrocytes, e.g. patients with thalassemia. Due to the high concentration of iron in red blood cell (1 ml blood contains ~0.5 mg iron), transfusions inevitably increases body iron stores greatly. In addition, the ineffectiveness in erythropoiesis in patients with thalassemia leads to the increased absorption of dietary iron, which also contributes to overloaded body iron stores (24).

1.2.2 Iron and oxidative stress

Free unbound iron can participate in reactions generating reactive oxygen species (ROS). If unshielded, iron can react with hydrogen peroxide (H_2O_2) resulting in the formation of highly ROS via Fenton chemistry and the Haber-Weiss reaction, which could lead to the damage of cellular integrity via oxidative stress (see Eqn. (1) - (3)). In the Fenton reaction, Fe^{2+} is oxidized to Fe^{3+}, coupled with the conversion of H_2O_2 into a hydroxyl radical ($OH^{\bullet}$) and a hydroxyl anion (OH^{-}). Fe^{3+}, in turn is reduced back to $Fe^{2+}$by the action of the superoxide radical ($^{\bullet}O_2^{-}$)

(see Eqn. (1) and (2)). The Haber-Weiss reaction, is the net reaction derived from the combination of the two reactions from Fenton Chemistry with iron being the catalyst. As can be seen from Eqn. (3), hydroxyl radicals ($OH^{\bullet}$) are generated from H_2O_2 and $^{\bullet}O_2^-$ catalyzed by Fe^{2+} through Fenton chemistry.

Fenton Chemistry:

$$Fe^{2+} + H_2O_2 \rightarrow Fe^{3+} + OH^{\bullet} + OH^- \quad (1)$$

$$Fe^{3+} + {}^{\bullet}O_2^- \rightarrow Fe^{2+} + O_2 \quad (2)$$

Haber-Weiss Reaction:

$$H_2O_2 + {}^{\bullet}O_2^- \rightarrow OH^{\bullet} + O_2 + OH^- \quad (3)$$

ROS serve as a source of oxidative stress that cause destruction in cellular components. ROS may refer to both relatively inactive compounds, such as $^{\bullet}O_2^-$ and H_2O_2, and extremely reactive ones, like $OH^{\bullet}$, peroxyl radicals and singlet oxygen (36). It is often assumed that ROS will always result in oxidative stress. This assumption is erroneous to a certain extent. The term ROS was introduced by introduced by Sies and Cadenas in 1985 and was defined as "a disturbance in the prooxidant-antioxidant balance in favor of the former" (37). Normal physiological variation in cellular redox equilibrium can be adjusted by the body. However, when the cellular levels of ROS surpasses the threshold of the redox regulatory capacity in the body, it subsequently results in oxidative stress and leads to cellular damages.

ROS are the by-products of normal metabolism in aerobic species. About 2% of the oxygen utilized in the electron chain reactions is metabolized into the potentially toxic ROS (see Fig. 1-1) (36, 38, 39). Oxygen is monovalently reduced

to water with the intermediate formation of superoxide anion, hydrogen peroxide and hydroxyl radicals (see Fig. 1-1) (36). In the cellular system, $^{\bullet}O_2^-$ is virtually the first oxidative stress associated ROS produced and is rapidly converted to H_2O_2. Both $^{\bullet}O_2^-$ and H_2O_2 are not very reactive but in the presence of iron, they can be turned into the highly reactive ROS like $OH^{\bullet}$, which can react with the adjacent cellular components and cause damages. As a result, redox-active ironsite-specifically determines the H_2O_2-mediated oxidation (40). Other metals like copper are more efficient catalysts than iron in the conversion to $OH^{\bullet}$, but iron is the main catalyst due to its high abundance and wide availability in living cells (41, 42)

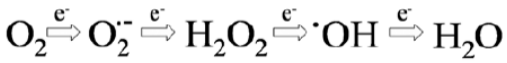

Fig. 1-1 Schematic representation of the reduction of oxygen to water

Under normal physiological conditions, the body copes with ROS and the resulting oxidative stress through an array of antioxidant defense systems, including antioxidant enzymes (glutathione peroxidases, superoxide dismutase and catalase) and non-enzymatic free radical scavengers (tocopherols, vitamin C, glutathione, etc.), which can inactivate superoxide radicals, hydrogen peroxide and lipid hydroperoxides (36, 43, 44). However, when the amount of the generated free radicals exceeds the cellular scavenging capability, they will damage DNA, lipids and proteins.

When free iron is exposed to H_2O_2, the generated ROS can possibly generate DNA lesions, resulting in DNA fragmentation and mutagenesis (45, 46). Among

lipid molecules, polyunsaturated fatty acids (PUFA) are more vulnerable to oxidative stress due to their electron-donating double bonds, which can react with $OH^{\bullet}$ and other radicals (47). These radicals can initiate lipid peroxidation in the cell membrane through reactions analogous to Fenton Chemistry in which iron can generate lipid radicals by splitting lipid hydroperoxides (LOOH) into alkoxyl ($LO^{\bullet}$) or peroxyl ($LOO^{\bullet}$) radicals. Peptides can be attacked by free radicals at the backbone and side-chain via oxidative modification (48). The resulting backbone modification leads to protein cross-linking or peptide-bond cleavage. The side-chain modification results in the change of chemical structure and thus properties via the modification of the amino acid side chains.

In light of the catalytic role of iron in the generation of ROS and the possible accompanying deleterious oxidative damage, evolution has equipped mammals with elegant regulatory mechanisms to maintain iron homeostasis at both at the systemic level and the cellular level by modulating iron absorption, iron reutilization and mobilization of stored iron which will be described in the following.

1.3 Body iron metabolism

1.3.1 Dietary iron sources

Dietary iron can be categorized by the form in which iron is bound at the molecular level as heme iron and non-heme iron, respectively. Heme iron can be found in animal foods, such as red meat, poultry and fish. It refers to all forms of

iron in which iron is present as hemoglobin and myoglobin in which iron is tightly bound within the porphyrin ring structure of the molecule. Non-heme iron, on the other hand, can be found in any food of plant origin. Heme iron is more effectively absorbed (25% to 35%) than non-heme iron (2% to 20%, on average). The absorption rate of heme-iron depends mainly on the proportion of iron enhancers and inhibitors in the diet, as well as the iron status of the individual. Although heme-iron constitutes about 10% to 15% of dietary iron, it may provide up to a third of total absorbed dietary iron (49-51). The recommended dietary allowances (RDA) for iron are 8 mg for adult males and18 mg for adult females (25).

1.3.2 Intestinal iron absorption

The absorption of iron occurs predominantly in the apical membrane of duodenal and proximal jejunum enterocytes (see Fig. 1-2) (34). The absorption of both heme iron and non-heme iron is regulated by the iron stores in the body. The former, however, is not regulated as tightly as the latter (52). But the absorption of heme iron is more efficient than non-heme iron as it remains soluble at intestinal pH as opposed to non-heme iron and its solubility does not seem to be affected by the oxidation state of heme iron. Moreover, in comparison to non-heme iron absorption, the absorption of heme iron is less sensitive to extrinsic factors (e.g. dietary iron absorption inhibitors or enhancers). Heme iron thus has a relatively high and constant bioavailability (ca. to 30%).

Heme iron is released into the lumen of the stomach and duodenum by proteolysis, before it can be taken up by enterocytes (53, 54). The uptake of heme iron by enterocytes is not as well understood. The heme carrier protein 1 (HCP1) on the apical surface of enterocytes is proposed be involved in this process due to its high expression in enterocytes (52). The principal role of HCP1 remains to be elucidated. It appears that in addition to the function of heme transport, it is also responsible for the uptake of folate (55). Heme iron binds to HCP1 and is absorbed intact into the cytoplasm through endocytosis (56). In the cytoplasm, the heme molecule is present in the membrane bound vesicles. Heme is then degraded to iron, carbon monoxide and bilirubin by the enzyme heme oxygenase-1 (HO-1). The degraded iron will then be released in ferrous form into the intracellular iron pool and follows the same metabolic pathways as non-heme iron as discussed below.

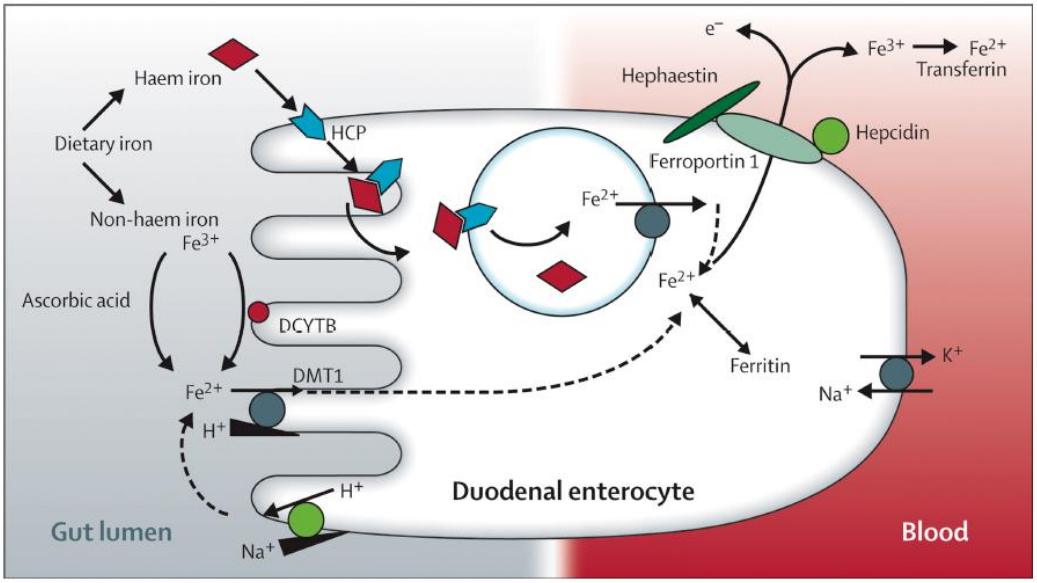

Fig. 1-2 Intestinal iron absorption
Fe^{3+} can be reduced to Fe^{2+} either by ascorbic acid and apical membrane ferrireductase cytochrome B (Dcytb). At the apical membrane, Fe^{2+} transport into the enterocytes can be driven by the H^+ electrochemical gradient via DMT1. Heme can be taken up by HCP1 via endocytosis. Fe^{2+} within the endosome is then

liberated inside the cytosol. Cytosolic iron is either stored in ferritin or exported through basolateral transfer via FPN, which is coupled to the ferroxidase activity of hephaestin. Exported iron binds to transferrin in the blood stream for distribution. (Figure source: Zimmermann and Hurrell, 2007) (57)

Non-heme iron, on the other hand, traverses into the cell via divalent metal ion transporter 1 (DMT1) after it has been enzymatically reduced (56). The ferric iron must first be reduced to the ferrous form, a pre-requisite for DMT1 mediated transport, by either the ferrireductase at the brush border membrane, duodenal cytochrome b (Dcytb), or reducing agents present in diet such as ascorbic acid before it can enter the intestinal enterocytes (58). Dcytb, a homolog of heme-containing cytochrome b, is a membrane-bound ferrireductase that can reduce ferric iron to ferrous iron (59). DMT1 was initially identified in rat duodenum and operates with a hydrogen-coupled mechanism for the transport of ferrous iron and other divalent metals across the cell membrane (60).

While some of the absorbed iron is sequestered into ferritin (see section 1.3.4.2) or incorporated into iron-containing enzymes within the cell, the rest enters blood circulation. The stored iron in ferritin can be liberated from the ferritin molecule in ferrous form should iron be needed for cellular metabolism. If it is not required by the body, the iron remains sequestrated in ferritin and is excreted when the short-lived (2-3 days) mucosal cells are sloughed off into the lumen of the gastrointestinal tract. Intestinal ferritin synthesis is directly regulated by body iron stores, with increased ferritin synthesis being associated with high iron stores. Iron is shuttled out of enterocytes by ferroportin (FPN) which enhances the rate of

iron export and generates the ferric form of iron (Fe^{3+}) with the aid of hephaestin (58, 61), a homologue of the serum ferroxidase ceruloplasmin (62).

1.3.3 Iron transport and cellular iron uptake

1.3.3.1 Plasma iron pool

Iron absorbed by the intestine or released from the tissues enters the plasma prior to further utilization. This intermediate state of iron in the plasma forms a plasma iron pool. The iron sources contributing mainly to the plasma iron pool mainly include 1) gastrointestinal absorbed dietary iron, 2) iron from reticulo-endothelial macrophages which catabolize and store red cell iron, and 3) iron from hepatocytes are storing iron. Iron released from myoglobin and iron-containing enzymes contributes only a small fraction of iron to the plasma iron pool for iron turnover (29).

Plasma iron turnover is estimated to be 20-30 mg of iron per day (63, 64). While only 10% of this turnover iron originates from duodenal absorption, the majority of turnover iron comes from macrophages pointing to the essential role of these cells in iron recycling from senescent erythrocytes and thus for the maintenance of body iron homeostasis (65). Iron turnover is therefore primarily determined by the degradation of senescent erythrocytes by the reticulo-endothelial system (66) but the role of dietary iron in iron turnover is also of great significance as the sole external source. In the human body, about 80% of functional iron is found in erythrocytes with an average lifetime of 120 days. Senescent erythrocytes are degraded by phagocytosis in macrophages, liberating iron from heme. About 85%

of the liberated iron re-enters circulation. Approximately 0.66% of total body is recycled in this manner each day (67). The regulation of iron release from macrophages is largely dependent on hepcidin (see section 1.3.7.2) (68), the dysregulation of which can result in the disruption of iron homeostasis as seen in hereditary hemochromatosis.

About 70–80% of plasma iron is incorporated subsequently by bone marrow into developing erythroid cells for hemoglobin synthesis which requires by far the greatest iron amount on a daily basis (58, 69). As the plasma pool of iron is commonly maintained at a level of less than 4 mg of iron and the iron demand for body metabolism is rather high, the half-life of plasma iron are therefore quite short.

1.3.3.2 Transferrin

As free iron is highly toxic, the exported Fe^{3+} from enterocytes to the blood stream is sequentially accepted by circulating plasma transferrin (Tf) (34, 56), a transporter used for iron delivery to organs where iron is required for metabolic processes. Tf is not only responsible for the delivery of iron from the basolateral surface of enterocytes to peripheral tissues, but also for the redistribution of iron to various body compartments. In addition, Tf also protects iron from body excretion during glomerular filtration by the formation of a large molecule, Tf-bound iron (Tf-Fe^{3+}) (50).

Tf (Mr ca. 80 kDa), a single chain of 680 amino acid residues, is a member of a closely related family of iron-binding glycoproteins that also includes lactoferrin, melanotransferrin, and ovotransferrin (70). It has two binding sites for Fe^{3+}in a ternary complex of protein ligands, bicarbonate and water with a very high affinity of 10^{-22} M for iron at pH 7.4 (50). The two binding sites, although 60% identical in amino acid sequence, are functionally distinct in sequestering iron and involve a conformational change during iron binding. In the plasma and other extracellular fluids, Tf exists as a mixture of apo-Tf (Tf that binds zero iron ions), monoferric Tf (Tf that binds to one Fe^{3+}) and diferric Tf (Tf that binds to two Fe^{3+}). Their relative abundance is dependent on the relative concentrations of iron and Tf (26).

Tf is able to bind two Fe^{3+} ions tightly, but reversibly with concomitant binding of two carbonate anions. The carbonate anions serve as bridging ligands to shield water from binding iron in the coordination sphere, to lock the iron ions firmly to the protein and to avoid hydrolysis (24). In the reversible binding mechanism, the release of iron from Tf is the result of the protonation of the carbonate anion. Several other metals may also bind to the iron-binding sites of Tf, e.g. aluminum, cadmium, and manganese. Iron, however, has the highest binding affinity and will displace the other metals (26).

Abundant amounts of circulating Tf are present in the blood plasma where the majority of non-heme iron binds to Tf. It is estimated that approximately 0.1% of

total body iron is found in Tf (51, 71). In normal adult plasma, the concentration of Tf is about 30μM whereas that of iron is approximately 20μM (69). Each Tf can bind up to two Fe^{3+} (72). Under normal conditions, plasma Tf is thus approximately saturated to only 1/3 with iron (73). The unoccupied iron binding sites on Tf offer a large buffering capacity in the case of an elevated level of plasma iron (72). Plasma Tf is thus always in excess of iron to prevent the body from the potential toxicity of free iron. Fasting Tf saturation can serve as one of the criteria for the assessment of iron status. Tf saturation for normal people is within the range of 16% - 45%. In establishing iron deficiency, Tf saturation should be <15% (35, 58), below the level of which, insufficient amount of iron is delivered to bone marrow and fails to maintain normal rates of erythropoiesis. If Tf saturation is above 45%, iron level in the body is considered elevated and further tests are required to be carried out to confirm the condition of iron overload.

In addition to the primary function of plasma Tf as a iron carrier in the plasma and interstitial fluid of the body, two secondary functions of Tf have been demonstrated, namely as a bacteriostatic agent and a growth factor, which is probably associated with the capacity of the protein to act as an iron donor (26).

1.3.3.3 Transferrin-dependent iron uptake mechanisms

Tf-Fe^{3+} in the plasma is nonreactive, but is also difficult to extract for utilization by organs. Several mechanisms for Tf-dependent iron uptake have thus been

adopted by the body to mediate the internalization of the entire Tf-Fe^{3+} complex (69).

Two transferrin receptors (TfR) have been identified in mammals to mediate the internalization of Tf into the cell, transferrin receptor 1 (TfR1) and transferrin receptor 2 (TfR2), both of which are type II transmembrane homodimer glycoproteins that share 45% of their chemical identity. They consist of two 90-kDa subunits linked by disulfide bonds (74).

The uptake of Tf-Fe^{3+} via the TfR1 mediated endocytic pathway has been most extensively investigated (75). Due to the ubiquitous expression of TfR1, most cell types might take up iron via TfR-mediated pathway. This appears to be the most important pathway for iron uptake in developing erythroid precursors, which require enormous iron for hemoglobin synthesis.

The Tf-TfR1 interaction depends on the iron saturated status of Tf and the pH of the milieu (64). At the extracellular pH of 7.4, TfR1 has high affinity to diferric Tf (dissociation constant of 10^{-7} - 10^{-9} M) whereas apo-Tf does not compete significantly. When the pH drops below 6.5, however, the affinity of TfR1 for diferric Tf decreases whereas that for apo-Tf increases. For instance, when between pH 5 to 6, the affinity of TfR1 for apo-Tf increases to the level that is comparable to that for diferric Tf at pH 7.4 (76, 77).

Following the binding of Tf-Fe^{3+} to TfR1 at the cell surface at the extracellular pH 7.4, Tf-Fe^{3+}/TfR1 complexes localize to clathrin-coated pits and enter the cell by endocytosis with the aid by the adaptor protein complex-2 (70) (see Fig. 1-3). Upon internalization, a smooth vesicle, is formed by shedding its clathrin coat into a sorting endosome. Early Tf-containing endosomes are acidified by a proton pump (H^+-ATPase) which lowers the pH in the endosome to pH 5-6, effecting conformational changes in both Tf and TfR1 to release iron. The released iron is subsequently reduced from Fe^{3+} to Fe^{2+} by an unidentified ferrireductase, possibly six-transmembrane epithelial antigen of the prostate 3 (STEAP3), allowing DMT1 to transfer Fe^{2+} across the endosomal membrane into the cytoplasm (78). This released iron is then channeled into one of three pathways: iron-utilizing proteins, iron-regulatory proteins, or storage iron (50). TfR1 and Apo-Tf are returned to the plasma membrane, where each can be recycled for iron uptake and binding. About 1% of the apo-Tf/TfR1 complex, however, enters the late endosomes and is directed to lysosomes for degradation (79)

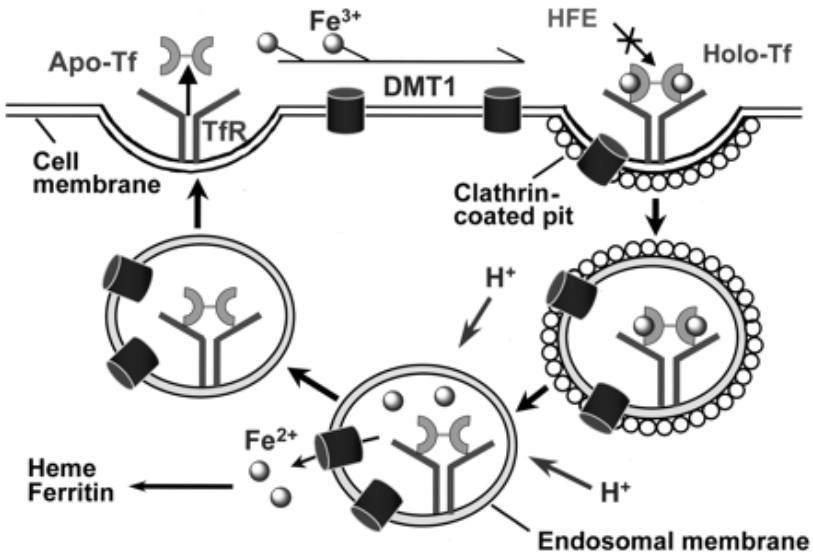

Fig. 1-3 Transferrin receptor mediated endocytosis for cellular iron uptake
$Tf\text{-}Fe^{3+}$ binds to TfR1 on the membrane. The $Tf\text{-}Fe^{3+}$/TfR1 complex is internalized and forms a endosome which is later acidified by a proton pump, resulting in the release of iron from Tf. The released iron is subsequently transported out of the endosomes via DMT1 into cytosol to participate in cellular metabolism or for storage. The apo-Tf/TfR1 complex are returned to the plasma membrane, where they dissociate at neural pH and can be recycled for iron uptake and binding.(Figure source: Qian et al., 2002 **) (70)**

In contrast to the ubiquitous expression of TfR1, TfR2 is mainly restricted to hepatocytes, suggesting a more specialized role (64, 80). TfR2 appears to have dual roles in iron metabolism: iron transport and iron regulation (81). TfR2 binds diferric Tf with an affinity approximately 25-fold lower than TfR1, possibly serving as an alternative pathway for the uptake of $Tf\text{-}Fe^{3+}$ by hepatocytes (81). Paradoxically, mutations in the human TfR2 gene result in a genetic disorder of iron overload - hemochromatosis (82), pointing to its role in iron regulation other than iron uptake.

Besides TfR1 and TfR2, cubilin, a 460-kDa protein that is located within the epithelium of intestine and kidneys, was demonstrated to be the third physiologically and quantitatively important TfR involved in iron uptake. Polarized epithelial cells of the kidney utilize this third uptake mechanism for $Tf\text{-}Fe^{3+}$, via megalin (coreceptor colocalizing with cubilin) dependent, cubilin-mediated endocytosis (83). Renal proximal tubules may acquire iron mainly via this pathway.

The cellular uptake of iron based on the TfR-mediated endocytosis is largely determined by the number of TfR present on the cell surface which is regulated by body iron status and the rate of cellular proliferation. Production of the receptor is

thus stimulated by iron deficiency and inhibited by increased iron supply. The regulation of the synthesis of receptors is achieved by a posttranscriptional mechanism known as the IRP/IRE system (see section 1.3.7.1) (26)

1.3.4 Body iron storage

1.3.4.1 Body iron distribution

While most of body iron (ca. 60%) is bound in erythrocytes for functional use (62), the liver and the reticulo-endothelial macrophages serve as the main sites of iron deposition and storage (84, 85). Distribution of storage iron, mainly in the form of ferritin, is heterogeneous among tissues. Approximately 60% of body ferritin is found in the liver whereas muscle tissues and reticulo-endothelial system contains the remaining 40% (73).

Under normal physiological conditions, ferritin constitutes 95% of liver iron and is stored in hepatocytes whereas the remaining 5% is found predominately as hemosiderin in Kupffer cell lysosomal remnants. Hepatocytes constitute 80% of the liver mass and play the most prominent role in hepatic iron metabolism (84). As a main site of iron storage, it has a high capacity for iron storage protein synthesis.

Macrophages of the reticulo-endothelial system are responsible for iron recycling from senescent erythrocytes. The structure of the erythrocyte membrane changes towards the end of the life cycle of the red blood cell. Once these changes are recognized, erythrocytes will be phagocytosed at extravascular sites by liver

Kupffer cells (resident macrophages in liver) and spleen macrophages. Iron released from heme by HO-1 either enters the cellular iron pool and is stored mainly as ferritin or returns to circulation.

1.3.4.2 Ferritin

Ferritin is ubiquitously distributed in the human body and is used, in general, for intracellular sequestration of iron and its detoxification and storage (26). It is a hollow spherical protein complex (molecular weight: ca. 450 kDa) composed of 24 subunits that are arranged in cubic symmetry surrounding a hollow cavity with an internal 8-nm diameter (86, 87). Ferritin can store up to 4,500 iron atoms inside the protein shell as an iron(III) mineral, traditionally described as ferrihydrite [$Fe^{III}_{10}O_{14}(OH)_2$] (88). Individual ions, such as water, metal cations and hydrophilic molecules of the appropriate size, can migrate into and out of the cavity through eight hydrophilic channels locating at the C_3 symmetry axis of ferritin (86, 88). Other biological molecules, on the other hand, are prevented from reacting with the iron mineral stored in the ferritin cavity (89). Ferritin is resistant to the change of temperature and pH. It is demonstrated to be stable at up to 70°C and over an extreme pH range of 3-10. At pH <3 the ferritin subunits dissociates but reversibly reassembles at pH > 3 (88).

The 24 subunits of the apoferritin shell can be classified into two types of polypeptide chains: the H (or heavy) subunits of 178 amino acids (21 kDa), and the L (or light) subunits with 171 amino acids (19 kDa). Despite their different physiological roles, H subunits and L subunits are structurally closely related

(~53% protein sequence identical in primary structure) (90, 91). H subunits possess the catalytic ferroxidase center for rapid iron (II) oxidation to detoxify iron. L subunits, however, possess the iron nucleation sites providing Fe^{3+}-binding ligands that initiate crystal growth within ferritin (92). L subunits are therefore responsible for mineralization and long term iron storage in the ferritin cavity (93). During the storage process, two Fe^{2+} are recognized by the ferritin molecule and bind to the ferroxidase center in H subunits where the Fe^{2+} ions are oxidized to Fe^{3+} (94). The oxidized Fe^{3+} thereafter diffuse into the interior of the ferritin cavity where Fe^{3+} binds to the nucleation sites of the L subunits for mineralization (92).

In agreement with the different roles of H and L subunits in iron storage, the H/L ratio in a ferritin shell varies widely in different tissues. H-rich ferritins predominate in organs that require mainly iron detoxification capacities, cellular protection and rapid iron turnover such as the macrophages, heart and brain while iron storage organs such as the liver and spleen contain mostly L-rich ferritins (95). For instance, the H/L ratio is 1:10 to 1:20 in human liver ferritin and 1:4 in rat liver ferritin (96, 97).

In contrast to the high expression of ferritin in tissues, ferritin is also present in plasma but with in very limited amounts. Plasma ferritin accounts for < 1% of the amount of iron bound to Tf. It is cleared from plasma by the liver via receptor-mediated endocytosis. The concentration of plasma ferritin correlates positively

with body iron stores and widely used as a indicator of body iron status in clinical practice (26).

1.3.4.3 Hemosiderin

Hemosiderin (molecular weight: 12.9 to 17.8 kDa), as the second iron storage molecule, is a water insoluble protein of ill-defined nature and considered a partial lysosomal degradation product of ferritin with a much higher iron to protein ratio found in hemosiderin than ferritin (24, 98-100). Hemosiderin is mainly found in pathological iron overload, e.g. hemochromatosis and siderosis (101). The mass accumulating rate of liver hemosiderin is 10 times that of ferritin during iron overload (102).

The protein shell of ferritin is usually partially degraded to form hemosiderin by lysosomal proteases when the average tissue ferritin capacity reaches approximately 4000 iron atoms per ferritin molecule (103). It is found that up to 40% of the mass of hemosiderin consists of iron. Depending on the sources and conditions under which the iron was obtained, the form of hemosiderin iron varies, including ferrhydrite, amorphous ferric oxide, and goethite (104). In general, the chemical reactivity of these forms of iron is lower than ferritin iron and their availability for mobilization is less.

1.3.5 Cellular iron metabolism

Cellular iron homeostasis includes iron uptake, utilization, storage and export. Iron taken up by the cell is mainly via a TfR-mediated endocytosis pathway (see section 1.3.3.3). The iron liberated into the cell will enter the cellular iron pool. A

labile intermediate iron pool within the cell has been hypothesized from which iron is accessible and ready for heme synthesis, for ferritin storage, and for the synthesis of iron-dependent enzymes within the cell, or for extracellular Tf after export from the cell (105-107).

The concept of the labile iron pool (LIP) was first proposed by Greenberg and Wintrobe in 1946 who defined it as “an intermediate stage which receives iron from hemoglobin breakdown or from oral absorption or iron that is injected parenterally” (106). It was later reintroduced by Jacobs (1976) and defined as a pool of redox-active iron complexes associated with proteins, serving as crossroads of metabolic pathways of iron-containing compounds (105, 107).

Although the actual functioning mechanism for LIP remains unexplained, its sources have been well defined. The LIP is replenished iron release from heme, from ferritin, iron export from endosome or from mitochondria etc. (108). To maintain cellular iron metabolism, a constant iron flux from an extracellular milieu to the cytoplasm is required. The daily dietary iron uptake (1–2 mg) is one of the major sources of LIP and theoretically should enter LIP prior to the distribution to the targeted proteins.

Iron in LIP can be complexed by a variety of low-molecular weight ligands with low affinity to iron ions, e.g. phosphate, carboxylates, citrate, nucleotides and nucleosides, polypeptides and phospholipids (107, 109, 110). The weakly

chelated iron (in both ionic form Fe^{2+} and Fe^{3+}) can potentially cause free radical generation, catalyze extensive oxidative modifications of cellular components and thus, cellular dysfunction (36). The loosely bound iron, however, can be scavenged by iron chelators.

LIP represents only a minor fraction (3–5%) of the total cellular iron (250 – 550μM) (111), however, it has been proposed to have two crucial functions: 1) provide a rapidly adjustable source of iron for immediate metabolic utilization, and 2) participate in iron regulation via sensing by iron regulatory proteins (108). The fraction of iron in the LIP covers a wide range, allowing a high tolerance for change in iron flux. However, in extreme cases when the change of iron influx exceeds the homeostatic capability of the LIP, the redox active forms of cellular iron may lead to a variety of physiological and pathological conditions via ROS induced oxidative stress (108, 109).

Due to the critical role that LIP plays in cellular homeostasis, the body stringently regulates the iron level in LIP to maintain normal cellular iron metabolism but also restricts iron to be involved in free radical generating chemistry (112). It is speculated that down regulation of labile iron may have a favorable impact on health in general and aging in particular (36). Iron chelators targeting LIP are therefore used clinically for the treatment of Parkinson's disease (see section 1.5.3.4).

The mechanism of cellular iron export has been far less extensively studied than that of iron uptake, but the molecular understanding has advanced recently. The main protein responsible for cellular iron export is FPN (see section 1.3.2). Iron is exported out of the cell via FPN with the aid of a ferroxidase. As the only current known cellular iron exporter in vertebrates (113, 114), FPN is distributed in cells such as hepatocytes, duodenal enterocytes and macrophages, where major iron flows are regulated. Studies on zebrafish (114) and mice (115) indicated that FPN is also the sole significant iron exporter in tissues involved in the process of iron absorption, storage and recycling.

1.3.6 Iron excretion

Evolutionally, the human body has not been equipped with a mechanism for active iron excretion (24). Prior to the presence of molecular oxygen, with the essentially reducing atmosphere on Earth, both the natural abundance of iron and its redox properties predisposed it to play a crucial role in the first stages of life on Earth. Since the advent of oxygen into the earth atmosphere, iron's bioavailability has been seriously compromised by the formation of iron hydroxide. Due to the crucial role of iron in life, the mammalian body has therefore developed a stringent regulatory system to conserve iron for reproduction and other biological functions.

As there is no mechanism for active iron excretion, it is of great importance to regulate dietary iron absorption to maintain body iron homeostasis (51). It is well established that under normal physiological conditions an adult person can absorb

only 1-2 mg of ingested dietary iron per day (116) which is shown to be adequate for the compensation of the ~1-2 mg of unregulated iron loss (see Fig. 1-4).

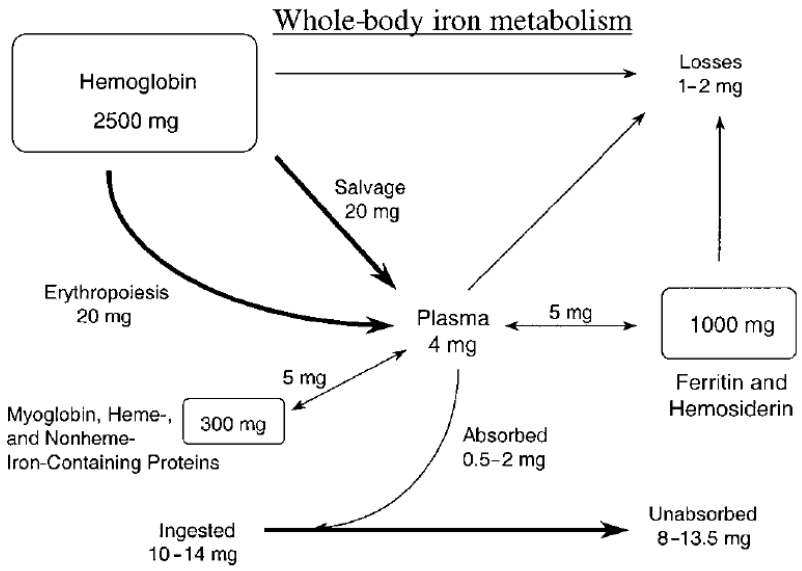

Fig. 1-4 Iron distribution in the body and exchange pools.
Figure source: Beard et al. (1996) **(50).**

The biggest contributor to the unregulatory iron losses is basal iron excretion. Basal iron excretion, predominantly arising from cellular exfoliation of the gastrointestinal tract, is limited, and is the primary determinant for nutritional requirements for absorbed iron in humans (117). Iron losses from this route amount to 0.6 mg/day in adult males via fecal excretion (67), derived from desquamated mucosal cells, minute blood loss, and biliary heme breakdown products. The skin losses of ~0.2 to 0.3 mg iron are due to desquamation of surface cells from the skin in adult males (66). Iron losses through the urogenital system are minimal and are estimated to be 0.08 mg iron (25). Increased losses of iron, however, may occur in people with gastrointestinal ulcers or intestinal parasites, or with hemorrhage induced by injury.

Other sources of unregulatory iron losses include menstruation, pregnancy, or other bleeding. The variation in iron losses with the gender of the individual is considerable. Daily iron losses by male have been determined to be ~0.9 to 1 mg/day while basal iron losses are slightly lower for postmenopausal women, ~0.7 to 0.9 mg/day, owing to their smaller surface area (25).

1.3.7 Regulation of body iron

Evolution left the body a closed system for iron metabolism with minimal iron excretion. The regulation of body iron content is therefore solely dependent on iron absorption efficiency. Iron absorption by the human body is regulated by the total amount and forms of consumed iron and the iron status of the individual**.** The iron absorptive efficiency has a wide range (118). The amount of iron absorbed by iron-loaded individuals is proportionally less (up to 15 times) than that by iron-deficient individuals (58). Regulation of intestinal iron absorption is the fundamental principle of body iron homeostasis (73).

Iron homeostasis must be maintained both at the cellular and the systemic level. Expression of proteins involved in iron absorption (DMT1), storage (ferritin), utilization (Tf and TfR), iron export pathway (FPN, HFE, the bone morphogenic proteins and hepcidin) and iron signaling (IRP/IRE system) must be regulated in a coordinated manner (119). Misregulation at each level can basically lead to physiological malfunction.

1.3.7.1 Cellular iron regulation – IRP/IRE system

At the cellular level, iron concentrations are sensed by two homologous cytoplasmic iron regulatory proteins (IRP)-IRP1 and IRP2 (64) and posttranscriptionally modulated by IRP/iron regulatory element (IRE) system. IRE-containing mRNAs encode key proteins of iron metabolism, such as H- and L-ferritin, TfR1, DMT1, FPN and others (120). When cytosolic iron levels are low, IRPs bind to IREs that possess hairpin structures in the untranslated regions (UTRs) of mRNAs of iron-associated proteins, and control their translation or stability. The synthesis of the iron-associated proteins is affected by the binding site on the IREs of mRNA: binding of IRPs to IREs in the 3'UTR results in the stabilization of mRNA, leading to elevated protein synthesis, whilst binding of IRPs to IREs in the 5'UTR inhibits the translation of mRNA, as a result protein synthesis decreases (see Fig. 1-5) (113)

The detailed operation of the IRP/IRE system can be exemplified by the translation of ferritin and TfR1. When cytoplasmic iron is high, the IRPs bind to iron instead of the IREs of ferritin and TfR1 mRNA. Due to the lack of IRP binding, the translation of the ferritin mRNA may precede forward whereas the TfR1 mRNA degrades, resulting in an elevated level of ferritin and reduced level of TfR1 synthesis. When cytoplasmic iron is low, IRP1 binds to the IRE in the 5'UTR of ferritin mRNA and 3'UTR of TfR1 mRNA, leading to the decreased translation of ferritin protein and increased TfR1 synthesis via the stabilization

and protection of the TfR mRNA from degradation. The expression of TfR2, on the contrary, is not regulated by the IRP/IRE system (51)

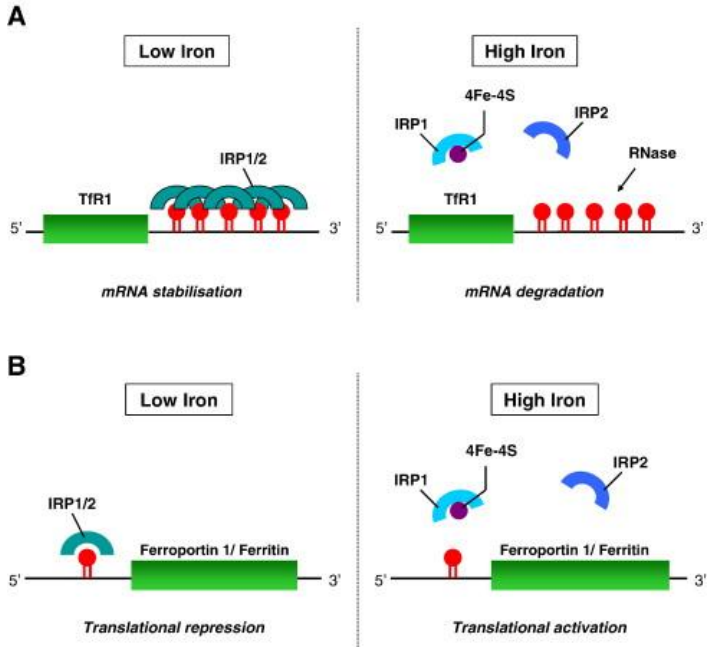

Fig. 1-5 The effect of cytoplasmic iron levels on IRE/IRP system.
When cytoplasmic iron concentrations are low, the binding affinity of IRP1/2 to mRNA is high. IRP1/2 binds to the IREs in the 5'UTR of ferritin mRNA and 3'UTR of TfR1 mRNA, leading to the decreased translation of ferritin protein and increased TfR1 synthesis. Under conditions of high cytoplasmic iron concentrations, IRP1 binds to the assembly of a [4Fe–4S] cluster whereas IRP2is targeted for proteasomal degradation (121, 122).

1.3.7.2 Systemic iron regulation - Hepcidin

Systemically, iron fluxes in the body are strictly controlled by a liver-derived regulatory hormone known as hepcidin (123). Hepcidin, with its ability to inhibit the functioning of the protein FPN that is responsible for cellular iron release, is demonstrated to affect iron homeostasis by the regulation of gastrointestinal iron absorption, hepatic iron storage and iron recycling from macrophages since enterocytes, hepatocytes and macrophages rely all on FPN for cellular iron export

(120). The secretion of hepcidin from the liver is largely in response to iron overload or inflammation. In the event that systemic iron increases (high iron stores), hepcidin can be secreted by the liver to target FPN on the basolateral membrane of duodenal enterocytes and tags it for internalization and lysosomal degradation, thereby effectively down-regulating dietary iron absorption (85). Within a day or two, the unabsorbed iron is removed concomitantly with the shedding of the short-lived enterocytes into the intestine. Conversely, synthesis of hepcidin is suppressed when iron stores are low. As a result FPN molecules are displayed on basolateral membranes to aid in iron transport to plasma Tf. Similarly, iron recycled from senescent erythrocytes is trapped in macrophages when hepcidin induces the degradation of FPN (113).

Iron fluxes in FPN-expressing organs is controlled by hepcidin (124) while the plasma level of hepcidin is in turn regulated by iron. Hepcidin regulatory system is likely to be extremely complex and remains to be further explored. It is reported that the *HAMP* gene encoding hepcidin is transcriptionally induced by high iron intake (125), resulting in the inhibition of iron efflux from the cytoplasm. Conversely, iron deficiency, anemia or hypoxia suppress hepcidin mRNA transcription (125, 126), allowing elevated iron absorption and iron release from macrophages.

Under physiological conditions, the level of *HAMP* is regulated via a complex cell signaling pathway that includes several cell membrane proteins such as bone

morphogenetic protein (BMP), hemojuvelin (HJV), TfR2 and HFE etc. (127). Mutations in these genes lead to iron loading syndrome, implicating their role in hepcidin synthesis in the liver (123). In cell cultures and murine models, hepcidin expression was shown to be associated with the BMP/SMAD pathway (128). The treatment with BMP results in increased hepcidin expression whereas the inactivation of the cofactor HJV of the pathway decreases hepcidin expression (129). In addition, the mRNA expression of hepcidin was reported to be influenced by inflammatory conditions and the transcription was induced by interleukin-6 (IL6) (130). Furthermore, hemochromatosis protein (HFE) might be involved in hepcidin regulation as previous human and animal studies demonstrated that this disorder was linked with lower level of hepcidin production (131)

By blocking cellular iron export, hepcidin may indirectly affect the cellular IRE/IRP system due to increased intracellular iron levels. Though the extent of interaction between hepcidin-FPN and the IRE/IRP system remains to be elucidated in detail, the effect of which on the expression of the IRE-containing proteins DMT1, TfR1, and FPN has been demonstrated (113).

The hepcidin regulatory system is compromised under pathological condition. Over expression of hepcidin is associated with severe iron deficiency anemia in transgenic mice (132) whereas considerably reduced hepcidin expression is found in patients with hereditary hemochromatosis (131, 133).

1.4 Brain iron homeostasis

Iron is not only the most abundant trace element in the body, but also in the brain (134). Like other organs in the body, the brain also requires iron for metabolic processes, which include electron transfer and oxygen transport, myelin production, neurotransmitter synthesis and neurogenesis (135).

1.4.1 Brain barriers

Brain is encompassed by the blood-brain barrier (BBB) and blood-cerebrospinal fluid barrier (BCB), across which iron traverses into the brain.

1.4.1.1 The blood-brain barrier

The BBB is a separation of circulating blood from the brain extracellular fluid and exists at the capillary endothelium, the cells of which are joined together by multiple bands of tight junctions that are not present in normal circulation. These junctions seal adjacent endothelial membranes, thereby closing off the paracellular diffusion space (136), allowing the cerebral microvasculature to selectively protect the brain from the rapid changing milieu of systemic circulation (137). Unlike small gas molecules (e.g. O_2 and CO_2) that can diffuse freely across lipid membranes into the brain (138), the lipophic nature of the BBB precludes circulating hydrophilic molecules from entering the brain. Mechanisms thus exist to ensure selective brain uptake of hydrophilic nutrients, amino acids, glucose, vitamins, and essential metals including iron (26).

1.4.1.2 The blood-cerebrospinal fluid barrier

The other barrier, BCB, is formed by the choroid plexus epithelial cells and the

arachnoid membrane (139). The choroid plexus, composed of many capillaries, is a vascular tissue present in cerebral ventricles. Unlike the capillaries that form the BBB, the endothelium of the capillaries in the choroid plexus has no tight junctions and allows the free movement of molecules. The epithelial cells, instead, are linked together by tight junctions. The BCB is therefore formed at the choroid plexus epithelial cells. The arachnoid membrane envelops the brain and its cells are also joined by tight junctions.

The choroid plexus produces the majority of cerebrospinal-fluid (CSF) in the brain (100-150 mL in normal adults), which circulates substances from ventricular cavities into the subarachnoid space. The CSF is then absorbed into venous sinus blood via the arachnoid villi, where the CSF may be filtered by the arachnoid membrane. While CSF is known as the major source of the transport of a variety of molecules into the brain, it also has a "sink action" by which it selectively removes molecules produced during metabolic activity in the nervous tissue. The turnover rate of CSF is very high, approximately 3-4 times a day.

1.4.2 Brain iron distribution

1.4.2.1 Brain regional iron distribution

An average adult brain contains approximately 60 mg non-heme iron, distributed heterogeneously in accordance to brain structures, with some regions, e.g. substantia nigra, caudate nucleus, globus palladus and putamen, containing iron well above average levels (140-142). The rank order for regional iron distribution in normal brain was found to be globus pallidus> putamen > substantia nigra >

caudate nucleus > cerebral cortex = cerebellum (143). It is noteworthy that the iron levels in substantia nigra and globus pallidus exceed hepatic iron levels, retaining iron at concentration of 3.3-3.8 mM in the normal adult brains. These two areas belong to the basal ganglia, which is situated at the base of the forebrain and which is associated with motor functions. The high brain iron levels can be attributed mainly to the high iron requirement in these areas to maintain ionic membrane gradients, synaptic transmission and axonal transport (144). Besides basal ganglia, iron concentration in hippocampus are also high at ca. 50 ng/mg (88). While it is widely accepted that the progressive degeneration of neurons in iron rich substantia nigra is involved in the development of PD, the loss of neurons cells in iron rich hippocampus is associated with AD.

1.4.2.2 Cellular iron distribution

The majority of brain iron is stored in the form of ferritin in brain cells. Neurons in many brain regions, however, do not contain ferritin. The abundant presence of TfR and the lack of ferritin indicate that the iron uptake by neurons is mainly for the immediate use for neuronal metabolic activities and non-utilized iron is exported out of the cell after use, possibly via FPN, instead of being stored as ferritin (145). In contrast to neurons, glial cells, except astrocytes which are largely responsible for iron transport into the brain, express the iron storage protein ferritin, indicating that these cells have the capacity to store iron (146). The ratio of H- to L- subunit in ferritin, however, varies in different cell types. H-subunits are mostly expressed in neurons**,** L-subunits are more abundant in microglia and both subunits are expressed in similar amounts in oligodendrocytes

(88, 147)**.** When the brain ages, ferritin that contains stable and soluble forms of iron is selectively changed into hemosiderin and other oxyhydroxide derivatives that sequester relatively highly reactive iron (148), making the brain more vulnerable to oxidative stress.

In the brain, the ferritin level in oligodendrocytes is much higher than in neurons (145, 149). Due to higher levels of iron, the oligodendrocyte is the principle cell type used for iron staining (150). This has led to the hypothesis that the main function of oligodendrocytes is myelin production (151), the process of which requires the participation of iron. Aberrations in the iron metabolism of oligodendrocytes are associated with hypomyelination. Previous studies demonstrated that hypomyelination in brain can result from dietary iron restriction, suggesting the importance of iron in myelin production (151, 152). During aging, the iron content in oligodendrocyte remains relatively constant (153).

Brain iron can also be stored in neuromelanin, one of the primary pigments in the human brain. Neuromelanin is a dark-colored, highly insoluble intracellular granular pigment that can bind to metals (147, 154). Neuromelanin has a much higher affinity for iron than other metals. On binding to iron, it forms stable octahedral complexes that contain oxy-hydroxide iron clusters. Neuronal iron is predominately bound to neuromelanin (155). In the human brain, neuromelanins are commonly found in dopaminergic neurons in the substantia nigra and the noradrenergic neurons in the locus coeruleus. Several studies have demonstrated

that neuromelanin accumulates during normal aging (154, 156, 157) and might be implicated in the development of PD (157, 158) (see section 1.5.2.2.2). The melanized dopaminergic neurons are more vulnerable than other neurons (157). The preferential loss of the melanized dopaminergic neurons is one of the characteristics of PD.

1.4.3 Brain iron uptake and export

1.4.3.1 Brain iron uptake

All tissues in the mammalian body share a common liver-dependent macro-regulatory system of iron delivery and homeostasis which is based on systemic iron circulation and involves regulation of intestinal iron uptake and circulating Tf. The three exceptions to this macro regulatory system are CNS, testes and retina (159, 160). The CNS is encompassed by the BBB and BCB across which iron traverses into the brain. The mechanism of brain iron uptake via these barriers has not yet been completely elucidated.

1.4.3.1.1 The blood-brain barrier pathway

It was believed for many years that iron uptake by the brain occur predominately during infancy before the BBB matured (159). In the last decade, with the discovery of the expression of TfR1 by endothelial cells on the luminal side of the capillaries (24), accumulating evidence reveals that TfR-mediated endocytosis is highly likely to be largely responsible for Tf bound iron uptake across BBB in adult mammals (138). Moreover, the expression of TfR on the luminal endothelial surface is modulated by iron status within the brain (159). In this pathway, Tf

binds to the extracellular portion of the TfR and the Tf-TfR complex gets incorporated into endosomes of the cerebral endothelial cells. The slightly acidic inner environment of endosomes facilitates iron release from Tf (see section 1.3.3.3). Besides the TfR-mediated pathway, iron might also transverse the BBB via a ferritin receptor mediated pathway as H-ferritin receptors were detected on the brain micro-vasculature (24, 161).

Additionally, previous studies report the possibility of non-transferrin-bound-iron (NTBI) transport across the BBB cells which serves as an alternative uptake pathway for iron in brain (162-164). The NTBI pathway is, however, responsible for only a small proportion of iron transport across the BBB especially at low serum Tf levels (165).

Iron taken up by the cerebral endothelial cells can be exported into the brain interstitial fluid by FPN (166). The existence of FPN in the membrane has been demonstrated by immunohistochemistry (167). Alternatively, iron can be released into the brain interior via the astrocytes, the end-feet of which encircle the cerebral endothelial cells and direct iron delivery into the brain. Under acidic conditions, Tf-Fe^{3+} releases Fe^{3+} to become apo-Tf, which has a high affinity to TfR. Apo-Tf thereafter reenters circulation (168). Astrocytes maintain high concentration of protons at the end-feet and release ATP and citrate, creating a favorable microenvironment for the release of iron from Tf (24, 166).

1.4.3.1.2 The blood cerebrospinal fluid barrier pathway

It has been reported that the expression of iron-related proteins, e.g. DMT1, FPN, ceruloplasmin and hephaestin, in the choroid plexus was higher than in virtually all other regions of the brain (85), suggesting that this could be another pathway for iron transport into the brain. Few previous radioactive isotope studies have demonstrated that the contribution of iron transported through the BCB is minute compared to the amount of iron transported through the BBB into the brain (165, 169).

1.4.3.2 Brain iron efflux

It was reported that the human brain conserves iron as the levels of iron-storage proteins like ferritin and neuromelanin in the human brains were revealed to increase with age (147, 170) (see section 1.5.1). The question remains whether iron uptake is uni-directional or bi-directional with a higher influx rate than efflux rate for iron.

Results obtained from some previous radio-isotope studies (171, 172) have demonstrated that iron uptake by the brain is a uni-directional process with no iron export occurring from brain. Other studies, however, suggest that the process is bidirectional (168, 173-176). Structurally, the tight junctions of the BCB are quantitatively leakier than those of the BBB. Very little is known about potential brain iron efflux mechanisms. It is speculated that BCB might be responsible not only for brain iron uptake (162) but also for iron efflux in the brain owing to its structure and functions (174, 175). Bradbury (1997) proposed a probable route to

export brain iron via the bulk drainage of CSF based on the estimation of the difference between iron influx rate in rats, iron concentration in CSF of rabbits, and the CSF drainage rate in rats (174). It was further demonstrated in rats that iron may efflux from the CSF to the blood via the re-absorption of Tf-Fe^{3+} into the blood, by the injection of radio-labeled iron into the lateral cerebral ventricle (168, 175, 177). However, the estimation by Bradbury (1997) was tentative and the method in the rat studies was too invasive to allow iron equilibrium for drawing valid conclusions. Despite the presence of fully iron-saturated Tf in CSF (174, 178), the low level of Tf in CSF lack of the capacity for iron export via this route. The CSF also contains other iron-bound proteins and molecules, such as ferritin, lactoferrin and non-protein-bound iron (178, 179), which can serve as additional means for brain iron export. Moreover, researchers speculated that the iron accumulation rate with age was slower than the rate of iron uptake from the blood at the different ages (24, 168), suggesting the presence of a route for brain iron efflux. Nevertheless, despite all the speculations and studies on iron efflux mechanisms, it is not clear whether iron is persistently conserved in the brain without exchange or just enters the brain with an influx rate higher than efflux rate that results ultimately in iron accumulation. The understanding of this question would shed light onto the pathological mechanisms responsible for excessive iron accumulation in the brain of AD and PD patients.

1.4.3.3 Cellular iron uptake and export in brain

Iron that crosses the BBB or BCB is most likely to be transported to different cells within the brain in interstitial fluid (IF) and CSF bound to brain-specific Tf

or in the form of NTBI (e.g. low-molecular-weight proteins such as citrate or ascorbate) (152, 162). The brain-specific Tf is synthesized in oligodendrocytes and choroid plexus epithelial cells and specifically for brain iron transport (162, 174, 178). The affinity of Tf to iron is 10^{10} times higher than affinity of citrate to iron. Tf is therefore the first molecule to bind free iron among all other iron transporters. When Tf in the CSF and IF is fully saturated with iron, the excess free iron will thus bind to other transporters (162).

As iron is indispensable for the development and survival of neurons, the mechanism for iron uptake by neurons has been investigated intensively (74, 145, 180). Due to the ubiquitous presence of Tf in the brain extracellular fluids and the detection of TfR in the neurons, it is widely accepted that neurons acquire iron mainly via a TfR-mediated pathway with the aid of DMT1 to release iron from the endosome into the cytosol. However, the role of TfR in iron uptake by glial cells is still unclear (181, 182). Though Tf is essential for oligodendrocyte media in culture and TfR was found in oligodendrocyte progenitors in cell culture, TfR has not yet been detected in oligodendrocytes *in vivo*. The immunoactivity of TfR has not been detected in oligodendrocytes, microglia and astrocytes in adult mice (180). Moreover, it has been shown that oligodendrocyte cultures continue to acquire iron under the conditions of Tf deprivation. These evidences suggest that oligodendrocytes might take up iron through a non-TfR dependent pathway. Supporting the notion, H-ferritin receptors were found to be present in

oligodendrocyte progenitors. It was proposed that glial cells may acquire iron via ferritin-receptor mediated endocytosis.

Owing to the existence of NTBI in the brain extracellular fluids, it was suggested that both neurons and glial cells might take up Tf-free iron as an alternative to the TfR-dependent pathway (145). The uptake of NTBI by the brain cells might be facilitated by the protein SFT (stimulator of Fe transport) across cell membranes (183, 184).

1.4.4 Brain iron regulation

Despite the tight regulation of iron uptake by BBB and BCB, systemic iron fluctuation may occur which could lead to neuronal dysfunction (185). A delicate intrinsic regulatory system that is partially independent of peripheral iron status was therefore, proposed to be in place to control brain iron metabolism (186). Scientists debate if there are similarities between systemic and CNS iron regulation (159). Studies indicate that, in response to iron-depletion, animals increase iron uptake in the CNS by increasing TfR expression in brain endothelial cells (174), while in HFE-related iron-overload hemochromatosis patients, iron was found to accumulate in specific regions in the brain. These studies have led to the suggestion of the involvement of the cellular IRP/IRE regulatory system and systemic hepcidin-mediated pathway in the maintenance of brain iron homeostasis.

Key proteins of iron metabolism that are encoded by IRE-containing mRNAs (120), are also found to be expressed in various cell types in the brain for different functions, including iron uptake (TfR1 and DMT1), iron storage (ferritin) and iron export (FPN). The possible role of IRP/IRE regulatory system on brain iron regulation has been further demonstrated by genetically modified animals with the deletion of IRP-related genes, which were shown to be involved in the process of neurodegeneration (24, 159, 187). In addition, an increased stability of the IRP-IRE complex in AD patients was revealed by Pinero et al. (2000) (188), resulting in an elevated level of TfR1 and a lower level of ferritin in the brain, possibly contributing to iron accumulation (189).

With regard to the hepcidin-mediated regulatory pathway (see section 1.3.7.2), it is unclear whether the CNS relies entirely on the peripheral hepcidin or utilizes intrinsic hepcidin (186). The gene expression for hepcidin was revealed to be widespread in both human and mouse brain although the expression of hepcidin protein was found to be low in mouse brain (186, 190). The expression of the hepcidin targeted protein, FPN, has been reported in neurons in mice and rats though controversies remain about the FPN expression in cell types, like endothelial cells and astrocytes (167, 191).

The hypothesis that the brain shares the similar hepcidin-mediated regulatory system with the liver is still in debate (186). The expression of hepcidin in liver is regulated by multiple proteins, e.g. HJV, TfR2 and HFE etc. Though the mutation

in these genes will induce iron-overload in the body system, the effect of their mutation on the brain iron status is known to be limited (159). This might be partly due to the low expressions of these proteins in the brain (192, 193).

In contrast to the liver, the brain might adopt other regulatory systems to control brain iron homeostasis (186, 194). One of the possible regulatory pathways might be blocking the brain iron uptake via HFE protein in response to high iron status. The expression of HFE protein is co-localized with that of TfR1, suggesting the role of HFE in brain iron uptake via the interaction with TfR1 (195). Bennett et al. (2000) and Feder et al. (1996) reported that the competition for TfR between HFE and Tf resulted in cellular iron change by the blocking of endocytosis of iron uptake (196, 197).

1.5 Iron and neurodegeneration

1.5.1 Age-related iron accumulation in brain

Age-related iron deposition in the brain has been observed in all species examined, including mice, rats, monkeys and humans (198-203). To date, both post-mortem (203-205) and *in vivo* MRI studies (142, 206, 207) have demonstrated that compared to younger controls iron deposits in the brain of older individuals are increased. The pioneering work of Hallgren and Sourander (1958) showed that the rate of accumulation of whole brain iron increases sharply during growth, slows down after the first three decades of life and reaches a “plateau” or increases very slowly after that (see Fig. 1-6) (203).

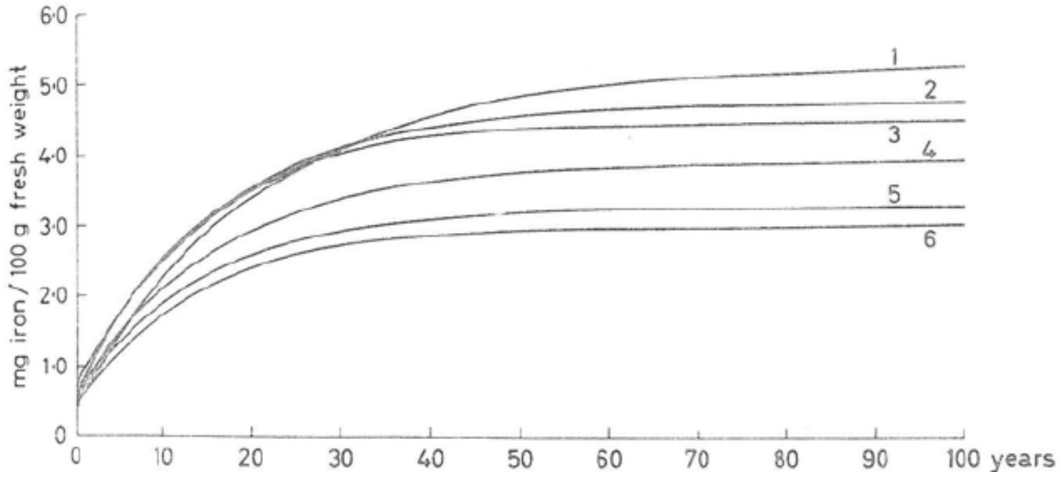

Fig. 1-6 Relation between the non-haemin iron and the age in different cortical fields
Relation between the non-haemin iron and the age in different cortical fields. (1) motor cortex; (2) occipital cortex; (3) sensory cortex; (4) parietal cortex; (5) temporal cortex; (6) prefrontal cortex. This figure is obtained from Hallgren and Sourander (1958) (203).

Moreover, iron accumulation is regionally clustered in the brain (206, 208). Motor function-related brain regions, e.g. basal ganglia and hippocampus, were demonstrated to have higher iron levels in adult individuals compared to other non-motor associated regions (163, 209-211). Studies have proven that these motor related regions have little iron at birth and accumulate significant amounts of iron with age (147, 209).

This age-related iron accumulation in the brain is consistent with "the free radical theory of aging" discussed below.

1.5.2 Iron and neurodegeneration

1.5.2.1 The free radical theory of aging

During the aging process, living organisms undergo gradual alterations that lead to both structural changes and functional decline, compromising the ability to

cope with internal and external challenges, which ultimately increase the probability of contracting diseases and causing death (36, 200, 212). Among the more than 300 theories on aging, the "free radical theory of aging" proposed by Harman 1956 has attracted a lot of interest (213) and reported to be the most prone to intervention (36, 214). The basic concept of the theory is that during aging, the balance between free radical induced damage in cell components and antioxidant defense system progressively shifts in favor of the former (36, 200). However, the exact molecular mechanisms underlying this theory remain an enigma. As excess free iron can possibly lead to the generation of ROS, iron may accumulate in the brain with age not only in general but also regional specifically, promoting the oxidative damage in the brain via free radicals.

Though iron also accumulates in other body organs with age, due to its special properties, the brain is considered more susceptible to oxidative damages accompanying aging than other tissues (39, 47). First of all, it has a high demand for oxygen, the main source of ROS, to maintain its normal function, consuming up to 20% of the total oxygen usage for its relatively small weight (2%). It also possesses more easily peroxidizable unsaturated fatty acids (20:4 and 22:6) which are vulnerable to the attack of free radicals (215). In addition, the CNS is not equipped with strong antioxidant defenses despite the needs. For instance, the catalase activity in brain is 10% lower than that in liver. The abovementioned properties collectively lead to a supposedly high age-related oxidative stress in the

brain, potentially resulting in a higher risk of developing dementia and neurodegenerative diseases in the aged populations.

Supporting the notion, recent studies have shown that iron accumulation in the brain with age may contribute to the functional cognitive decline (216-220). Penke et al. (2012) demonstrated that higher iron deposits were correlated with lower cognitive ability in human subjects with various ages using MRI (217). Similarly, another study identified that higher iron level in the basal ganglia was associated with lower scores on the Dementia Rating Scales and longer reaction times with the semi-quantifying method for iron deposits with MRI (220). Iron levels elevating in other brain regions, e.g. hippocampus and frontal cortex, was revealed to correlate with DNA strand breaks, potentially jeopardizing the functional ability of the brain (219). On the other hand, one study conducted on monkeys discovered that lower level of brain iron in basal ganglia and temporal cortex might lead to a reduction in age-related inflammation and oxidative stress (218).

1.5.2.2 The roles of iron in Alzheimer's and Parkinson's diseases

Neurodegenerative disorders (NDD), are on the rise with AD and PD, the two most common NDD, expected to reach epidemic levels in the coming decades (1, 2). This situation will pose tremendous economic and social burden on the society, necessitating a better understanding of the etiology of the two diseases for the development of effective therapeutic and preventive interventions.

Although the etiologies of AD and PD are still not completely understood, many lines of evidences support that iron accumulation in the brain with age is implicated in the pathogenesis of age-related AD and PD with the iron induced oxidative stress as the underlying mechanism. A good deal of studies have shown that, as compared to the age-matched control subjects, elevated levels of iron were observed in hippocampus of AD patients and substantia nigra of PD patients, although it remains unclear whether this represents a cause or a result of neuronal destruction. In addition, the abnormal iron deposits in the brain of AD/PD patients could be a consequence of malfunction in iron homeostasis, which might serve as one of the primary causes of the diseases (33, 147, 221, 222). Advancing the understanding of the relationship between iron and AD/PD can help us identify the cause of the diseases and the development of relevant therapeutic and preventive measures.

1.5.2.2.1 The role of iron in Alzheimer's diseases

An imbalance of brain iron homeostasis is suggested to be implicated in the pathogenesis of AD (4). As mentioned, increased levels of iron demonstrated by brain MRI scans were observed in hippocampus in AD patients as compared to healthy age-matched controls (223). In addition, a growing body of evidence supports the role of iron-associated oxidative stress in AD, which is manifested by elevated levels of lipid peroxidation, free radical formation, oxidation products of DNA and proteins (e.g. HNE, 8-HO-guanidine and protein respectively) in the brain (224-227).

More specifically, brain iron is inextricably linked with the two pathological hallmarks of AD: senile plaques and neurofibrillary tangles (NFT). The former is created by extracellular insoluble amyloid-β peptide (Aβ) whereas the latter is formed by the aggregation of protein *tau* and collapsing of microtubule that results from it (228).

Goodman in 1953 first described the presence of large amount of iron in AD-associated senile plaques (229), where the accumulation of iron is up to 3 times that of normal neutrophil levels (940 μM compared to 340 μM) (230). In line with the abovementioned findings, Aβ deposition was observed in the same regions in AD brains where iron also accumulated, such as hippocampus (231, 232). Iron might be implicated in the process of Aβ aggregation since the binding of metal ions is supposed to be an integral part of this process (233, 234). In presence of iron, Aβ can efficiently reduce Fe^{3+} to generate hydrogen peroxide. The generated H_2O_2 may degrade to form unstable ROS via Haber-Weiss reaction and Fenton Chemistry, resulting in cellular oxidative damage and subsequent cell loss and neuronal dysfunction (235). This may explain the observed increased oxidative stress in concurrence with increases iron deposits and Aβ aggregation. Furthermore, iron is also involved in Aβ formation,

Aβ is produced by the proteolysis of amyloid-β protein precursor (APP). The production of Aβ however, can be terminated by the cleavage of APP via α-secretase to form a neuroprotective sAβPPα fragment. This process is promoted

by furin protein, which is capable of converting precursor proteins into their biologically active form (236). The expression of furin protein is modulated by the brain iron level. When brain iron concentration increases, the furin protein is down-regulated, leading to the reduced level of neuroprotective sAβPPα fragment and promoting production of Aβ (237). It was therefore proposed that the regulatory role of iron in the expression of furin protein may also play a role in AD development which would explain elevated levels of iron and Aβ found in brains of AD patients.

Moreover, it is also reported that APP might potentially play a role in iron regulation. The two most notable features of APP implicated in the process are, 1) an IRE is located on the 50 untranslated region of APP and the subsequent APP translation event is influenced by iron levels (228, 238, 239), 2) APP contains a REXXE ferroxidase consensus motif (184), implying a ferroxidase activity in neurons (235). As iron is present in cytosol in ferrous form, the cellular Fe^{2+} export is thus aided by ferroxidases to oxidize Fe^{2+} to Fe^{3+}, which is subsequently transported out via FPN on the cell surface (34). Numerous studies indicated that APP possesses ferroxidase activity and is able to facilitate the export of Fe^{2+} from cultured neurons, in an attempt likely to minimize the potential ROS generation by the presence of reactive iron (240, 241). However, the ferroxidase activity of APP is inhibited in AD patients, causing neuronal iron accumulation (242).

Furthermore, iron deposition was also observed in neurons with NFT (243). Ferric iron was reported to have the ability to bind to the *tau* protein, promoting of the aggregation of hyperphosphorylated *tau* and the subsequent formation of NFT. It was also recently revealed that the amount of *tau* protein is inversely correlated with the number of APP on neuronal surface. The increase of *tau* protein in specific regions of AD patients can potentially lead to neuronal iron retention by decreasing the number of APP on the cell surface (242).

1.5.2.2.2 The role of iron in Parkinson's diseases

PD is clinically manifested by the degeneration of the dopaminergic neurons in the substantia nigra pars compacta (SNpc) (228), to which chemical properties of iron have been linked (5). Under normal physiological condition, iron distribution within the brain is cell-type dependent and iron is found most abundant in regions rich in dopaminergic neurons in globus pallidus and SN of the basal ganglia (143, 244-246). However, an augmented iron level was demonstrated in SN in PD by studies employing different techniques as compared to age-matched controls (247, 248). Furthermore, the iron changes observed in SN in PD exhibits a shift of the Fe^{3+} : Fe^{2+} ratio from 2 : 1 in normal subjects to 1 : 2 in PD (249, 250). This abnormal deposition of iron in the brains of PD patients reflects a dysfunction of brain iron homeostasis (245, 248, 251). To date, the mechanism behind the altered iron level in PD, however, remains an enigma.

A growing body of evidence has suggested that the ability to sequester the excess redox active metals in the brain has been compromised in PD patients. In healthy

individuals, excess iron in the brain can be sequestered in ferritin and neuromelanin. Approximately half of the total neuromelanin is saturated with iron, suggesting a neuroprotective role. As brain iron content is found to be increased in PD as compared to normal subjects, the normal physiological response would be an up-regulation of ferritin and neuromelanin expression in PD. However, a marked reduction of both ferritin (248, 251) and neuromelanin (252) coupled with the alteration of neuromelanin structure was demonstrated in PD patients (33) and may compromise their abilities to sequester the redox active metal, leading to the accumulation of free iron that is able to produce free radicals, ultimately resulting in cell death.

Iron is also shown to be associated with the hallmark of PD, Lewy bodies, which are formed by the aggregation of intracellular, eosinophilic protein. They mainly consist of α-synuclein and are observed in dopaminergic neurons, axons, and synapses of SN (253). The aggregation of α-synuclein was shown to be promoted by iron (254, 255). Previous studies reveal that the removal of free iron with the iron chelators desferrioxamine can block the aggregation of α-synuclein (256, 257). In addition, α-synuclein can exacerbate oxidative damage via the generation of $OH^{\bullet}$, triggering the PUFA peroxidation, promoting the formation of HNE, a reliable oxidative stress marker, which was identified immunohistochemically to be present in Lewy bodies in PD (166).

PD is characterized by the loss of dopamine-secreting neurons in SN. Although iron is a pivotal cofactor of tyrosine hydroxylase and monoamine oxidase, both of which are important for dopamine metabolism (228), iron can also promote the oxidation of dopamine that may lead to oxidative stress via the generation of hydrogen peroxide catalyzed by iron. Furthermore, iron is able to catalyze the conversion of excess dopamine to neuromelanin, a redox active iron sequester with a high affinity for Fe^{3+}. Neuromelanin tends to become a pro-oxidant when bound to excess Fe^{3+}, converting Fe^{3+} back to Fe^{2+}, which is then released due to its weak affinity. The released Fe^{2+} thus increases the fraction of iron participating in the ROS-generating reactions.

1.5.3 Dietary iron and neurodegeneration

Neurodegeneration, accounting for the major impediment of healthy aging, can be influenced by numerous factors namely genetic factors, environmental factors, and life style factors. In the absence of effective curative treatments for NDD like AD and PD at present, preventive measures are of significance to lessen the disease burden. The potential effect of nutrition has become a topic of increasing scientific and public interest (12, 258, 259). In light of the effect of dietary iron on brain iron and that iron is implicated in the pathogenesis of AD/PD, the role of dietary iron in the development of AD/PD starts to gain research interest. Even after age correction, the prevalence of the age-related AD and PD still increases (6, 7).

This increasing trend could be attributable to the worldwide rising affluence, which shifted the diet paradigms to a high-iron based pattern – an increased dietary intake of highly bioavailable form of iron (red meat, iron-fortified food and iron supplements) (8). Evolutionary, the human body is virtually a closed system for iron with minimal habitual losses (117) to store iron for reproduction as iron is vital for life (260). With increased dietary iron intake, high iron stores might result from body iron accumulation if ingested dietary iron overcorrects for habitual losses.

High iron stores, however, is associated with increased oxidative stress in the body, which can accelerate the aging process (214, 261, 262). Data showed that abnormally high body iron stores were observed in approximately 10% westerners for various reasons, e.g. genetics, diet and others (263). Whether high body iron stores are associated with higher risk of NDD, however, remains unclear (264). But studies demonstrated that individuals with iron metabolism protein encoding gene variants (hemochromatosis H63D; HFE H63D) have higher iron stores, higher brain iron levels (265) and shorter life expectancy (266).High body iron store, therefore, might be related to increased iron accumulation in the brain, which is implicated in age-related neurodegeneration (267). The understanding of the effect of dietary iron on adult brain iron and its implication in the development of AD/PD are therefore, of utmost importance.

1.5.3.1 The effect of high dietary iron intake on brain iron homeostasis

Some researchers demonstrated that, unlike the liver (268), moderate dietary iron supplementation had minimal effect on brain iron content of both young animals (269, 270) and adult animals (271, 272). However, extremely high dietary iron can induce a detectable increase in total brain iron content (270) as well as regional brain iron of young rats (cortex, hippocampus, striatum and substantia nigra) (273). The abovementioned observations suggest that brain iron is highly regulated even if dietary iron supply is moderately high (<5 g per kg body weight per day); however, the brain iron regulative system is compromised when dietary iron intake is extreme (>10 g iron per kg body weight per day). This was further supported by the observation that increased glutathione levels (antioxidant defense) were associated with moderately high iron intake whereas reduced glutathione levels were linked with extremely high-iron diet (274).

The high tolerance of brain iron in response to high dietary iron intakes can be basically attributed to the tight regulation of iron transport through the BBB. It was suggested that the expressions of TfR as well as TfR mRNA in endothelial cells were decreased in response to dietary iron overload (273, 275). Alternatively, similar to the response observed in low-iron diet (166), in the event of high peripheral iron supply, the brain might regulate the brain iron uptake via a slower TfR turnover in the brain capillary endothelial cells as compared to normal body iron status.

Besides the changes in brain iron uptake, high dietary iron may result in subtle changes in other iron-relevant gene and protein expressions in the brain, e.g. an elevated level of ferritin and a decreased level of Tf (188). In addition, microarray analysis of mouse brain gene expression showed that transcripts for IRP1 decreased and transcripts for L-ferritin increased in response to high dietary iron (263). On the contrary, another study demonstrated that ferritin expressions were not altered by dietary iron overload (26).

1.5.3.2 The effect of systemic iron deficiency on brain iron homeostasis

As iron deficiency and iron-deficiency anemia remain severe nutritional problems worldwide among infants and adolescents, the effect of iron-depleted diet on brain iron has been extensively studied during the developmental stage of humans (32, 152) and animals (176, 276-279), but much less during adulthood.

In light of the role of iron in neuronal function and metabolism, the lack of iron in the infant diet was reported to lead to the delay of neuronal development as a result of alterations in neurotransmitter synthesis, myelin formation and other iron iron-involved neuronal processes (152).

Animal studies demonstrated that dietary restriction on young animals resulted in a decrease in brain iron content as well as ferritin level (277, 278, 280). The brain iron, however, is less responsive to dietary iron alteration than liver iron, the level of which was largely reduced (174). But brain iron repletion is much slower than that of liver, probably due to the slower iron turnover rate of brain (174, 176,

276). Besides the decrease in brain ferritin levels to maintain brain iron homeostasis in the event of low body iron status, the brain also increases the Tf levels to accelerate brain iron transport (277), especially in hippocampus (281).

The uptake of brain iron is highly regulated upon entering the BBB via the TfR-dependent endocytosis pathway. Although expression of TfR in endothelial cells in response to low dietary iron is still not completely understood, it was shown that brain iron uptake was greater in iron-deficient animals than that in controls (169, 282). It was revealed that an increased number of TfR in brain capillary endothelial cells was observed in iron-deficient animals (74, 275). In addition, TfR turnover rate was found to be elevated by the brain iron regulation system to cope with low body iron status (26, 166).

Different from the early stage of life when iron is in high demand for neuronal development in the brain, brain requirements are much lower later in life. However, as the brain is designed to conserve its iron, the iron obtained in the early stage might be largely retained within the brain. This concept is supported by the observation of age-related iron accumulation in different brain regions (203). In adults, the body might be less sensitive to the alteration of dietary restriction as previous studies reported that total body iron store increased with age (283) and potentially had higher tolerance for low-iron diet. This was reflected by relatively constant brain iron content in adult rats treated with iron-deficient diet as compared to the control (280).

1.5.3.3 Dietary iron and risks of Alzheimer's and Parkinson's diseases

In light of the above-discussed effect of dietary iron on brain iron, the relationship between dietary iron and the development of AD/PD is worth investigating.

Albeit relationships between the diet and cognitive decline or AD/PD have been extensively investigated in previous epidemiological studies, research focus lied largely on the combined effect of dietary factors (284-286). Very few studies investigated the effect of a specific dietary component such as iron on the development of AD/PD.

Most epidemiological studies revealed that dietary iron intake correlates with cognitive decline or risks of contracting AD/PD while a few studies could not find such a correlation or found an opposite effect. A study conducted in Japan has shown that higher iron intakes have a protective effect against PD (12) while other studies suggest that high dietary iron intake may contribute to the risk of developing PD (9-11). Interestingly, data obtained by Logroscino et al. (2008) failed to support an association between total iron consumption and risk of PD but suggested that a diet containing high non-heme iron increases the risk of PD (13). With regard to AD, it was proposed that excessive iron intake should be avoided in order to prevent AD (14, 287) whereas findings reported by Ortega et al. (1997) suggest that increasing iron intake may be advisable not only to improve cognitive function but also to improve the general health of the elderly (15). However,

epidemiological studies are chronically sensitive to unidentified confounding factors which may explain contradictory findings.

In contrast to epidemiological studies, animal studies point to a clearer correlation between dietary iron intake and risks of age-related NDD. Arruda et al. (2013) proposed that iron supplementation accelerates the aging process whereas iron restriction retards it (268). In line with this finding, Shoham et al. (2004) reported that nutritional iron deprivation attenuates the neurotoxicity induced in rats (288). As progressive neurodegenerative diseases do not afflict rats or mice (289), researchers commonly induce the disease-like symptoms in a rodent model by the injection of neurotoxins (e.g. 6-hydroxydopamine (6-OHDA) or 1-methyl-4-phenyl-1,2,3,6-tetrapyridine (MPTP) for PD) or use transgenic mouse models (e.g. Tg2546 mice generated for AD based on double mutation in *APP* gene) to test new neuroprotective agents or strategies (21, 290, 291).

The results obtained from dietary iron manipulation studies in animal models of AD/PD suggest that iron-loaded diet shall be avoided for the prevention of AD/PD. In MPTP-treated mice, researchers found that an iron-loaded diet contributed to the etiology of PD (292, 293). In addition, dietary iron restriction protected the mice against PD-inducing insults but the essential role of iron in neuron production and dopamine synthesis should also be taken into consideration (290, 294). In a transgenic mouse model of AD, spatial memory impairment was observed in the iron supplemented group as compared to the control group (295).

1.5.3.4 Strategies for reducing brain iron content

In consideration of the protective effect of iron deprivation on PD/AD, clinical iron chelators (e.g. clioquinol, VK-28, M30 and desferrioxamine etc.) have been tested for their efficacy to alleviate disease symptoms of AD/PD both in animal models and in clinical trials (16-21, 296-299). The results obtained from these studies are promising. However, problems accompanying iron-chelator treatment are emerging: 1) the side effects of the long-term treatment, e.g. iron chelators interact with other metabolic pathways in the body and thus affect the homeostasis of the interacting substances; 2) the toxicity of the inactive iron chelators deposited in the body - chelators are supposed to be designed to scavenge free iron and be excreted them safely through urine; 3) the sizes of the iron chelators are required to be small enough to cross the BBB to target the labile iron in the brain.

In light of the current obstacles in the application of clinical iron chelators, dietary iron chelators/free radical scavengers/antioxidants/iron absorptive inhibitors (phytic acid in legumes/cereals/seeds and polyphenols in tea) can serve as alternatives in the prevention of AD/PD or to alleviate the symptoms (22, 23, 300-305).

In line with previous findings that tea consumption is able to lower the risk of AD/PD (302, 306), it has been extensively reported that polyphenolic compounds (22, 301, 305, 307, 308) present in tea have the ability to penetrate the BBB (244,

304) and are proven to be effective in neuroprotection. However, as compared to green tea, black tea which accounts for 80% tea consumption worldwide (309), received much less research attention. The differences between these two types of tea are the distinct multimeric polyphenols (thearubigins and theaflavins) present in black tea as a result of the oxidation and fermentation of catechins, the processes of which are absent in green tea production (23). As theaflavins are the strongest antioxidants among catechins (310) and black tea is a more potent inhibitor in iron absorption than green tea (311), black tea consumption, not green tea, is inversely correlated with risks of PD.

Phytic acid, enriched in legumes and seeds, is an effective iron-chelating agent, promoting the oxidation of Fe^{2+} to Fe^{3+} but suppressing the hydroxyl radical formation catalyzed by iron (312). Studies both *in vivo* and *in vitro* demonstrated that phytic acid protects the neurons against dopaminergic cellular apoptosis (300) and has beneficial effect on amyloid-β pathology (313).

On the whole, a majority of evidences indicate that dietary iron can serve as a possible intervention approach to prevent AD/PD or delay their onset while some other studies raised doubts on the effect of dietary iron. The conflicting statements may rise from the incomplete understanding of the role of dietary iron on brain iron homeostasis.

Chapter 2 Methodology

Due to limited information on the effect of dietary iron intake on brain iron balance in adulthood, a novel technique was developed in this project for long-term tracing of dietary iron into brain in adult rats.

There are several reasons why rats were chosen as a model organism, one of them is the large library of neurological information of rats (314). Furthermore, iron metabolism and the sequence of events in iron transport to the rat brain share many common features with those of humans and connections can easily be made (28, 315). Having a life-span of 2-3 years, the rat is also among the shortest-lived mammals (316). This makes rats ideal for long-term feeding experiments in relation to ageing processes. In fact, the observational period of 4 months in rats in our experiments is equivalent to approximately 7-10 human years (317). Mice can also be used as a model organism to study long-term dietary iron effect on brain. However, due to the small size of the animal, the amount of iron inside the mouse brain is limited and thus requires extremely demanding technique for quantification. It is therefore less suitable for iron tracing studies. Despite all the listed advantages of rat models, data obtained from rat studies still requires extremely careful interpretation as humans and rats are still different organisms.

In the conducted experiments, we were interested to understand how dietary iron intake affects brain iron accumulation during young adulthood as iron accumulation at this stage of life might be related to the development of AD/PD at

advanced age. The rate of whole brain iron accumulation in humans was reported to increase steeply during the first two decades of life, slow down during the third and fourth decades and reach a "plateau" thereafter or the increment is minimal (203). A similar trend was also observed in rats and the increment slows down at about the fourth month of life (172, 275, 318-320). Adult rats that are 6-8-month old were therefore chosen, corresponding to an age of twenty-odd human years. In this project, stable isotope techniques were used to trace the fate of dietary iron and to investigate the effect of dietary iron intake on brain iron at the systemic level.

2.1 The application of isotope tracing techniques in nutritional studies

2.1.1 Stable isotopes versus radioactive isotopes

Isotopes have been widely used as tracers. The use of isotopes as tracers in metabolic research can be traced back to 1923 (321). Hevesy published the first study on the application of radioactive isotopes in studying metabolic processes of plant in 1923. He used the naturally radioactive ^{212}Pb as radioactive tracer to follow the absorption and translocation of lead in the plant. Later in 1942, the first tracer study to investigate mineral metabolism in animals was conducted using a radioactive iron isotope – ^{59}Fe (322). The application of radioisotopes was soon extended to human studies (323). With the increasing availability of enriched stable isotopes of minerals after the Manhattan Project during World War II, the use of stable-isotope tracer started to gain popularity in mineral metabolic

research (324). The use of stable-isotope tracer was further expanded in the last few decades with the advances in mass spectrometric instrumentation for providing highly accurate and precise isotope ratio measurement.

With regard to the study of iron metabolism in the body, both radioisotopes and stable isotopes are commonly used as tracers; however, both types of tracers have their own merits and limitations, which are summarized in Table 2-1 (325).

Table 2-1 Merits and limitations of the use of radioisotopes and stable isotopes as metabolic tracers
(This table is modified from Patterson et al. (2001) (324))

	Radioisotopes	**Enriched stable isotopes**
Safety	Potential risks for the subjects and the researchers	No risks
Dose	True tracers, relatively lower dose	Sufficient amounts must be given to be detectable
Study time	Dependent on the half-life of the radioisotope	No time restrictions
Sample storage time	Dependent on the half-life of the radioisotope	No time restrictions
Study design	One radioisotope is generally given	Multiple isotopes of an element and/or isotopes of different elements can be given simultaneously
Cost	Relatively inexpensive	Generally expensive
Analysis and Detection	Direct quantification via the detection of emitting particles and/or gamma rays; Whole-body counting allows *in vivo* measurement; Less demanding for instruments and researchers due to good measurement sensitivity.	Indirect quantification via the induced changes in isotopic abundances; Whole-body counting not available; Extensive sample preparation; Sophisticated instruments and technicians are required for good measurements.

In most nutritional studies, dietary iron is the tracee and iron isotopes can serve as tracers. Naturally occurring iron consists of four stable isotopes, ^{54}Fe, ^{56}Fe, ^{57}Fe and ^{58}Fe with their natural abundances as 5.85%, 91.75%, 2.12% and 0.28% respectively (326). The enriched forms of the isotopes with lower natural

abundances can be used as tracers, e.g. enriched ^{54}Fe, ^{57}Fe and ^{58}Fe. In addition, iron has a number of radioactive isotopes, out of which ^{55}Fe (67, 327, 328) and ^{59}Fe (176, 329, 330) are widely used as tracers due to their relatively long half-lives. The former has a half-life of 2.73 years and emits X-rays in the electron capture decay process, whereas the latter has a half-life of 44.5 days and emits γ-radiation in the β-decay process (331). The strong penetrating power of γ-radiation has enabled a wider use of ^{59}Fe as tracers in this field as compared to ^{55}Fe.

2.1.2 The application of radioisotopes to assess brain iron metabolism

Brain iron uptake mechanisms and underlying kinetics have been extensively investigated using radioisotopes. These studies were, however, largely based on the single administration of a radiotracer (^{59}Fe) to groups of young animals, usually through intravenous or peritoneal injection, and sacrifice of animals some time after dose administration (Table 2-2). While this technique permit to study short-term iron turnover in the brain, it is less suitable to assess the effect of diet on brain iron content as well as brain iron balance due to the short half-lives of the radiotracers. For a single dose, the time span between injection and sampling must be long enough to take brain iron turnover into account. Moreover, tracer administration by injection circumvents the intestine as the main regulatory barrier for maintaining body iron homeostasis. In consequence, this approach does not take a possible adaptive response at the level of intestinal absorption into account.

Unlike radioisotopes, stable isotope techniques can be applied in long term nutritional studies and pose no risks to the involved personnel (324). However, to the best of our knowledge, long-term studies involving continuous feeding of stable isotopes have not been conducted so far. Such an approach allows not only to study brain iron uptake as in earlier experiments but also, for the first time ever, to study efflux of iron from brain that has been taken up earlier by the brain through physiological mechanisms.

Table 2-2 Summary of studies on brain iron uptake using radioactive isotope techniques on animal models*.

Authors/Years	Species	Iron Status	Age/wt.	Chemical State	Type of Injection	Observational Period	Way of Sacrifice	Observation/Conclusion
Dallman and Spirito, 1977 (176)	Male SD rats	Normal	2-59 days	$^{59}FeCl_3$	I.P.	24 hrs	Perfusion	Iron uptake by rat brain increased from Day 3 to 15, and dropped sharply from Day 15 to 35; Brain iron content thereafter remained relatively constant.
			15 days	$^{59}FeCl_3$		6 -135 days	Perfusion	Slow brain iron turnover: virtually no loss of counts from the brain from 50-150 days
			35 days	$^{59}FeCl_3$		6 - 80 days	Perfusion	
Banks et.al., 1988 (173)	Male ICR mice	Normal	17-25g	$^{59}Fe^{3+}$	I.V.	90 mins	Decapitation	Iron and Tf have transport systems across the BBB that are bidirectional and slow
Dwork et.al., 1990 (332)	SD rats	Normal	15 days	$^{59}FeCl_3$	I.P.	2-57 days	Perfusion	Iron acquired by the rat brain at 15-days was sequestered but translocated from different areas with development.
			28 days			14 -28 days		
			42 days			14 days		
Taylor and Morgan, 1990 (172)	Wistar rats	Normal	7-70 days	$^{59}FeCl_3$	I.V.	2 hrs	Perfusion	Iron uptake in to the rat brain climbed rapidly during the first 15 days of life, reaching the peakat the 15th day and declined thereafter.
			15 days	[^{59}Fe-^{125}I] Tf	I.V.	0-312 hrs	Perfusion	Iron transport into the brain in the 15-day rat is a unidirectional process
Taylor et.al., 1991 (275)	Wistar rats	ID/IL/normal	15-63 days	[^{59}Fe-^{125}I] Tf	I.V.	2 hrs	Perfusion	1. Iron uptake is greater in ID rats and lower in IO rats 2. The expression of TfR on the brain capillary endothelial cells is highly sensitive to the body iron status.
Crowe and Morgan, 1992 (169)	Wistar rats	Normal	15 - 63 days	[^{59}Fe-^{125}I] Tf	I.V.	6 hrs	Perfusion Non-perfusion	1. Iron uptake by the rat brain is unidirectional 2. Iron uptake into the brain and CSF decreased with age 3. Iron uptake by the brain was greater in the ID rats than in controls at the age of 21 days.
			63 days			56 days	Non-perfusion	
		ID	18 days			56 days	Non-perfusion	
			21 days			6 hrs	Perfusion	
Morris et.al., 1992 (333)	Wistar Rat	Normal	650-700g	$^{59}FeCl_3$	I.V.	5 min-8 days	Decapitation	1. The BBB permeability to iron is ~15 times higher than to Tf; 2. Regional iron distribution by autography and histochemistry 3. The route of brain iron uptake

*Abbreviations: SD: Sprague Dawley; WT: Wild-type; HP: hypertransferrinemic; IL: iron loaded; ID: iron deficient; IV: intravenous; IP: intraperitoneal.

Table 2-2 (continued) Summary of studies on brain iron uptake using radioactive isotope techniques on animal models*.

Authors/Years	Species	Iron Status	Age/wt.	Chemical State	Type of Injection	Observational Period	Way of Sacrifice	Observation/Conclusion
Ueda and Bradbury, 1992 (334)	Male rats and mice	Normal	N/A	$^{59}FeCl_2$	Intravenous infusion	N/A	Decapitation followed by washing of vascular space	Iron influx into the brain is dependent on TfR
Ueda et.al., 1993 (165)	Wistar Rats To mice	Normal	Adult Rats (300g) Adult Mice (35g)	[^{59}Fe] Tf or ^{59}Fe-ascorbic acid	Intravenous infusion	3-4 hrs	Decapitation followed by washing of vascular space	Iron uptake by the mouse brain occurred in the following order: cerebellum > brainstem > frontal cerebral cortex > parietal cortex > occipital cortex > hippocampus > caudate nucleus.
	Wistar/ HP rats	Normal	Young rats (100-160g)	^{59}Fe-ascorbic acid				Although iron transport across the BBB is largely TfR dependent, NTBI pathways are also available
Crowe and Morgan, 1994 (335)	Wistar rats (both sexes)	Iron chelator	15 days	[^{59}Fe-^{125}I] Tf	I.V.	2/24 hrs	Perfusion	1. Once ^{59}Fe had entered the brain no chelator used was able to mediate its release 2.Similar iron uptake mechanisms for femur and brain 3. Certain chelators can reduce brain iron uptake.
	Male Wistar rats		63 days					
Dwork, 1995 (336)	Male Wistar rats	ID diet (Age 28 - 56 days)	14 days	$^{59}FeCl_3$	I.P. on Day 14	42 days	Perfusion	Sequestration of cerebral iron acquired at age 2 wks and its distribution were not affected by ID diet
		Normal	28 days		I.P. on Day 28	14 days		Regional iron distribution
		ID diet (Age 21 - 49 days)	21 days		I.P. on Day 50	13 days		The choroid plexus might buffer the brain against rapid rises in plasma iron content.
Crowe and Morgan, 1996 (269)	Wistar rats	ID (lead/non-lead diet)	15 - 63 days	[^{59}Fe-^{125}I] Tf	I.V.	2 hrs	Perfusion	1. ID rats had lower liver iron levels and elevated brain iron uptake as compared to the controls. 2. The level of lead intoxication produced in this investigation had no impact on iron uptake by the brain

*Abbreviations: SD: Sprague Dawley; WT: Wild-type; HP: hypertransferrinemic; IL: iron loaded; ID: iron deficient; IV: intravenous; IP: intraperitoneal.

Table 2-2 (continued) Summary of studies on brain iron uptake using radioactive isotope techniques on animal models*.

Authors/Years	Species	Iron Status	Age/wt.	Chemical State	Type of Injection	Observational Period	Way of Sacrifice	Observation/Conclusion
Moos and Morgan, 1998 (178)	Male Wistar rats	Normal	15-56 days	[^{59}Fe-^{125}I] Tf	I.V.	2 hrs	Perfusion	NTBI is present extracellularly in CSF and probably in brain interstitium
Moos and Morgan, 1998 (175)	Male Wistar rats	Normal	50 days (180g)7 days	[^{59}Fe-^{125}I] Tf	Injection into lateral cerebral ventricle	4-72 hrs	Perfusion	1. Injected Tf disappeared after 24 hrs, whereas 18% ^{59}Fe retained in brain parenchyma in 50-day rats. 2 .^{59}Fe was remained to a higher degree in young rats than in adult rats.
Malecki et.al., 1999 (337)	HP and WT mice	Normal/IL	12 wks	$^{59}FeCl_3$	I.V.	1 hr/1 wk	Perfusion	Comparison of regional distribution of iron and manganese
Takeda et.al., 2001 (338)	HP and WT mice	Normal/IL	7 days	$^{59}FeCl_3$	Subcutaneous injection	24 hrs	Decapitation	1.Brain iron distribution is changed by Tf deficiency; 2.Iron abnormally accumulates in the brain of HP mice
Takeda et.al., 2002 (339)	Male ddY mice	Normal/IL	10 wk	$^{59}FeCl_3$	I.V.	24 hrs	Decapitation	The concentrations of ^{59}Fe in all brain regions tested of iron-loaded mice were approximately 40–50% of those of control mice except the choroid plexus, in which ^{59}Fe concentration was equal
Deane et.al., 2004 (164)	Male SD rats	Normal	9-12 wks	^{59}Fe; [^{59}Fe]Tf	Infusion	5-30 mins	Perfusion	For iron delivery to the CNS, the transport of circulating Tf-bound and free iron could be equally important
Moos and Morgan, 2004 (145)	DMT1-mutated Belgrade rat and WT rats	Normal/ID	17-19 days; 10 wks	[^{59}Fe-^{125}I] Tf	I.V.	120 mins	Perfusion	Brain iron transport and distributional pattern of DMT1

*Abbreviations: SD: Sprague Dawley; WT: Wild-type; HP: hypertransferrinemic; IL: iron loaded; ID: iron deficient; IV: intravenous; IP: intraperitoneal.

Table 2-2 (continued) Summary of studies on brain iron uptake using radioactive isotope techniques on animal models*

Authors/Years	Species	Iron Status	Age/wt.	Chemical State	Type of Injection	Observational Period	Way of Sacrifice	Observation/Conclusion
Beard et.al., 2005 (282)	HP and WT mice	Normal diet/ID diet (8 wks feeding)	~11-12 wks	$^{59}FeCl_3$	I.V.	24 hrs	Perfusion	1. Iron uptake by the brain may be constitutive and independent of plasma Tf, Tf saturation, or regional brain iron concentration; 2. The data is supportive of a NTBI pathway.
Moos et.al., 2006 (191)	DMT1-mutated Belgrade rats	Normal/ID	16 days; 10 wks	[^{59}Fe-^{125}I] Tf	I.V.	5-60 mins	Perfusion	Brain capillary endothelial cells probably mediate iron delivery into the brain by separating iron from Tf without the involvement of DMT1
Lopes et.al., 2010 (171)	C57BL6 mice	Normal/IL/IO diet (5 wks feeding)	25 g	^{59}Fenitrate in complex with nitrolotria-ceticacid	I.V.	12 hrs-28 days	Non-perfusion	A kinematic model of the dynamic system of iron pools and fluxes, including the brain

*Abbreviations: SD: Sprague Dawley; WT: Wild-type; HP: hypertransferrinemic; IL: iron loaded; ID: iron deficient; IV: intravenous; IP: intraperitoneal.

2.2 The use of stable isotopes as tracers

To trace iron from diet in and out of brain or other tissues in an animal model, the iron in the test diet (tracee) has to be labeled isotopically. When using enriched stable isotopes as labels (tracers), they are not distinguishable from the stable isotopes in the sample due to their identical physical and chemical characteristics (340). The amount of iron tracer retained in the brain/other tissues, therefore, can only be quantified indirectly via the induced changes in the iron isotopic abundances in the sample by the tracer addition. As isotopic abundances in nature are highly constant, the greater amount of the tracer present in the sample, the more the isotopic abundances are altered (341). The underlying mathematical concept is known as the 'isotope dilution' principle (see section 2.2.1). With the calculated amount of iron tracer detected in the brain and the ratio of the tracer to tracee in the diet, the amount of iron in the brain originating from the diet can be obtained.

The number of stable isotopic labels in isotope dilution that can be used in parallel is determined by the number of stable isotopes that exists for a given element (341). For an element having n stable isotopes, (n-1) isotopic labels are available. For iron with its four stable isotopes ^{54}Fe, ^{56}Fe, ^{57}Fe and ^{58}Fe, three isotopic labels can be used in parallel. Since ^{56}Fe is the most abundant iron isotope, it is more difficult to induce changes in its abundance than other less abundant isotopes. ^{54}Fe, ^{57}Fe and ^{58}Fe are therefore commonly used as isotopic labels.

2.2.1 Study Design

In this project, enriched iron isotopes were administered continuously via the drinking water (see Section 3.3.1), which was fed together with feed to the rats for a period of 4 to 6 months (see Chapter 3, 4 and 5). The amount of consumed tracer in the drinking water was determined by weighing the drinking bottle before and after water consumption. All drinking bottles were checked for water dripping or leaking before use. Monthly blood samples were taken for isotopic analysis to assess the change of iron absorption rate with time. At the end of each study, rats were hyper-perfused to remove the blood from the brain as well as other organs to minimize interferences between blood iron and tissue iron. Relevant tissues were harvested and stored for iron quantification and isotopic analysis.

2.2.2 Isotope Dilution Mass Spectrometry (IDMS)

Quantification of stable isotope tracers in the tissues or body fluids can be performed with high precision and accuracy using Isotope Dilution Mass Spectrometry (IDMS) which is derived from the isotope dilution principle and originally developed to quantify elements (342, 343)

2.2.2.1 Quantification of iron content in tissues using IDMS

To assess changes in tissue iron induced by dietary iron in tracing studies, an accurate assessment of total tissue iron content is as important as the quantification of the tracer uptake by the brain so that the relative brain iron uptake (the amount of iron uptake by the tissue from diet relative to total brain iron) can be reliably determined. Tissue iron contents in our studies were

therefore analyzed using IDMS via isotope ratio analysis (see Chapter 4). IDMS is widely considered as a reference technique for elemental analysis as all sources of analytical uncertainty can be identified and quantitatively assessed (342, 344, 345). Although more tedious steps are required, this approach permits a more accurate assessment of iron contents than what can be achieved by conventional elemental analysis using colorimetry (346), inductively coupled plasma atomic emission spectroscopy (ICP-AES), atomic absorption spectrometry (AAS), or inductively coupled plasma mass spectrometry (ICP-MS).

The basic principle of IDMS is illustrated in Fig. 2-1. In IDMS, the unknown amount of the element in the sample can be determined by the addition of a known amount of a stable isotope tracer (enriched isotope [mass number X] of the element) to alter the abundances of the natural isotopes in the sample (340, 342). The isotopic composition change in the sample is in proportion to the mixing ratio of the natural element (n_{nat}) in the sample and the tracer (n_{iso}). This mixing ratio can be obtained from the abundances (a) of the isotope with mass number X and a reference isotope with mass number W of both the tracer ($^{X}a_{iso}$ and $^{W}a_{iso}$) and the natural element ($^{X}a_{nat}$ and $^{W}a_{nat}$) together with the measured isotope ratio of the mixture $^{X/W}R_{sample}$ (Eqn. (4)). Since the amount of the stable isotope tracer added (n_{iso}) is known, the amount of natural iron in the sample (n_{nat}) can easily be obtained. For example, a known amount of enriched ^{57}Fe can be added to native rat brain (rats that are not fed with enriched iron isotopes) prior to sample analysis to determine the exact amount of natural iron in the native rat brain, provided that

the mixture is homogenized (Eqn. (5). With regard to the brain samples obtained from the rats fed with enriched iron isotopes, the method for determination still follows the basic IDMS principle though the calculation is more complicated, which will be illustrated in detail in Chapter 4.

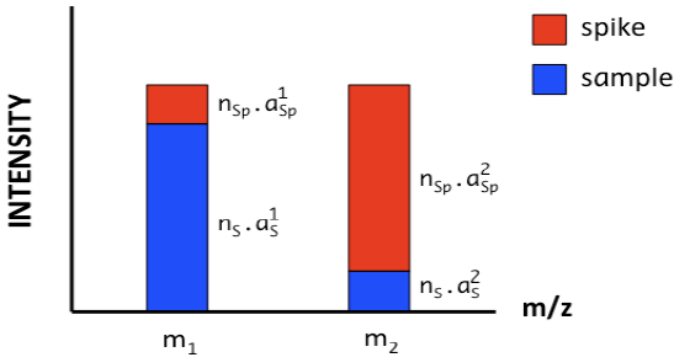

Fig. 2-1 The illustration of the principle of IDMS
In IDMS, to determine the element of interest in the sample (S), a known amount of an enriched stable isotope of that particular element (spike or Sp) is required to mix with the sample. Fig. 2-1 illustrates the schematic mass spectrum of an element with two isotopes (mass 1 and mass 2) of the mixture of the sample and the spike. In Fig. 2-1, **n** represents the number of atoms whereas **a** refers to the isotopic abundance. The amount ratio of sample and spike can be expressed as $(n_S \cdot a_S^{\ 1} + n_S \cdot a_S^{\ 2})/(n_{Sp} \cdot a_{Sp}^{\ 1} + n_{Sp} \cdot a_{Sp}^{\ 2})$.

$$\frac{n_{iso}}{n_{nat}} = \frac{{}^{X}a_{iso} - {}^{X/W}R_{sample} \cdot {}^{W}a_{iso}}{{}^{X/W}R_{sample} \cdot {}^{W}a_{nat} - {}^{X}a_{nat}} \quad (4)$$

$$\frac{n_{iso,57}}{n_{nat}} = \frac{{}^{57}a_{iso} - {}^{57/56}R_{sample} \cdot {}^{56}a_{iso,57}}{{}^{57/56}R_{sample} \cdot {}^{56}a_{nat} - {}^{56}a_{nat}} \quad (5)$$

2.2.3 Instrumentations for iron isotope ratio measurement

Since the first mass spectrometer was constructed by J.J. Thomson in 1912 to study the isotopic nature of neon (347), mass spectrometry has evolved as the primary, although not only, tool to measure the ratio of stable isotope abundances of an element. Thermal Ionization Mass Spectrometry (TIMS) and Multi-Collector Inductively Coupled Plasma Mass Spectrometry (MC-ICP-MS) are

currently the two most widely used methods for the determination of metal isotope ratios, both of which have their own merits and limitations.

2.2.3.1 Thermal Ionization Mass Spectrometry (TIMS)

TIMS has long been the reference technique for isotope ratio determinations at highest precision and accuracy (324, 348-350) and has been applied to many stable isotope studies for the determination of iron isotope ratios (351-354).

A TIMS is composed of three main components: an ion source where ions are produced, accelerated, and focused; a magnetic analyzer where ions are separated based on their mass-to-charge ratio; and one or more detectors for measuring beam intensities.

2.2.3.1.1 Filament arrangement

In an isotope ratio measurement by TIMS, the pre-treated sample is loaded on a filament made of a refectory metal, rhenium or tantalum, of high melting point. Two different filament configurations can be used for the thermal ionization process, single- or double-filament. A single-filament arrangement is preferred if evaporation and ionization of the element of interest take place at the same temperature. For elements that evaporate and ionize at different temperatures, use of a double-filament arrangement can be advantageous (see
Fig. 2-2) (348, 355). In the case of iron, a double-filament ion source made of rhenium is the configuration of choice due differences in the optimal evaporation and ionization temperature for FeF4- ion generation.

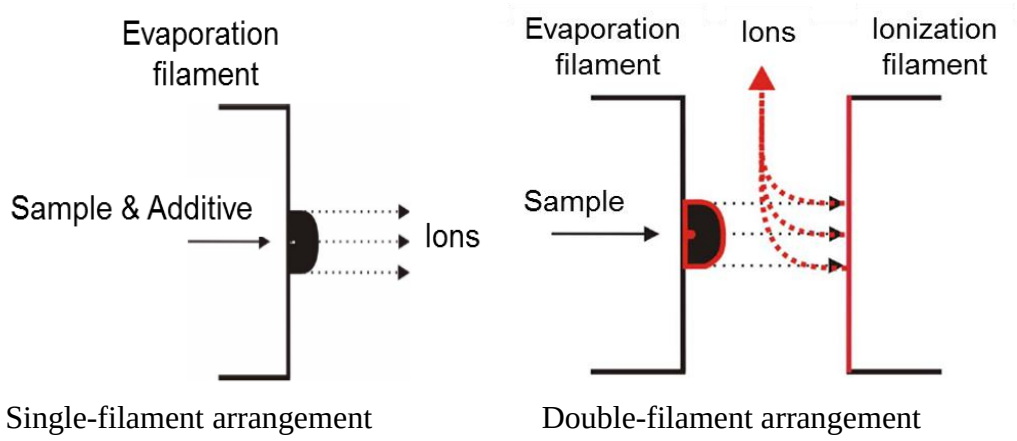

Fig. 2-2 Ion source configuration used in thermal ionization mass spectrometry
(Figure source: Triton Manual)

2.2.3.1.2 Principles of TIMS

In the ion source, the sample is evaporated and ionized by passing a current through a filament under vacuum (see Fig. 2-3). The ionization process is theoretically described by the Langmuir–Saha equation, which states that elements with a high ionization potential are ionized at higher temperatures than elements with low ionization potential (348). The generated ions move randomly and slowly, forming an ion cloud which are later focused into an ion beam by acceleration across an electrical potential gradient via a set of slits and plates at high voltage (up to 10,000V) (356). Ions are extracted out of the source by the first slit plate which has a potential just a few volts below 10,000 V. After passing the last slit which is at ground potential, ions that share the same charge will have the same velocity. Based on Lorentz force law and Newton's second law, the focused ion beam will be forced into different circular paths in the magnetic field,, the radius of which are dependent on the mass to charge ratio of the ions. The lighter the ions are, the smaller the radius and vice versa. Ions are commonly collected by Faraday cups inside which the ions flow to ground potential via a

large resistor (e.g. $10^{11}\Omega$ for the model used in the study). Several Faraday cup detectors can be set up such that the isotope beams are measured simultaneously to perform isotope ratio measurements at high precision (multi-collector TIMS). The ratio of the ions of different mass to charge ratio can be obtained via the measured ratio of ion currents in the respective detectors. For detection of low abundant isotope and for isotopic analysis of very small quantities of analyte, mass spectrometers with Faraday cup detectors can also be equipped with Secondary Electron Multipliers (SEM) to further extend the sensitivity of the instruments by several orders of magnitude (up to 10^4), either in current amplification or ion-counting modes (357). SEM is the most sensitive detectors for measuring extremely small ion current or particle count rates.

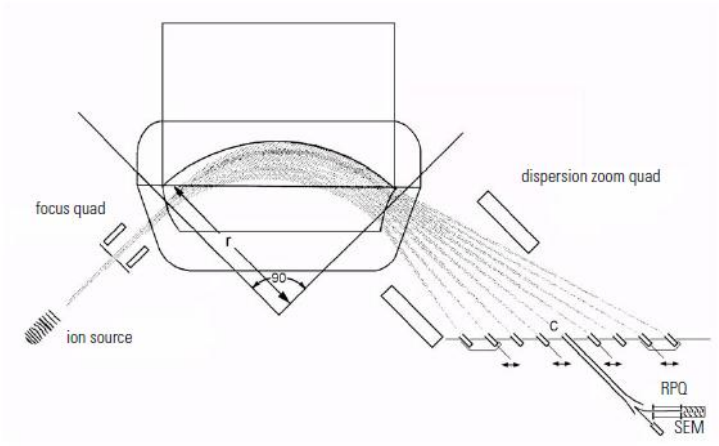

Fig. 2-3 Analyzer system of the TRITON
(Courtesy of Thermo Finnigan)

2.2.3.2 Multi-Collector Inductively Coupled Plasma Mass Spectrometry (MC-ICP-MS)

ICP-MS has been introduced as a new tool for elemental and isotopic analysis in the 1980s (358). During the past three decades, tremendous improvements have

been made on both the instrumentation and the methodology of iron isotope analysis of biological samples using ICP-MS (359, 360). This refers in particular to the advent of MC-ICP-MS (Fig. 2-4), which opened up the possibility for high-throughput isotope ratio measurements at high precision and sensitivity.

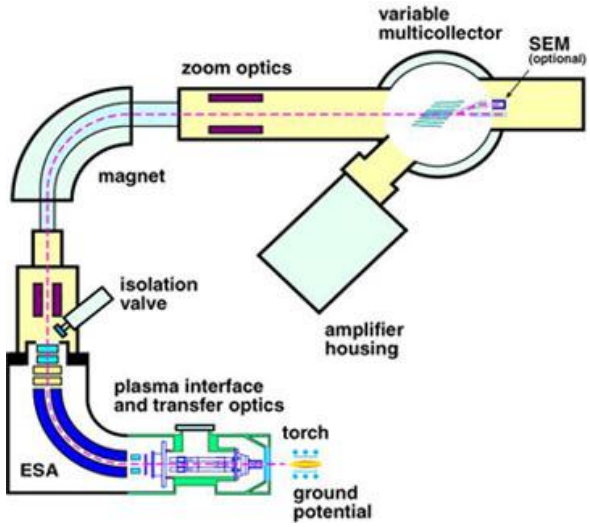

Fig. 2-4 Schematic of a Neptune MC-ICP-MS
(Courtesy of Thermo Finnigan)

The main difference between ICP-MS and TIMS is the ion source. Usually liquid samples are introduced into the high energy plasma by pneumatic or ultrasonic nebulization for ionization. The ions are later accelerated and focused into an ion beam for separation of ions by their mass to charge ratio (355). The ability to reach close to 100% ionization efficiency for nearly all the elements of the periodic table has contributed to the popularity of ICP-MS in isotope ratio mass spectrometry (349).

With regard to iron isotope ratio measurements, the accuracy and precision of the data obtained using ICP-MS is limited by isobaric and polyatomic interferences (Table 2-3) generated during the measurement either in the samples or through

chemical interactions in the plasma of the ICP (361, 362). For instance, the presence of calcium in incompletely purified biological samples can lead to the formation of oxygenated calcium molecular ions (e.g. $^{40}Ca^{18}O^{+}$, $^{42}Ca^{16}O^{+}$) showing the same nominal mass-to-charge ratio as the iron isotopes. Similarly, the use of the noble gas Ar in the plasma source system can produce Ar-based molecular ions (e.g. $^{40}Ar^{14}N^{+}$, $^{40}Ar^{18}O^{+}$). Besides interferences from molecular ions, trace amounts of Cr and Ni can also compromise the accuracy of isotope analysis of ^{54}Fe and ^{58}Fe due to their respective interfering ions $^{54}Cr^{+}$ and $^{58}Ni^{+}$ (362, 363)

Table 2-3 Interferences encountered in iron analysis by ICP-MS*

Isotope	Abundance (atom %)**	Interfering species
$^{54}Fe^{+}$	5.85	$^{54}Cr^{+}$, $^{40}Ar^{14}N^{+}$
$^{56}Fe^{+}$	91.75	$^{40}Ar^{16}N^{+}$, $^{40}Ca^{16}O^{+}$
$^{57}Fe^{+}$	2.12	$^{40}Ar^{16}N^{1}H^{+}$, $^{40}Ca^{16}O^{1}H^{+}$
$^{58}Fe^{+}$	0.28	$^{58}Ni^{+}$, $^{40}Ar^{18}O^{+}$, $^{40}Ca^{18}O^{+}$, $^{42}Ca^{16}O^{+}$

*Table source: Ingle et al. (2002) (350).
** Rosman *et al.* 1999 (326)

The double-focusing magnetic-sector technology applied to MC-ICP-MS offers the possibility to remove isobaric interferences to the biggest extent via the increased mass resolution (364, 365). The mass analyzer of double sector instrument consists of two analyzers, an electrostatic analyzer and a magnetic sector field. When combined together, the former filters out ions of the same energy while the latter separates them by their mass-to-charge ratio. By varying the slit width, mass resolution can be modified. In addition, interfering species can be removed by interacting with a cell gas in collision or reaction cells. 'Cool plasma' also facilitates the suppression of interfering effects. To further minimize

the effect of interfering ions, sample purification prior to analysis and mathematical corrections of the measured the isotope ratios can also be applied.

2.2.3.3 TIMS versus MC-ICP-MS

Modern high resolution MC-ICP-MS is now widely considered as the tool of choice for iron isotope ratio measurements of high accuracy and precision due to its flexible sample introduction system (either in solution or aerosol form) as well as the high ionization efficiency (366, 367). In contrast, TIMS requires the sample to be in the solid form and isolated from the matrix by a series of steps prior to the measurement.

Advantages of MC-ICP-MS, however, are balanced by unrecognized isobaric interferences and the larger mass fractionation of isotope in the ion source as compared to TIMS (368, 369, 370). Ideally, the measured isotope ratio should reflect the true isotope ratio of the sample. However, due to inevitable isotope fractionation occurring in the mass spectrometer during sample ionization, the measured isotope ratio inevitably deviates from the true ratio. Isotope fractionation thus becomes the limiting factor for isotope ratio measurement with high precision and accuracy by mass spectrometers (369). While matrix effects on isotope fractionation are minimal for TIMS, they can be significant for MC-ICP-MS. As a consequence, the element of interest must be separated from the sample matric for MC-ICP-MS analysis as in TIMS which reduces advantages in terms of analytical efforts. In addition, MC-ICP-MS is more susceptible to artifacts which requires more robust quality control measures and repeated analysis of samples in case of doubt.

Samples were analyzed in thesis by TIMS as the more robust technique delivering isotope ratio measurements on par with MC-ICP-MS in terms of precision. Both Positive TIMS (P-TIMS) and Negative TIMS (N-TIMS) have been used for iron isotope ratio analysis (9, 371-374). In P-TIMS, singly charged iron ions (e.g. $^{56}Fe^{+}$) represent the forms of the ionized isotopes to be detected. However, one drawback of this technique is that molecular ions with same nominal mass-to-charge ratio as the iron isotopes can be formed during the ionization process, e.g. $^{40}Ca^{18}O^{+}$ interferes with $^{58}Fe^{+}$. To achieve a better precision of iron isotope ratio measurement, Walczyk (1997) developed a technique using N-TIMS, in which iron isotopes were in the form of FeF_4^- (375). This technique offers a variety of advantages as compared to the conventional iron isotope ratio measurement by P-TIMS: a better control of mass-fractionation effect (375-376), the improved sensitivity as opposed to P-TIMS (377), as well as the capability to circumvent the problem of isobaric interferences using the monoisotopic fluoride (375).

Bibliography

1. Brookmeyer R, Johnson E, Ziegler-Graham K, & Arrighi HM (2007) Forecasting the global burden of Alzheimer's disease. *Alzheimers Dement* 3(3):186-191.
2. Dorsey ER, *et al.* (2007) Projected number of people with Parkinson disease in the most populous nations, 2005 through 2030. *Neurology* 68(5):384-386.
3. Prince M, Prina M, & Guerchet M (2013) World Alzheimer report: Journey of caring-an analysis of long-term care for dementia (Alzheimer's Disease International, London).
4. Bush AI (2013) The metal theory of Alzheimer's disease. *J Alzheimers Dis* 33:S277-S281.
5. Hare D, Austin C, & Doble P (2012) Quantification strategies for elemental imaging of biological samples using laser ablation-inductively coupled plasma-mass spectrometry. *Analyst* 137(7):1527-1537.
6. Kokmen E, Beard CM, OBrien PC, & Kurland LT (1996) Epidemiology of dementia in Rochester, Minnesota. *Mayo Clin Proc* 71(3):275-282.
7. Sekita A, *et al.* (2010) Trends in prevalence of Alzheimer's disease and vascular dementia in a Japanese community: the Hisayama Study. *Acta Psychiat Scand* 122(4):319-325.
8. FAO (2010) *The state of food and agriculture 2009: live stock in the balance* (Bernan Assoc).
9. Powers KM, *et al.* (2003) Parkinson's disease risks associated with dietary iron, manganese, and other nutrient intakes. *Neurology* 60(11):1761-1766.
10. Powers KM, *et al.* (2009) Dietary fats, cholesterol and iron as risk factors for Parkinson's disease. *Parkinsonism Relat D* 15(1):47-52.
11. Johnson CC, Gorell JM, Rybicki BA, Sanders K, & Peterson EL (1999) Adult nutrient intake as a risk factor for Parkinson's disease. *Int J Epidemiol* 28(6):1102-1109.
12. Miyake Y, *et al.* (2011) Dietary intake of metals and risk of Parkinson's disease: A case-control study in Japan. *J Neurol Sci* 306(1-2):98-102.
13. Logroscino G, Gao X, Chen HL, Wing A, & Ascherio A (2008) Dietary iron intake and risk of Parkinson's disease. *Am J Epidemiol* 168(12):1381-1388.
14. Grant WB (1997) Dietary links to Alzheimer's disease. *Alz Dis Rev* 2:42-55.
15. Ortega RM, *et al.* (1997) Dietary intake and cognitive function in a group of elderly people. *Am J Clin Nutr* 66(4):803-809.
16. Grunblatt E, Mandel S, & Youdim MBH (2000) MPTP and 6-hydroxydopamine-induced neurodegeneration as models for Parkinson's disease: neuroprotective strategies. *J Neurol* 247:95-102.
17. Betarbet R, Sherer TB, & Greenamyre JT (2002) Animal models of Parkinson's disease. *Bioessays* 24(4):308-318.
18. Bush AI (2002) Metal complexing agents as therapies for Alzheimer's disease. *Neurobiol Aging* 23(6):1031-1038.
19. Levenson CW (2003) Iron and Parkinson's disease: chelators to the rescue? *Nutr Rev* 61(9):311-313.
20. Ben Shachar D, Kahana N, Kampel V, Warshawsky A, & Youdim MBH (2004) Neuroprotection by a novel brain permeable iron chelator, VK-28, against 6-hydroxydopamine lession in rats. *Neuropharmacology* 46(2):254-263.
21. Schober A (2004) Classic toxin-induced animal models of Parkinson's disease: 6-OHDA and MPTP. *Cell Tissue Res* 318(1):215-224.

22. Levites Y, Weinreb O, Maor G, Youdim MBH, & Mandel S (2001) Green tea polyphenol (-)-epigallocatechin-3-gallate prevents N-methyl-4-phenyl-1,2,3,6-tetrahydropyridine-induced dopaminergic neurodegeneration. *J Neurochem* 78(5):1073-1082.
23. Tan LC, *et al.* (2008) Differential effects of black versus green tea on risk of Parkinson's disease in the Singapore Chinese Health Study. *Am J Epidemiol* 167(5):553-560.
24. Crichton RR (2009) Brain iron homeostasis and its perturbation in various neurodegenerative diseases. *Iron metabolism: from molecular mechanisms to clinical consequences*, ed Crichton RR (John Wiley & Sons), 3rd Ed, pp 371-372.
25. Gropper SAS, Smith JL, & Groff JL (2009) *Advanced nutrition and human metabolism* (Wadsworth Cengage Learning).
26. Moos T (2002) Brain iron homeostasis. *Dan Med Bull* 49(4):279-301.
27. Perutz MF (1979) Regulation of oxygen-affinity of hemoglobin - Influence of structure of the globin on the heme iron. *Annu Rev Biochem* 48:327-386.
28. Dallman PR (1986) Biochemical basis for the manifestations of iron deficiency. *Annu Rev Nutr* 6:13-40.
29. Beard JL (2001) Iron biology in immune function, muscle metabolism and neuronal functioning. *J Nutr* 131(2):568s-579s.
30. Rattehalli D, Pickard L, Tselepis C, Sharma N, & Iqbal TH (2013) Iron deficiency without anaemia: Do not wait for the haemoglobin to drop? *Health Policy and Technology* 2(1):45-58.
31. WHO (2002) *The world health report 2002* (WHO, Geneva), Reducing risks, promoting healthy life.
32. Lozoff B & Georgieff MK (2006) Iron deficiency and brain development. *Semin Pediatr Neurol* 13(3):158-165.
33. Sian-Hulsmann J, Mandel S, Youdim MBH, & Riederer P (2011) The relevance of iron in the pathogenesis of Parkinson's disease. *J Neurochem* 118(6):939-957.
34. De Domenico I, Ward DM, & Kaplan J (2008) Regulation of iron acquisition and storage: consequences for iron-linked disorders. *Nat Rev Mol Cell Bio* 9(1):72-81.
35. Andrews NC (2000) Iron metabolism: Iron deficiency and iron overload. *Annu Rev Genom Hum G* 1:75-98.
36. Galaris D, Mantzaris M, & Amorgianiotis C (2008) Oxidative stress and aging: the potential role of iron. *Horm-Int J Endocrino* 7(2):114-122.
37. Sies H & Cadenas E (1985) Oxidative stress - damage to intact-cells and organs. *Philos T Roy Soc B* 311(1152):617-631.
38. Chance B, Sies H, & Boveris A (1979) Hydroperoxide metabolism in mammalian organs. *Physiol Rev* 59(3):527-605.
39. Floyd RA (1999) Antioxidants, oxidative stress, and degenerative neurological disorders. *P Soc Exp Biol Med* 222(3):236-245.
40. Chevion M (1988) A site-specific mechanism for free-radical induced biological damage: the essential role of redox-active transition-metals. *Free Radic Bio Med* 5(1):27-37.
41. Mello AC & Meneghini R (1991) Iron is the intracellular metal involved in the production of DNA damage by oxygen radicals. *Mutat Res* 251(1):109-113.
42. Barbouti A, Doulias PT, Zhu BZ, Frei B, & Galaris D (2001) Intracellular iron, but not copper, plays a critical role in hydrogen peroxide-induced DNA damage. *Free Radic Bio Med* 31(4):490-498.
43. Bokov A, Chaudhuri A, & Richardson A (2004) The role of oxidative damage and stress in aging. *Mech Ageing Dev* 125(10-11):811-826.

44. Wickens AP (2001) Ageing and the free radical theory. *Resp Physiol* 128(3):379-391.
45. Halliwell B & Aruoma OI (1991) DNA damage by oxygen-derived species - its mechanism and measurement in mammalian systems. *Febs Lett* 281(1-2):9-19.
46. Kryston TB, Georgiev AB, Pissis P, & Georgakilas AG (2011) Role of oxidative stress and DNA damage in human carcinogenesis. *Mutat Res-Fund Mol M* 711(1-2):193-201.
47. Poon HF, Calabrese V, Scapagnini G, & Butterfield DA (2004) Free radicals and brain aging. *Clin Geriatr Med* 20(2):329-+.
48. Butterfield DA & Stadtman ER (1997) Chapter 7 Protein oxidation processes in aging brain. *Advances in Cell Aging and Gerontology*, eds Paula ST & Bittar EE (Elsevier), Vol Volume 2, pp 161-191.
49. Bjorn-Rasmussen E, Hallberg L, Isaksson B, & Arvidsso.B (1974) Food iron absorption in man - Applications of two-pool extrinsic tag method to measure heme and nonheme iron absorption from whole diet. *J Clin Invest* 53(1):247-255.
50. Beard JL, Dawson H, & Pinero DJ (1996) Iron metabolism: a comprehensive review. *Nutr Rev* 54(10):295-317.
51. Valerio LG (2007) Mammalian iron metabolism. *Toxicol Mech Method* 17(9):497-517.
52. McKie A & Simpson R (2012) Intestinal iron absorption. *Iron physiology and pathophysiology in humans*, Nutrition and Health, eds Anderson GJ & McLaren GD (Humana Press), pp 101-116.
53. Raffin SB, Woo CH, Roost KT, Price DC, & Schmid R (1974) Intestinal absorption of hemoglobin iron-heme cleavage by mucosal heme oxygenase. *J Clin Invest* 54(6):1344-1352.
54. Rosenberg DW & Kappas A (1989) Characterization of heme oxygenase in the small intestinal epithelium. *Arch Biochem Biophys* 274(2):471-480.
55. Qiu AD, *et al.* (2006) Identification of an intestinal folate transporter and the molecular basis for hereditary folate malabsorption. *Cell* 127(5):917-928.
56. Walczyk T & von Blanckenburg F (2005) Deciphering the iron isotope message of the human body. *Int J Mass Spectrom* 242(2-3):117-134.
57. Zimmermann MB & Hurrell RF (2007) Nutritional iron deficiency. *The Lancet* 370(9586):511-520.
58. Beard J & Han O (2009) Systemic iron status. *Bba-Gen Subjects* 1790(7):584-588.
59. McKie AT, *et al.* (2001) An iron-regulated ferric reductase associated with the absorption of dietary iron. *Science* 291(5509):1755-1759.
60. Gunshin H, *et al.* (1997) Cloning and characterization of a mammalian proton-coupled metal-ion transporter. *Nature* 388(6641):482-488.
61. Wessling-Resnick M (2006) Iron imports. III. Transfer of iron from the mucosa into circulation. *Am J Physiol Gastrointest Liver Physiol* 290(1):G1-6.
62. Mesquita SD, *et al.* (2012) Modulation of iron metabolism in aging and in Alzheimer's disease: relevance of the choroid plexus. *Front Cell Neurosci* 6.
63. Frazer DM & Anderson GJ (2003) The orchestration of body iron intake: how and where do enterocytes receive their cues? *Blood Cell Mol Dis* 30(3):288-297.
64. Hentze MW, Muckenthaler MU, & Andrews NC (2004) Balancing acts: Molecular control of mammalian iron metabolism. *Cell* 117(3):285-297.
65. Weiss G (2012) Iron and the reticuloendothelial system. *Iron physiology and pathophysiology in humans*, Nutrition and Health, eds Anderson GJ & McLaren GD (Humana Press), pp 211-231.
66. Finch CA, *et al.* (1970) Ferrokinetics in man. *Medicine* 49(1):17-&.

67. Green R, *et al.* (1968) Body iron excretion in man - a collaborative study. *Am J Med* 45(3):336-&.
68. Nemeth E, *et al.* (2004) Hepcidin regulates cellular iron efflux by binding to ferroportin and inducing its internalization. *Science* 306(5704):2090-2093.
69. Graham RM, Chua ACG, & Trinder D (2012) Plasma iron and iron delivery to the tissues. *Iron Physiology and Pathophysiology in Humans,* Nutrition and Health, eds Anderson GJ & McLaren GD (Humana Press), pp 117-139.
70. Qian ZM, Li H, Sun H, & Ho K (2002) Targeted drug delivery via the transferrin receptor-mediated endocytosis pathway. *Pharmacol Rev* 54(4):561-587.
71. Andrews NC (2000) Iron homeostasis: Insights from genetics and animal models. *Nat Rev Genet* 1(3):208-217.
72. Laurell CB (1952) Plasma iron and the transport of iron in the organism. *Pharmacol Rev* 4(4):371-395.
73. Bothwell TH (1979) *Iron metabolism in man* (Blackwell Scientific Publications ; St. Louis : Distributors USA, Blackwell Mosby Book Distributors).
74. Moos T & Morgan EH (2000) Transferrin and transferrin receptor function in brain barrier systems. *Cell Mol Neurobiol* 20(1):77-95.
75. Cheng Y, Zak O, Alsen P, Harrison SC, & Walz T (2004) Structure of the human transferrin receptor-transferrin complex. *Cell* 116(4):565-576.
76. Dautry-Varsat A, Ciechanover A, & Lodish HF (1983) Ph and the recycling of transferrin during receptor-mediated endocytosis. *P Natl Acad Sci-Biol* 80(8):2258-2262.
77. Morgan EH (1983) Effect of pH and iron content of transferrin on its binding to reticulocyte receptors. *Biochim Biophys Acta* 762(4):498-502.
78. Fleming MD, *et al.* (1998) Nramp2 is mutated in the anemic Belgrade (b) rat: Evidence of a role for Nramp2 in endosomal iron transport. *P Natl Acad Sci USA* 95(3):1148-1153.
79. Maxfield FR & McGraw TE (2004) Endocytic recycling. *Nat Rev Mol Cell Bio* 5(2):121-132.
80. Kawabata H, *et al.* (1999) Molecular cloning of transferrin receptor 2. A new member of the transferrin receptor-like family. *J Biol Chem* 274(30):20826-20832.
81. Graham RM, *et al.* (2008) Transferrin receptor 2 mediates uptake of transferrin-bound and non-transferrin-bound iron. *J Hepatol* 48(2):327-334.
82. Camaschella C, *et al.* (2000) The gene TFR2 is mutated in a new type of haemochromatosis mapping to 7q22. *Nat Genet* 25(1):14-15.
83. Kozyraki R, *et al.* (2001) Megalin-dependent cubilin-mediated endocytosis is a major pathway for the apical uptake of transferrin in polarized epithelia. *P Natl Acad Sci USA* 98(22):12491-12496.
84. Anderson GJ & Frazer DM (2005) Hepatic iron metabolism. *Semin Liver Dis* 25(4):420-432.
85. Rouault TA, Zhang DL, & Jeong SY (2009) Brain iron homeostasis, the choroid plexus, and localization of iron transport proteins. *Metab Brain Dis* 24(4):673-684.
86. Watt RK (2011) The many faces of the octahedral ferritin protein. *Biometals* 24(3):489-500.
87. Crichton RR & Declercq JP (2010) X-ray structures of ferritins and related proteins. *Bba-Gen Subjects* 1800(8):706-718.
88. Carmona F, *et al.* (2013) Ferritin iron uptake and release in the presence of metals and metalloproteins: chemical implications in the brain. *Coord Chem Rev*.

89. Arosio P, Ingrassia R, & Cavadini P (2009) Ferritins: A family of molecules for iron storage, antioxidation and more. *Bba-Gen Subjects* 1790(7):589-599.
90. Levi S, *et al.* (1992) Evidence that H-chains and L-chains have cooperative roles in the iron-uptake mechanism of human ferritin. *Biochem J* 288:591-596.
91. Hempstead PD, *et al.* (1997) Comparison of the three-dimensional structures of recombinant human H and horse L ferritins at high resolution. *J Mol Biol* 268(2):424-448.
92. Santambrogio P, Levi S, Cozzi A, Corsi B, & Arosio P (1996) Evidence that the specificity of iron incorporation into homopolymers of human ferritin L- and H-chains is conferred by the nucleation and ferroxidase centres. *Biochem J* 314:139-144.
93. Theil EC (2011) Ferritin protein nanocages use ion channels, catalytic sites, and nucleation channels to manage iron/oxygen chemistry. *Curr Opin Chem Biol* 15(2):304-311.
94. Lawson DM, *et al.* (1989) Identification of the ferroxidase center in ferritin. *Febs Lett* 254(1-2):207-210.
95. Wagstaff M, Worwood M, & Jacobs A (1978) Properties of human tissue isoferritins. *Biochem J* 173(3):969-977.
96. Brock JH, Halliday JW, Pippard MJ, & Powell LW (1994) *Iron metabolism in health and disease* (Saunders).
97. Harrison PM & Arosio P (1996) Ferritins: molecular properties, iron storage function and cellular regulation. *Bba-Bioenergetics* 1275(3):161-203.
98. Richter GW (1978) Iron-loaded cell - cytopathology of iron storage - review. *Am J Pathol* 91(2):361-404.
99. Ward RJ, *et al.* (1994) Further characterization of forms of hemosiderin in iron-overloaded tissues. *Eur J Biochem* 225(1):187-194.
100. Ward RJ, *et al.* (1992) Chemical and structural characterization of iron cores of haemosiderins isolated from different sources. *Eur J Biochem* 209(3):847-850.
101. Quintana C, *et al.* (2006) Study of the localization of iron, ferritin, and hemosiderin in Alzheimer's disease hippocampus by analytical microscopy at the subcellular level. *J Struct Biol* 153(1):42-54.
102. Selden C, Owen M, Hopkins JMP, & Peters TJ (1980) Studies on the concentration and intracellular-localization of iron proteins in liver-biopsy specimens from patients with iron overload with special reference to their role in lysosomal disruption. *Brit J Haematol* 44(4):593-603.
103. Weir MP, Gibson JF, & Peters TJ (1984) Biochemical studies on the isolation and characterization of human spleen hemosiderin. *Biochem J* 223(1):31-38.
104. Crichton RR & Ward RJ (1992) Iron metabolism - new perspectives in view. *Biochemistry-Us* 31(46):11255-11264.
105. Jacobs A (1976) An intracellular transit iron pool. *Ciba Foundation symposium* (51):91-106.
106. Greenberg GR & Wintrobe MM (1946) A labile iron pool. *J Biol Chem* 165(1):397-398.
107. Kruszewski M (2003) Labile iron pool: the main determinant of cellular response to oxidative stress. *Mutat Res-Fund Mol M* 531(1-2):81-92.
108. Breuer W, Shvartsman M, & Cabantchik ZI (2008) Intracellular labile iron. *Int J Biochem Cell B* 40(3):350-354.
109. Kakhlon O & Cabantchik ZI (2002) The labile iron pool: Characterization, measurement, and participation in cellular processes. *Free Radic Bio Med* 33(8):1037-1046.

110. Petrat F, de Groot H, Sustmann R, & Rauen U (2002) The chelatable iron pool in living cells: A methodically defined quantity. *Biol Chem* 383(3-4):489-502.
111. Epsztejn S, *et al.* (1999) H-ferritin subunit overexpression in erythroid cells reduces the oxidative stress response and induces multidrug resistance properties. *Blood* 94(10):3593-3603.
112. Kaur D & Andersen JK (2002) Ironing out Parkinson's disease: is therapeutic treatment with iron chelators a real possibility? *Aging Cell* 1(1):17-21.
113. Nemeth E & Ganz T (2006) Regulation of iron metabolism by hepcidin. *Annu Rev Nutr* 26:323-342.
114. Donovan A, *et al.* (2000) Positional cloning of zebrafish ferroportin1 identifies a conserved vertebrate iron exporter. *Nature* 403(6771):776-781.
115. Donovan A, *et al.* (2005) The iron exporter ferroportin/Slc40a1 is essential for iron homeostasis. *Cell Metab* 1(3):191-200.
116. Council NR (2001) Iron. *Dietary Reference Intakes for Vitamin A, Vitamin K, Arsenic, Boron, Chromium, Copper, Iodine, Iron, Manganese, Molybdenum, Nickel, Silicon, Vanadium, and Zinc*, (The National Academies Press, Washington, DC).
117. Hunt JR, Zito CA, & Johnson LK (2009) Body iron excretion by healthy men and women. *Am J Clin Nutr* 89(6):1792-1798.
118. Cook JD (1990) Adaptation in iron metabolism. *Am J Clin Nutr* 51(2):301-308.
119. Jellen LC, Beard JL, & Jones BC (2009) Systems genetics analysis of iron regulation in the brain. *Biochimie* 91(10):1255-1259.
120. Sebastiani G & Pantopoulos K (2011) Disorders associated with systemic or local iron overload: from pathophysiology to clinical practice. *Metallomics* 3(10):971-986.
121. Wallander ML, Leibold EA, & Eisenstein RS (2006) Molecular control of vertebrate iron homeostasis by iron regulatory proteins. *Bba-Mol Cell Res* 1763(7):668-689.
122. Richardson DR, Kalinowski DS, Lau S, Jansson PJ, & Lovejoy DB (2009) Cancer cell iron metabolism and the development of potent iron chelators as anti-tumour agents. *Bba-Gen Subjects* 1790(7):702-717.
123. Anderson GJ, Frazer DM, & McLaren GD (2009) Iron absorption and metabolism. *Curr Opin Gastroen* 25(2):129-135.
124. Rivera S, *et al.* (2005) Synthetic hepcidin causes rapid dose-dependent hypoferremia and is concentrated in ferroportin-containing organs. *Blood* 106(6):2196-2199.
125. Pigeon C, *et al.* (2001) A new mouse liver-specific gene, encoding a protein homologous to human antimicrobial peptide hepcidin, is overexpressed during iron overload. *J Biol Chem* 276(11):7811-7819.
126. Nicolas G, *et al.* (2002) The gene encoding the iron regulatory peptide hepcidin is regulated by anemia, hypoxia, and inflammation. *J Clin Invest* 110(7):1037-1044.
127. Schmidt PJ, Toran PT, Giannetti AM, Bjorkman PJ, & Andrews NC (2008) The transferrin receptor modulates Hfe-dependent regulation of hepcidin expression. *Cell Metab* 7(3):205-214.
128. Rhodes SL & Ritz B (2008) Genetics of iron regulation and the possible role of iron in Parkinson's disease. *Neurobiol Dis* 32(2):183-195.
129. Babitt JL, *et al.* (2006) Bone morphogenetic protein signaling by hemojuvelin regulates hepcidin expression. *Nat Genet* 38(5):531-539.

130. Nemeth E, *et al.* (2004) IL-6 mediates hypoferremia of inflammation by inducing the synthesis of the iron regulatory hormone hepcidin. *J Clin Invest* 113(9):1271-1276.
131. Bridle KR, *et al.* (2003) Disrupted hepcidin regulation in HFE-associated haemochromatosis and the liver as a regulator of body iron homoeostasis. *Lancet* 361(9358):669-673.
132. Nicolas G, *et al.* (2002) Severe iron deficiency anemia in transgenic mice expressing liver hepcidin. *P Natl Acad Sci USA* 99(7):4596-4601.
133. Gehrke SG, *et al.* (2003) Expression of hepcidin in hereditary hemochromatosis: evidence for a regulation in response to the serum transferrin saturation and to non-transferrin-bound iron. *Blood* 102(1):371-376.
134. Quintana C & Gutierrez L (2010) Could a dysfunction of ferritin be a determinant factor in the aetiology of some neurodegenerative diseases? *Bba-Gen Subjects* 1800(8):770-782.
135. Takeda A (2004) Analysis of brain function and prevention of brain diseases: the action of trace metals. *J Health Sci* 50(5):429-442.
136. Smith QR (2003) A review of blood-brain barrier transport techniques. *The Blood-Brain Barrier*, Methods in Molecular Medicine™, ed Nag S (Humana Press), Vol 89, pp 193-208.
137. Shah GN & Mooradian AD (1997) Age-related changes in the blood-brain barrier. *Exp Gerontol* 32(4-5):501-519.
138. Mills E, Dong XP, Wang FD, & Xu HX (2010) Mechanisms of brain iron transport: insight into neurodegeneration and CNS disorders. *Future Med Chem* 2(1):51-64.
139. Laterra J, Keep R, Betz LA, & Goldstein G (1999) Blood-cerebrospinal fluid barrier. *Basic neurochemistry: molecular, cellular and medical aspects*, eds Siegel GJ, Agranoff BW, & Albers RW (Lippincott-Raven, Philadelphia), 6th Ed.
140. Schenck JF & Zimmerman EA (2004) High-field magnetic resonance imaging of brain iron: birth of a biomarker? *Nmr Biomed* 17(7):433-445.
141. Martin WRW, Ye FQ, & Allen PS (1998) Increasing striatal iron content associated with normal aging. *Movement Disord* 13(2):281-286.
142. Bartzokis G, *et al.* (1997) MR evaluation of age-related increase of brain iron in young adult and older normal males. *Magn Reson Imaging* 15(1):29-35.
143. Dexter DT, Sian J, Jenner P, & Marsden CD (1993) Implications of alterations in trace-element levels in brain in Parkinson's disease and other neurological disorders affecting the basal ganglia. *Adv Neurol* 60:273-281.
144. Kozlowski H, *et al.* (2009) Copper, iron, and zinc ions homeostasis and their role in neurodegenerative disorders (metal uptake, transport, distribution and regulation). *Coord Chem Rev* 253(21-22):2665-2685.
145. Moos T & Morgan EH (2004) The metabolism of neuronal iron and its pathogenic role in neurological disease - Review. *Ann Ny Acad Sci* 1012:14-26.
146. Kumar H, *et al.* (2012) The Role of Free Radicals in the Aging Brain and Parkinson's Disease: Convergence and Parallelism. *Int J Mol Sci* 13(8):10478-10504.
147. Zecca L, Youdim MBH, Riederer P, Connor JR, & Crichton RR (2004) Iron, brain ageing and neurodegenerative disorders. *Nat Rev Neurosci* 5(11):863-873.
148. Crichton RR & Boelaert JR (2001) *Inorganic biochemistry of iron metabolism: from molecular mechanisms to clinical consequences* (Wiley).
149. Zecca L, *et al.* (2004) The role of iron and copper molecules in the neuronal vulnerability of locus coeruleus and substantia nigra during aging. *P Natl Acad Sci USA* 101(26):9843-9848.

150. Connor JR, Snyder BS, Arosio P, Loeffler DA, & Lewitt P (1995) A Quantitative-analysis of isoferritins in select regions of aged, parkinsonian, and, Alzheimers diseased brains. *J Neurochem* 65(2):717-724.
151. Todorich B, Pasquini JM, Garcia CI, Paez PM, & Connor JR (2009) Oligodendrocytes and myelination: The role of iron. *Glia* 57(5):467-478.
152. Beard J (2003) Iron deficiency alters brain development and functioning. *J Nutr* 133(5):1468s-1472s.
153. Connor JR, Menzies SL, Stmartin SM, & Mufson EJ (1990) Cellular distribution of transferrin, ferritin, and iron in normal and aged human brains. *J Neurosci Res* 27(4):595-611.
154. Double KL, Maruyama W, Naoi M, Gerlach M, & Riederer P (2011) Biological role of neuromelanin in the human brain and its importance in Parkinson's disease. *Melanins and Melanosomes*, (Wiley-VCH Verlag GmbH & Co. KGaA), pp 225-246.
155. Gotz ME, Double K, Gerlach M, Youdim MBH, & Riederer P (2004) The relevance of iron in the pathogenesis of Parkinson's disease. *Ann Ny Acad Sci* 1012:193-208.
156. Wakamatsu K, Murase T, Zucca FA, Zecca L, & Ito S (2012) Biosynthetic pathway to neuromelanin and its aging process. *Pigm Cell Melanoma R* 25(6):792-803.
157. Zecca L, *et al.* (1996) Interaction of neuromelanin and iron in substantia nigra and other areas of human brain. *Neuroscience* 73(2):407-415.
158. Zecca L, Zucca FA, Wilms H, & Sulzer D (2003) Neuromelanin of the substantia nigra: a neuronal black hole with protective and toxic characteristics. *Trends Neurosci* 26(11):578-580.
159. Rouault TA & Cooperman S (2006) Brain iron metabolism. *Semin Pediatr Neurol* 13(3):142-148.
160. Rouault TA (2001) Systemic iron metabolism: A review and implications for brain iron metabolism. *Pediatr Neurol* 25(2):130-137.
161. Fisher J, *et al.* (2007) Ferritin: a novel mechanism for delivery of iron to the brain and other organs. *Am J Physiol-Cell Ph* 293(2):C641-C649.
162. Ke Y & Qian ZM (2007) Brain iron metabolism: Neurobiology and neurochemistry. *Prog Neurobiol* 83(3):149-173.
163. Burdo JR & Connor JR (2003) Brain iron uptake and homeostatic mechanisms: An overview. *Biometals* 16(1):63-75.
164. Deane R, Zheng W, & Zlokovic BV (2004) Brain capillary endothelium and choroid plexus epithelium regulate transport of transferrin-bound and free iron into the rat brain. *J Neurochem* 88(4):813-820.
165. Ueda F, Raja KB, Simpson RJ, Trowbridge IS, & Bradbury MWB (1993) Rate of Fe-59 uptake into brain and cerebrospinal-fluid and the influence thereon of antibodies against the transferrin receptor. *J Neurochem* 60(1):106-113.
166. Crichton RR, Dexter DT, & Ward RJ (2011) Brain iron metabolism and its perturbation in neurological diseases. *Monatsh Chem* 142(4):341-355.
167. Wu LJC, *et al.* (2004) Expression of the iron transporter ferroportin in synaptic vesicles and the blood-brain barrier. *Brain Res* 1001(1-2):108-117.
168. Moos T, Nielsen TR, Skjorringe T, & Morgan EH (2007) Iron trafficking inside the brain. *J Neurochem* 103(5):1730-1740.
169. Crowe A & Morgan EH (1992) Iron and transferrin uptake by brain and cerebrospinal fluid in the rat. *Brain Res* 592(1-2):8-16.

170. Zecca L, *et al.* (2001) Iron, neuromelanin and ferritin content in the substantia nigra of normal subjects at different ages: consequences for iron storage and neurodegenerative processes. *J Neurochem* 76(6):1766-1773.
171. Lopes TJS, *et al.* (2010) Systems analysis of iron metabolism: the network of iron pools and fluxes. *Bmc Syst Biol* 4.
172. Taylor EM & Morgan EH (1990) Developmental changes in transferrin and iron uptake by the brain in the rat. *Dev Brain Res* 55(1):35-42.
173. Banks WA, Kastin AJ, Fasold MB, Barrera CM, & Augereau G (1988) Studies of the slow bidirectional transport of iron and transferrin across the blood-brain-barrier. *Brain Res Bull* 21(6):881-885.
174. Bradbury MWB (1997) Transport of iron in the blood-brain-cerebrospinal fluid system. *J Neurochem* 69(2):443-454.
175. Moos T & Morgan EH (1998) Kinetics and distribution of [Fe-59-I-125]transferrin injected into the ventricular system of the rat. *Brain Res* 790(1-2):115-128.
176. Dallman PR & Spirito RA (1977) Brain iron in rat: extremely slow turnover in normal rats may explain long-lasting effects of early iron deficiency. *J Nutr* 107(6):1075-1081.
177. Su CK, *et al.* (2010) In vivo monitoring of the transfer kinetics of trace elements in animal brains with hyphenated inductively coupled plasma mass spectrometry techniques. *Mass Spectrom Rev* 29(3):392-424.
178. Moos T & Morgan EH (1998) Evidence for low molecular weight, non-transferrin-bound iron in rat brain and cerebrospinal fluid. *J Neurosci Res* 54(4):486-494.
179. Terent A, Hallgren R, Venge P, & Bergstrom K (1981) Lactoferrin, lysozyme, and beta 2-microglobulin in cerebrospinal fluid. Elevated levels in patients with acute cerebrovascular lesions as indices of inflammation. *Stroke* 12(1):40-46.
180. Moos T (1996) Immunohistochemical localization of intraneuronal transferrin receptor immunoreactivity in the adult mouse central nervous system. *J Comp Neurol* 375(4):675-692.
181. Todorich B, Zhang XS, & Connor JR (2011) H-ferritin is the major source of iron for oligodendrocytes. *Glia* 59(6):927-935.
182. Takeda A, Devenyi A, & Connor JR (1998) Evidence for non-transferrin-mediated uptake and release of iron and manganese in glial cell cultures from hypotransferrinemic mice. *J Neurosci Res* 51(4):454-462.
183. Knutson MD, Levy JE, Andrews NC, & Wessling-Resnick M (2001) Expression of stimulator of Fe transport is not enhanced in Hfe knockout mice. *J Nutr* 131(5):1459-1464.
184. Gutierrez JA, Yu JM, Rivera S, & WesslingResnick M (1999) Functional expression cloning and characterization of SFT, a stimulator of Fe transport. *J Cell Biol* 147(1):205-205.
185. Nandar W & Connor JR (2011) HFE gene variants affect iron in the brain. *J Nutr* 141(4):729s-739s.
186. Johnstone D & Milward EA (2010) Molecular genetic approaches to understanding the roles and regulation of iron in brain health and disease. *J Neurochem* 113(6):1387-1402.
187. Smith SR, *et al.* (2004) Severity of neurodegeneration correlates with compromise of iron metabolism in mice with iron regulatory protein deficiencies. *Ann Ny Acad Sci* 1012:65-83.
188. Pinero DJ, Li NQ, Connor JR, & Beard JL (2000) Variations in dietary iron alter brain iron metabolism in developing rats. *J Nutr* 130(2):254-263.

189. Ke Y & Qian ZM (2003) Iron misregulation in the brain: a primary cause of neurodegenerative disorders. *Lancet Neurol* 2(4):246-253.
190. Zechel S, Huber-Wittmer K, & von Bohlen und Halbach O (2006) Distribution of the iron-regulating protein hepcidin in the murine central nervous system. *J Neurosci Res* 84(4):790-800.
191. Moos T, Skjoerringe T, Gosk S, & Morgan EH (2006) Brain capillary endothelial cells mediate iron transport into the brain by segregating iron from transferrin without the involvement of divalent metal transporter 1. *J Neurochem* 98(6):1946-1958.
192. Martinez AR, Niemela O, & Parkkila S (2004) Hepatic and extrahepatic expression of the new iron regulatory protein hemojuvelin. *Haematologica* 89(12):1441-1445.
193. Hanninen MM, *et al.* (2009) Expression of iron-related genes in human brain and brain tumors. *Bmc Neurosci* 10.
194. Gebril OH, Simpson JE, Kirby J, Brayne C, & Ince PG (2011) Brain iron dysregulation and the risk of ageing white matter lesions. *Neuromol Med* 13(4):289-299.
195. Connor JR, Menzies SL, Burdo JR, & Boyer PJ (2001) Iron and iron management proteins in neurobiology. *Pediatr Neurol* 25(2):118-129.
196. Bennett MJ, Lebron JA, & Bjorkman PJ (2000) Crystal structure of the hereditary haemochromatosis protein HFE complexed with transferrin receptor. *Nature* 403(6765):46-53.
197. Feder JN, *et al.* (1996) A novel MHC class I-like gene is mutated in patients with hereditary haemochromatosis. *Nat Genet* 13(4):399-408.
198. Hahn P, *et al.* (2009) Age-dependent and gender-specific changes in mouse tissue iron by strain. *Exp Gerontol* 44(9):594-600.
199. Massie HR, Aiello VR, & Banziger V (1983) Iron accumulation and lipid peroxidation in aging C57bL/6J Mice. *Exp Gerontol* 18(4):277-285.
200. Cook CI & Yu BP (1998) Iron accumulation in aging: modulation by dietary restriction. *Mech Ageing Dev* 102(1):1-13.
201. Hardy PA, *et al.* (2005) Correlation of R2 with total iron concentration in the brains of rhesus monkeys. *J Magn Reson Imaging* 21(2):118-127.
202. Maynard CJ, *et al.* (2002) Overexpression of Alzheimer's disease amyloid-beta opposes the age-dependent elevations of brain copper and iron. *J Biol Chem* 277(47):44670-44676.
203. Hallgren B & Sourander P (1958) The effect of age on the non-haemin iron in the human brain. *J Neurochem* 3(1):41-51.
204. Loeffler DA, *et al.* (1995) Transferrin and iron in normal, Alzheimer's disease, and Parkinson's disease brain regions. *J Neurochem* 65(2):710-716.
205. Hebbrecht G, Maenhaut W, & De Reuck J (1999) Brain trace elements and aging. *Nucl Instrum Meth B* 150(1-4):208-213.
206. Xu JZ, Knutson MD, Carter CS, & Leeuwenburgh C (2008) Iron accumulation with age, oxidative stress and functional decline. *Plos One* 3(8).
207. Bartzokis G, *et al.* (2007) Brain ferritin iron may influence age- and gender-related risks of neurodegeneration. *Neurobiol Aging* 28(3):414-423.
208. Haacke EM, *et al.* (2005) Imaging iron stores in the brain using magnetic resonance imaging. *Magn Reson Imaging* 23(1):1-25.
209. Koeppen AH (1995) The history of iron in the brain. *J Neurol Sci* 134:1-9.
210. Aquino D, *et al.* (2009) Age-related iron deposition in the basal ganglia: quantitative analysis in healthy subjects. *Radiology* 252(1):165-172.
211. Drayer B, *et al.* (1986) MRI of brain iron. *Am J Roentgenol* 147(1):103-110.

212. Yu BP (1996) Aging and oxidative stress: Modulation by dietary restriction. *Free Radic Bio Med* 21(5):651-668.
213. Harman D (1956) Aging: a theory based on free radical and radiation chemistry. *J Gerontol* 11(3):298-300.
214. Polla AS, Polla LL, & Polla BS (2003) Iron as the malignant spirit in successful ageing. *Ageing Res Rev* 2(1):25-37.
215. Barja G (2004) Free radicals and aging. *Trends Neurosci* 27(10):595-600.
216. House MJ, Pierre TGS, Milward EA, Bruce DG, & Olynyk JK (2010) Relationship between brain R-2 and liver and serum iron concentrations in elderly men. *Magn Reson Med* 63(2):275-281.
217. Penke L, *et al.* (2012) Brain iron deposits are associated with general cognitive ability and cognitive aging. *Neurobiol Aging* 33(3):510-U607.
218. Kastman EK, *et al.* (2010) A calorie-restricted diet decreases brain iron accumulation and preserves motor performance in old rhesus monkeys. *J Neurosci* 30(23):7940-7947.
219. Vasudevaraju P, *et al.* (2010) New evidence on iron, copper accumulation and zinc depletion and its correlation with DNA integrity in aging human brain regions. *Indian J Psychiatry* 52(2):140-144.
220. Sullivan EV, Adalsteinsson E, Rohlfing T, & Pfefferbaum A (2009) Relevance of iron deposition in deep gray matter brain structures to cognitive and motor performance in healthy elderly men and women: exploratory findings. *Brain Imaging Behav* 3(2):167-175.
221. Berg D, Becker G, Riederer P, & Riess O (2002) Iron in neurodegenerative disorders. *Neurotox Res* 4(7-8):637-653.
222. Berg D, *et al.* (2002) Echogenicity of the substantia nigra: Association with increased iron content and marker for susceptibility to nigrostriatal injury. *Arch Neurol-Chicago* 59(6):999-1005.
223. Bartzokis G & Tishler TA (2000) MRI evaluation of basal ganglia ferritin iron and neurotoxicity in Alzheimer's and Huntingon's disease. *Cell Mol Biol* 46(4):821-833.
224. Markesbery WR (1997) Oxidative stress hypothesis in Alzheimer's disease. *Free Radic Bio Med* 23(1):134-147.
225. Butterfield DA, Drake J, Pocernich C, & Castegna A (2001) Evidence of oxidative damage in Alzheimer's disease brain: central role for amyloid beta-peptide. *Trends Mol Med* 7(12):548-554.
226. Butterfield DA, Castegna A, Lauderback CM, & Drake J (2002) Evidence that amyloid beta-peptide-induced lipid peroxidation and its sequelae in Alzheimer's disease brain contribute to neuronal death. *Neurobiol Aging* 23(5):655-664.
227. Butterfield DA & Lauderback CM (2002) Lipid peroxidation and protein oxidation in Alzheimer's disease brain: potential causes and consequences involving amyloid beta-peptide-associated free radical oxidative stress. *Free Radic Bio Med* 32(11):1050-1060.
228. Altamura S & Muckenthaler MU (2009) Iron toxicity in diseases of aging: Alzheimer's disease, Parkinson's disease and atherosclerosis. *J Alzheimers Dis* 16(4):879-895.
229. Goodman L (1953) Alzheimer's disease; a clinico-pathologic analysis of twenty-three cases with a theory on pathogenesis. *J Nerv Ment Dis* 118(2):97-130.
230. Lovell MA, Robertson JD, Teesdale WJ, Campbell JL, & Markesbery WR (1998) Copper, iron and zinc in Alzheimer's disease senile plaques. *J Neurol Sci* 158(1):47-52.

231. Good PF, Perl DP, Bierer LM, & Schmeidler J (1992) Selective accumulation of aluminum and iron in the neurofibrillary tangles of Alzheimer's disease: a laser microprobe (LAMMA) study. *Ann Neurol* 31(3):286-292.
232. Connor JR, Snyder BS, Beard JL, Fine RE, & Mufson EJ (1992) Regional distribution of iron and iron-regulatory proteins in the brain in aging and Alzheimer's disease. *J Neurosci Res* 31(2):327-335.
233. Barrow CJ, Yasuda A, Kenny PTM, & Zagorski MG (1992) Solution conformations and aggregational properties of synthetic amyloid β-peptides of Alzheimer's disease: Analysis of circular dichroism spectra. *J Mol Biol* 225(4):1075-1093.
234. Barrow CJ & Zagorski MG (1991) Solution structures of beta peptide and its constituent fragments: relation to amyloid deposition. *Science* 253(5016):179-182.
235. Greenough MA, Camakaris J, & Bush AI (2013) Metal dyshomeostasis and oxidative stress in Alzheimer's disease. *Neurochem Int* 62(5):540-555.
236. Seidah N, Chretien M, & Day R (1994) The family of subtilisin/kexin Like pro-protein and prohormone convertases: divergent or shared functions. *Biochimie* 76(3-4):197-209.
237. Zemlan FP, Thienhaus OJ, & Bosmann HB (1989) Superoxide dismutase activity in Alzheimer's disease: Possible mechanism for paired helical filament formation. *Brain Res* 476(1):160-162.
238. Rogers JT, *et al.* (2002) An iron-responsive element type II in the 5'-untranslated region of the Alzheimer's amyloid precursor protein transcript. *J Biol Chem* 277(47):45518-45528.
239. Venti A, *et al.* (2004) The integrated role of desferrioxamine and phenserine targeted to an iron-responsive element in the APP-mRNA 5'-untranslated region. *Annals of the New York Academy of Sciences* 1035:34-48.
240. Duce JA & Bush AI (2010) Biological metals and Alzheimer's disease: Implications for therapeutics and diagnostics. *Prog Neurobiol* 92(1):1-18.
241. Bonda DJ, *et al.* (2011) Role of metal dyshomeostasis in Alzheimer's disease. *Metallomics* 3(3):267-270.
242. Lei P, *et al.* (2012) Tau deficiency induces parkinsonism with dementia by impairing APP-mediated iron export. *Nat Med* 18(2):291-295.
243. Smith MA, Harris PLR, Sayre LM, & Perry G (1997) Iron accumulation in Alzheimer disease is a source of redox-generated free radicals. *P Natl Acad Sci USA* 94(18):9866-9868.
244. Youdim KA, Qaiser MZ, Begley DJ, Rice-Evans CA, & Abbott NJ (2004) Flavonoid permeability across an in situ model of the blood-brain barrier. *Free Radic Bio Med* 36(5):592-604.
245. Sofic E, Paulus W, Jellinger K, Riederer P, & Youdim MB (1991) Selective increase of iron in substantia nigra zona compacta of parkinsonian brains. *J Neurochem* 56(3):978-982.
246. Hirsch EC, Brandel JP, Galle P, Javoy-Agid F, & Agid Y (1991) Iron and aluminum increase in the substantia nigra of patients with Parkinson's disease: an X-ray microanalysis. *J Neurochem* 56(2):446-451.
247. Earle KM (1968) Studies on Parkinson's disease including x-ray fluorescent spectroscopy of formalin fixed brain tissue. *J Neuropath Exp Neur* 27(1):1-14.
248. Dexter DT, *et al.* (1991) Alterations in the levels of iron, ferritin and other trace metals in Parkinson's disease and other neurodegenerative diseases affecting the basal ganglia. *Brain* 114 (Pt 4):1953-1975.

249. Riederer P, *et al.* (1988) Biochemical fundamentals of Parkinson's disease. *Mt Sinai J Med* 55(1):21-28.
250. Sofic E, *et al.* (1988) Increased iron (III) and total iron content in post mortem substantia nigra of parkinsonian brain. *J Neural Transm* 74(3):199-205.
251. Faucheux BA, *et al.* (2002) Lack of up-regulation of ferritin is associated with sustained iron regulatory protein-1 binding activity in the substantia nigra of patients with Parkinson's disease. *J Neurochem* 83(2):320-330.
252. Zecca L, *et al.* (2002) The neuromelanin of human substantia nigra and its interaction with metals. *J Neural Transm* 109(5-6):663-672.
253. Goedert M (2001) Alpha-synuclein and neurodegenerative diseases. *Nat Rev Neurosci* 2(7):492-501.
254. Golts N, *et al.* (2002) Magnesium inhibits spontaneous and iron-induced aggregation of alpha-synuclein. *J Biol Chem* 277(18):16116-16123.
255. Ostrerova-Golts N, *et al.* (2000) The A53T alpha-synuclein mutation increases iron-dependent aggregation and toxicity. *J Neurosci* 20(16):6048-6054.
256. Sangchot P, *et al.* (2002) Deferoxamine attenuates iron-induced oxidative stress and prevents mitochondrial aggregation and alpha-synuclein translocation in SK-N-SH cells in culture. *Dev Neurosci* 24(2-3):143-153.
257. Hashimoto M, *et al.* (1999) Oxidative stress induces amyloid-like aggregate formation of NACP/alpha-synuclein in vitro. *Neuroreport* 10(4):717-721.
258. Gillette-Guyonnet S, Secher M, & Vellas B (2013) Nutrition and neurodegeneration: epidemiological evidence and challenges for future research. *Brit J Clin Pharmaco* 75(3):738-755.
259. Luchsinger JA, Noble JM, & Scarmeas N (2007) Diet and Alzheimer's disease. *Curr Neurol Neurosci* 7(5):366-372.
260. Brewer GJ (2010) Risks of copper and iron toxicity during aging in humans. *Chem Res Toxicol* 23(2):319-326.
261. Polla BS (1999) Therapy by taking away: The case of iron. *Biochem Pharmacol* 57(12):1345-1349.
262. Xu JZ, *et al.* (2010) The emerging role of iron dyshomeostasis in the mitochondrial decay of aging. *Mech Ageing Dev* 131(7-8):487-493.
263. Johnstone D & Milward EA (2010) Genome-wide microarray analysis of brain gene expression in mice on a short-term high iron diet. *Neurochem Int* 56(6-7):856-863.
264. Pichler I, *et al.* (2013) Serum iron levels and the risk of Parkinson disease: a mendelian randomization study. *PLoS Med* 10(6):e1001462.
265. Bartzokis G, *et al.* (2011) Gender and iron genes may modify associations between brain iron and memory in healthy aging. *Neuropsychopharmacol* 36(7):1375-1384.
266. Bathum L, *et al.* (2001) Association of mutations in the hemochromatosis gene with shorter life expectancy. *Arch Intern Med* 161(20):2441-2444.
267. Jellen LC, *et al.* (2012) Systems genetic analysis of the effects of iron deficiency in mouse brain. *Neurogenetics* 13(2):147-157.
268. Arruda LF, Arruda SF, Campos NA, de Valencia FF, & Siqueira EMD (2013) Dietary iron concentration may influence aging process by altering oxidative stress in tissues of adult rats. *Plos One* 8(4).
269. Crowe A & Morgan EH (1996) Iron and copper interact during their uptake and deposition in the brain and other organs of developing rats exposed to dietary excess of the two metals. *J Nutr* 126(1):183-194.
270. Sobotka TJ, *et al.* (1996) Neurobehavioral dysfunctions associated with dietary iron overload. *Physiol Behav* 59(2):213-219.

271. Sotogaku N, Oku N, & Takeda A (2000) Manganese concentration in mouse brain after intravenous injection. *J Neurosci Res* 61(3):350-356.
272. Monnot AD, Behl M, Ho SN, & Zheng W (2011) Regulation of brain copper homeostasis by the brain barrier systems: Effects of Fe-overload and Fe-deficiency. *Toxicol Appl Pharm* 256(3):249-257.
273. Ke Y, *et al.* (2005) Age-dependent and iron-independent expression of two mRNA isoforms of divalent metal transporter 1 in rat brain. *Neurobiol Aging* 26(5):739-748.
274. Yu SY, Feng Y, Shen ZL, & Li M (2011) Diet supplementation with iron augments brain oxidative stress status in a rat model of psychological stress. *Nutrition* 27(10):1048-1052.
275. Taylor EM, Crowe A, & Morgan EH (1991) Transferrin and iron uptake by the brain: effects of altered iron status. *J Neurochem* 57(5):1584-1592.
276. Dallman PR, Siimes MA, & Manies EC (1975) Brain iron: persistent deficiency following short-term iron deprivation in young rat. *Brit J Haematol* 31(2):209-215.
277. Chen Q, Connor JR, & Beard JL (1995) Brain Iron, transferrin and ferritin concentrations are altered in developing iron-deficient rats. *J Nutr* 125(6):1529-1535.
278. Beard JL, *et al.* (2006) Moderate iron deficiency in infancy: Biology and behavior in young rats. *Behav Brain Res* 170(2):224-232.
279. Felt BT & Lozoff B (1996) Brain iron and behavior of rats are not normalized by treatment of iron deficiency anemia during early development. *J Nutr* 126(3):693-701.
280. Williamson AM & Ng KT (1980) Behavioral effects of iron deficiency in the adult rat. *Physiol Behav* 24(3):561-567.
281. Erikson KM, Pinero DJ, Connor JR, & Beard JL (1997) Regional brain iron, ferritin and transferrin concentrations during iron deficiency and iron repletion in developing rats. *J Nutr* 127(10):2030-2038.
282. Beard JL, Wiesinger JA, Li N, & Connor JR (2005) Brain iron uptake in hypotransferrinemic mice: influence of systemic iron status. *J Neurosci Res* 79(1-2):254-261.
283. Ahluwalia N, *et al.* (2000) Iron status and stores decline with age in Lewis rats. *J Nutr* 130(9):2378-2383.
284. Solfrizzi V, Panza F, & Capurso A (2003) The role of diet in cognitive decline. *J Neural Transm* 110(1):95-110.
285. Sofi F, Cesari F, Abbate R, Gensini GF, & Casini A (2008) Adherence to Mediterranean diet and health status: meta-analysis. *Brit Med J* 337(7671).
286. Butterfield D, *et al.* (2002) Nutritional approaches to combat oxidative stress in Alzheimer's disease. *J Nutr Biochem* 13(8):444.
287. Loef M & Walach H (2012) Copper and iron in Alzheimer's disease: a systematic review and its dietary implications. *Brit J Nutr* 107(1):7-19.
288. Shoham S & Youdim MBH (2004) Nutritional iron deprivation attenuates kainate-induced neurotoxicity in rats: Implications for involvement of iron in neurodegeneration. *Ann Ny Acad Sci* 1012:94-114.
289. Gallagher M & Rapp PR (1997) The use of animal models to study the effects of aging on cognition. *Annu Rev Psychol* 48:339-370.
290. Levenson CW, *et al.* (2004) Role of dietary iron restriction in a mouse model of Parkinson's disease. *Exp Neurol* 190(2):506-514.

291. Gomez M, Esparza JL, Cabre M, Garcia T, & Domingo JL (2008) Aluminum exposure through the diet: Metal levels in A beta PP transgenic mice, a model for Alzheimer's disease. *Toxicology* 249(2-3):214-219.
292. Yantiri F & Andersen JK (1999) The role of iron in Parkinson disease and 1-methyl-4-phenyl-1,2,3,6-tetrahydropyridine toxicity. *Iubmb Life* 48(2):139-141.
293. Lan J & Jiang DH (1997) Excessive iron accumulation in the brain: a possible potential risk of neurodegeneration in Parkinson's disease. *J Neural Transm* 104(6-7):649-660.
294. Love R (2004) Dietary iron in Parkinson's disease: a double edged sword. *Lancet Neurol* 3(12):699-699.
295. Railey AM, Groeber CM, & Flinn JM (2011) The effect of metals on spatial memory in a transgenic mouse model of Alzheimer's disease. *J Alzheimers Dis* 24(2):375-381.
296. Youdim MB (2012) M30, a brain permeable multitarget neurorestorative drug in post nigrostriatal dopamine neuron lesion of parkinsonism animal models. *Parkinsonism Relat Disord* 18 Suppl 1:S151-154.
297. Mounsey RB & Teismann P (2012) Chelators in the treatment of iron accumulation in Parkinson's disease. *Int J Cell Biol* 2012:12.
298. Kupershmidt L, Amit T, Bar-Am O, Youdim MBH, & Weinreb O (2012) Neuroprotection by the multitarget iron chelator M30 on age-related alterations in mice. *Mech Ageing Dev* 133(5):267-274.
299. Bonda DJ, *et al.* (2012) Nanoparticle delivery of transition-metal chelators to the brain: oxidative stress will never see it coming! *Cns Neurol Disord-Dr* 11(1):81-85.
300. Xu Q, Kanthasamy AG, & Reddy MB (2011) Phytic acid protects against 6-hydroxydopamine-induced dopaminergic neuron apoptosis in normal and iron excess conditions in a cell culture model. *Parkinson's Disease* 2011.
301. Mandel SA, *et al.* (2005) Multifunctional activities of green tea catechins in neuroprotection - Modulation of cell survival genes, iron-dependent oxidative stress and PKC signaling pathway. *Neurosignals* 14(1-2):46-60.
302. Mandel SA & Youdim MB (2012) In the rush for green gold: Can green tea delay age-progressive brain neurodegeneration? *Recent Pat CNS Drug Discov* 7(3):205-217.
303. Halliwell B (2007) Dietary polyphenols: Good, bad, or indifferent for your health? *Cardiovasc Res* 73(2):341-347.
304. Chaturvedi RK, *et al.* (2006) Neuroprotective and neurorescue effect of black tea extract in 6-hydroxydopamine-lesioned rat model of Parkinson's disease. *Neurobiol Dis* 22(2):421-434.
305. Rossi L, Mazzitelli S, Arciello M, Capo CR, & Rotilio G (2008) Benefits from dietary polyphenols for brain aging and Alzheimer's disease. *Neurochem Res* 33(12):2390-2400.
306. Pan TH, Jankovic J, & Le WD (2003) Potential therapeutic properties of green tea polyphenols in Parkinson's disease. *Drug Aging* 20(10):711-721.
307. Dajas F, *et al.* (2005) Flavonoids and the brain: Evidences and putative mechanisms for a protective capacity. *Curr Neuropharmacol* 3(3):193-205.
308. Dajas F, *et al.* (2003) Cell culture protection and in vivo neuroprotective capacity of flavonoids. *Neurotox Res* 5(6):425-432.
309. Ames BN, Shigenaga MK, & Hagen TM (1993) Oxidants, antioxidants, and the degenerative diseases of aging. *P Natl Acad Sci USA* 90(17):7915-7922.
310. Leung LK, *et al.* (2001) Theaflavins in black tea and catechins in green tea are equally effective antioxidants. *J Nutr* 131(9):2248-2251.

311. Dufresne CJ & Farnworth ER (2001) A review of latest research findings on the health promotion properties of tea. *J Nutr Biochem* 12(7):404-421.
312. Graf E, Empson KL, & Eaton JW (1987) Phytic acid - a natural antioxidant. *J Biol Chem* 262(24):11647-11650.
313. Anekonda TS, *et al.* (2011) Phytic acid as a potential treatment for Alzheimer's pathology: Evidence from animal and in vitro models. *J Alzheimers Dis* 23(1):21-35.
314. Nadon NL (2006) Chapter 25 - Gerontology and Age-Associated Lesions. *The Laboratory Rat (Second Edition)*, eds Mark AS, Steven HW, Craig L. FranklinA2 - Mark A. Suckow SHW, & Craig LF (Academic Press, Burlington), pp 761-772.
315. Gallaher DD (1992) Animal models in human nutrition research. *Nutr Clin Pract* 7(1):37-39.
316. Baker E, Morton AG, & Tavill AS (1980) The regulation of iron release from the perfused rat liver. *Brit J Haematol* 45(4):607-620.
317. Quinn R (2005) Comparing rat's to human's age: How old is my rat in people years? *Nutrition* 21(6):775-777.
318. Roskams AJI & Connor JR (1994) Iron, transferrin, and ferritin in the rat brain during development and aging. *J Neurochem* 63(2):709-716.
319. Takahashi S, *et al.* (2001) Age-related changes in the concentrations of major and trace elements in the brain of rats and mice. *Biol Trace Elem Res* 80(2):145-158.
320. Tarohda T, Yamamoto M, & Amano R (2004) Regional distribution of manganese, iron, copper, and zinc in the rat brain during development. *Anal Bioanal Chem* 380(2):240-246.
321. Hevesy G (1923) The Absorption and Translocation of Lead by Plants: A Contribution to the Application of the Method of Radioactive Indicators in the Investigation of the Change of Substance in Plants. *Biochem J* 17(4-5):439-445.
322. Hahn PF, Bale WF, & Balfour WM (1942) Radioactive iron used to study red blood cells over long periods - The constancy of the total blood volume in the dog. *Am J Physiol* 135(3):0600-0605.
323. Balfour WM, Hahn PF, Bale WF, Pommerenke WT, & Whipple GH (1942) Radioactive iron absorption in clinical conditions: normal, pregnancy, anemia, and hemochromatosis. *J Exp Med* 76(1):15-30.
324. Patterson KY & Veillon C (2001) Stable isotopes of minerals as metabolic tracers in human nutrition research. *Exp Biol Med* 226(4):271-282.
325. Jackson M & Lowe N (2002) *Advances in isotope methods for the analysis of trace elements in man* (Taylor & Francis) pp 1-34.
326. Rosman KJR & Taylor PDP (1999) Isotopic compositions of the elements 1997. *J Anal Atom Spectrom* 14(1):5N-24N.
327. Peacock WC, *et al.* (1946) The Use of 2 Radioactive Isotopes of Iron in Tracer Studies of Erythrocytes. *J Clin Invest* 25(4):605-615.
328. Finch CA (1959) Body iron exchange in man. *J Clin Invest* 38(2):392-396.
329. Pollycove M & Mortimer R (1961) Quantitative determination of iron kinetics and hemoglobin synthesis in human subjects. *J Clin Invest* 40(5):753-&.
330. Van Campen D (1973) Enhancement of iron absorption from ligated segments of rat intestine by histidine, cysteine, and lysine: effects of removing ionizing groups and of stereoisomerism. *J Nutr* 103(1):139-142.
331. Jackson M & Lowe N (2002) *Advances in isotope methods for the analysis of trace elements in man* (Taylor & Francis) pp 25-27.
332. Dwork AJ, *et al.* (1990) An autoradiographic study of the uptake and distribution of iron by the brain of the young rat. *Brain Res* 518(1-2):31-39.

333. Morris CM, Keith AB, Edwardson JA, & Pullen RGL (1992) Uptake and distribution of iron and transferrin in the adult-rat brain. *J Neurochem* 59(1):300-306.
334. Ueda F & Bradbury MWB (1992) Rate and mechanism of 59Fe transport into brain and other tissues of the anaesthetized rat and mouse. *J Physiol* 446(Proceedings of the Physiological Society):98P.
335. Crowe A & Morgan EH (1994) Effects of chelators on iron uptake and release by the brain in the rat. *Neurochem Res* 19(1):71-76.
336. Dwork AJ (1995) Effects of diet and development upon the uptake and distribution of cerebral iron. *J Neurol Sci* 134:45-51.
337. Malecki EA, Cook BM, Devenyi AG, Beard JL, & Connor JR (1999) Transferrin is required for normal distribution of Fe-59 and Mn-54 in mouse brain. *J Neurol Sci* 170(2):112-118.
338. Takeda A, Takatsuka K, Connor JR, & Oku N (2001) Abnormal iron accumulation in the brain of neonatal hypotransferrinemic mice. *Brain Res* 912(2):154-161.
339. Takeda A, Takatsuka K, Sotogaku N, & Oku N (2002) Influence of iron-saturation of plasma transferrin in iron distribution in the brain. *Neurochem Int* 41(4):223-228.
340. Walczyk T (2012) The use of stable isotope techniques for studying mineral and trace element metabolism in humans. *Isotopic Analysis*, (Wiley-VCH Verlag GmbH & Co. KGaA), pp 435-494.
341. Bohn T (2003) Magnesium absorption in humans. Doctor of Natural Sciences (Swiss Federal Institute of Technology Zurich).
342. Heumann KG (1992) Isotope-dilution mass-spectrometry. *Int J Mass Spectrom Ion Process* 118:575-592.
343. Debievre P (1994) Stable isotope dilution: an essential tool in metrology. *Fresen J Anal Chem* 350(4-5):277-283.
344. Debievre P (1990) Isotope-dilution mass-spectrometry - what can it contribute to accuracy in trace analysis. *Fresen J Anal Chem* 337(7):766-771.
345. Debievre P, Savory J, Lamberty A, & Savory G (1988) Meeting the need for reference measurements. *Fresen Z Anal Chem* 332(6):718-721.
346. Kaldor I (1954) Studies on intermediary iron metabolism .5. The Measurement of non-haemoglobin tissue iron. *Aust J Exp Biol Med* 32(6):795-799.
347. Thomson JJ (1912) Further experiments on positive rays. *Philos Mag* 24(140):209-253.
348. Heumann KG, *et al.* (1995) Recent developments in thermal ionization mass spectrometric techniques for isotope analysis - a review. *Analyst* 120(5):1291-1299.
349. Yang L (2009) Accurate and precise determination of isotopic ratios by MC-ICP-MS: A review. *Mass Spectrom Rev* 28(6):990-1011.
350. Ingle C, *et al.* (2002) Development of a high-resolution ICP-MS method, suitable for the measurement of iron and iron isotope ratios in acid digests of faecal samples from a human nutrition study. *J Anal At Spectrom* 17(11):1498-1501.
351. Walczyk T, Davidsson L, Zavaleta N, & Hurrell RF (1997) Stable isotope labels as a tool to determine the iron absorption by Peruvian school children from a breakfast meal. *Fresen J Anal Chem* 359(4-5):445-449.
352. Dixon PR, *et al.* (1993) Measurement of iron isotopes (Fe-54, Fe-56, Fe-57, and Fe-58) in submicrogram quantities of iron. *Anal Chem* 65(15):2125-2130.
353. Fox TE, Eagles J, & Fairweather-Tait SJ (1998) Bioavailability of iron glycine as a fortificant in infant foods. *Am J Clin Nutr* 67(4):664-668.

354. O'Brien KO, Zavaleta N, Caulfield LE, Yang DX, & Abrams SA (1999) Influence of prenatal iron and zinc supplements on supplemental iron absorption, red blood cell iron incorporation, and iron status in pregnant Peruvian women. *Am J Clin Nutr* 69(3):509-515.
355. Denk E (2005) Evaluation of Ca-41 as a novel isotopic tool to assess the impact of diet on bone health. Doctor of Natural Sciences (Swiss Federal Institute of Technology Zurich).
356. Calsteren P (1998) Thermal ionization mass spectrometry. *Geochemistry*, Encyclopedia of Earth Science, (Springer Netherlands), pp 623-624.
357. Wieser ME & Schwieters JB (2005) The development of multiple collector mass spectrometry for isotope ratio measurements. *Int J Mass Spectrom* 242(2–3):97-115.
358. Houk, R. S., V. A. Fassel, G. D. Flesch, et al. (1980). Inductively coupled argon plasma as an ion source for mass spectrometric determination of trace elements. *Anal Chem* 52(14): 2283-2289.
359. Chen, Z. S., I. J. Griffin, L. M. Plumlee, et al. (2005). High resolution inductively coupled plasma mass spectrometry allows rapid assessment of iron absorption in infants and children. *J Nutr* 135(7): 1790-1795.
360. Gonzalez-Iglesias, H., M. L. Fernandez-Sanchez, J. Lopez-Sastre, et al. (2012). Nutritional iron supplementation studies based on enriched Fe-57, added to milk in rats, and isotope pattern deconvolution-ICP-MS analysis. *Electrophoresis* 33(15): 2407-2415.
361. Ingle, C. P., N. Langford, L. J. Harvey, et al. (2004). Comparison of three different instrumental approaches to the determination of iron and zinc isotope ratios in clinical samples. *J Anal At Spectrom* 19(3): 404-406.
362. Benkhedda, K., H. Chen, R. Dabeka, et al. (2008). Isotope ratio measurements of iron in blood samples by multi-collector ICP-MS to support nutritional investigations in humans. *Biol Trace Elem Res* 122(2): 179-192.
363. Fantle, M. S. and T. D. Bullen (2009). Essentials of iron, chromium, and calcium isotope analysis of natural materials by thermal ionization mass spectrometry. *Chem Geol* 258(1-2): 50-64.
364. Giessmann, U. and U. Greb (1994). High resolution ICP-MS - a new concept for elemental mass spectrometry. *Fresenius J Anal Chem* 350(4-5): 186-193.
365. Thomas, R. (2001). A beginner's guide to ICP-MS - Part VII: Mass separation devices - Double-focusing magnetic-sector technology. *Spectroscopy* 16(11): 22-27.
366. Malinovsky, D., A. Stenberg, I. Rodushkin, et al. (2003). Performance of high resolution MC-ICP-MS for Fe isotope ratio measurements in sedimentary geological materials. *J Anal At Spectrom* 18(7): 687-695.
367. Dauphas, N., A. Pourmand and F. Z. Teng (2009). Routine isotopic analysis of iron by HR-MC-ICPMS: How precise and how accurate? *Chem Geol* 267(3-4): 175-184.
368. Heumann, K. G., S. M. Gallus, G. Radlinger, et al. (1998). Precision and accuracy in isotope ratio measurements by plasma source mass spectrometry. *J Anal At Spectrom* 13(9): 1001-1008.
369. Walczyk, T. (2004). TIMS versus multicollector-ICP-MS: coexistence or struggle for survival? *Anal Bioanal Chem* 378(2): 229-231.
370. Yang, L., Z. Mester, L. Zhou, et al. (2011). Observations of large mass-independent fractionation occurring in MC-ICPMS: implications for determination of accurate isotope amount ratios. *Anal Chem* 83(23): 8999-9004.

371. Johnson CC, Gorell JM, Rybicki BA, Sanders K, & Peterson EL (1999) Adult nutrient intake as a risk factor for Parkinson's disease. *Int J Epidemiol* 28(6):1102-1109.
372. Logroscino G, Gao X, Chen H, Wing A, & Ascherio A (2008) Dietary iron intake and risk of Parkinson's disease. *Am J Epidemiol* 168(12):1381-1388.
373. Loef M & Walach H (2011) Copper and iron in Alzheimer's disease: a systematic review and its dietary implications. *Br J Nutr* 107(01):7-19.
374. Miyake Y, *et al.* (2011) Dietary intake of metals and risk of Parkinson's disease: a case-control study in Japan. *J Neurol Sci* 306(1-2):98-102.
375. Walczyk T (1997) Iron isotope ratio measurements by negative thermal ionisation mass spectrometry using FeF4- molecular ions. *Int J Mass Spectrom Ion Process* 161(1-3):217-227.
376. Aggarwal SK & Jain HC (1995) Polyatomic ions in thermal ionization mass-spectrometry - challenges and opportunities. *Int J Mass Spectrom Ion Process* 141(2):149-160.1-4
377. Walczyk T & Heumann KG (1993) Iridium Isotope Ratio Measurements by Negative Thermal Ionization Mass-Spectrometry and Atomic-Weight of Iridium. *Int J Mass Spectrom Ion Process* 123(2):139-147.

Chapter 3

Stable iron isotope tracing reveals significant brain iron uptake in the adult rat

Jie-Hua Chen[a], Shahreena Shahnavas[a], Nadia Singh[a], Wei-Yi Ong[b], Thomas Walczyk[a,c]

[a] Department of Chemistry, National University of Singapore, 3 Science Drive 3, Singapore, 117543;
[b] Department of Anatomy, National University of Singapore, 4 Medical Drive, Singapore, 117597;
[c] Department of Biochemistry, National University of Singapore, 8 Medical Drive, Singapore, 117597;

Corresponding author: Thomas Walczyk
Department of Chemistry,
3 Science Drive 3,
Singapore, 117543
Tel.: (65) 6516 7986
Fax: (65) 6775 7895
Email: walczyk@nus.edu.sg

3.1 Abstract

Iron deposits in brain are a common hallmark of Alzheimer's disease and Parkinson's disease. This has spurred the hypothesis that iron may play a functional role in the pathogenesis of neurodegenerative disorders through free radical damage. Previous short-term studies using radiotracers suggested that brain iron uptake is small as compared to other tissues in adult rodents. This has led to the assumption that brain iron uptake must also be marginal in humans after brain development is complete. In this study we applied a novel approach to determine directly the fraction of iron that was transferred over time from diet to brain and other organs in adult rats. A known amount of a stable iron isotope (^{57}Fe) was fed with drinking water to adult rats over 4 months. Uptake of tracer iron and final iron content in tissues were assessed by Negative Thermal Ionization Mass Spectrometry (NTI-MS). We found that only a very small amount of dietary iron has entered the brain (0.000537 ± 0.000076%). This amount, however, is considerable relative to total brain iron content (9.19 ± 0.71%), which was lower but comparable to percentage uptake in other tissues. Whereas it remains unclear if excessive dietary iron intake is a risk factor in neurodegenerative diseases or if high systemic iron correlates to iron deposits in brain, our study suggests that uptake of dietary iron is much higher than previously thought. This finding challenges current beliefs and points to a possible role of iron nutrition in the pathogenesis of neurodegenerative disorders.

3.2 Introduction

Neurodegenerative disorders are on the rise with Alzheimer's disease (AD) and Parkinson's disease (PD) expected to reach epidemic levels in the coming decades. In 2006, 26.6 million people worldwide were living with AD. It has been predicted that more than 100 million people will suffer from AD in 2050 (1), while prevalence of PD may double from about 4.3 to 9 million people worldwide over the next 25 years (2). The projected rise in these neurodegenerative disorders necessitates a better understanding of the etiology of the disease.

AD and PD are age-related disorders without a known isolated cause (3). Their prevalence is increasing, even when adjusted for aging demographics (4, 5). This points to a possible role of environmental and lifestyle factors in the development of AD and PD in addition to ageing. Economic welfare has increased significantly over the past decades in industrialized countries and has affected lives in many ways, including diet. One significant change is the sharp increase in consumption of red meat over the past 50 years in industrialized countries and more recently in the developing world, with its consequent increase in dietary iron supply (6). Over the same time span, iron fortification of foods has become common practice due to its undisputed benefits for children and women of fertile age. In parallel, dietary supplements became widely available and easily accessible to the consumer beyond the control of health professionals.

Iron is vital for brain development, neurogenesis as well as normal brain function

(7). Free unbound iron, however, can induce oxidative stress through catalysis of Fenton and Haber-Weiss chemistry which results ultimately in the formation of highly reactive free radicals (8, 9). Iron deposits in brain in AD and PD patients have led to the suggestion that iron is possibly involved in the pathogenesis of neurodegenerative disorders (10) with many lines of evidence pointing to free radical damage as the underlying mechanism (11-13). A recent report also suggests an iron-dependent cell-death pathway to be critical in neuronal injury (14). Potential links between dietary iron and incidence of AD and PD have been studied in rats (15, 16) as well as humans (17-21) but, as yet, no firm conclusions can be drawn.

Although abnormal iron deposits are a common observation in the brain of AD and PD patients, the actual cause of this accumulation remains unknown. Iron deposits in the brain of AD and PD patients can result, theoretically, from iron translocation within the body due to a pathological impairment of brain iron uptake and/or release. Alternatively, deposits can be reflective of dietary iron exposure and an overall accumulation of iron in the body. Evolution has left the human body with no pathway to actively excrete iron. Systemic losses are uncontrolled and accidental with menstrual blood loss, occult bleedings in the intestine or secretion of digestive juices being major routes of iron loss from the body. This lack of control over iron excretion requires iron homeostasis to be exclusively maintained by tight regulation of iron absorption in the intestine (22, 23). If absorbed iron overcorrects for habitual losses, iron inevitably accumulates

in the body. This occurs, for example, in hereditary hemochromatosis as the most common genetic disorder in western populations. Some studies have shown that homozygotes for this disease show not only an excessive iron uptake in the intestine but are also at higher risk to contract neurodegenerative disorders (24, 25). For healthy individuals, however, it remains to be seen if excessive iron intake is a risk factor and if high body iron correlates with iron deposits in brain.

Our current understanding of brain iron dynamics has primarily come from radioisotope studies. To date, about a dozen short-term studies have been published in which brain iron uptake was studied in mice or rats using radioactive isotope tracers followed by tracer quantification in brain (26-34). These have been based on a single administration of a radiotracer to groups of animals at a given age, usually through intravenous or peritoneal injection, and sacrifice of animals relatively shortly after dose administration. While such an approach permits to study the effect of growth on brain iron uptake and underlying mechanisms and kinetics, it is less suitable to assess the effect of diet on brain iron content, particularly considering the importance of the intestine for systemic iron homeostasis. Furthermore, studies to date have not quantified brain iron uptake relative to total brain iron content, which is critical to assess proportional uptake and risks of iron accumulation.

In this study we have used for the first time ever a stable iron isotope (^{57}Fe) in brain research which has a low enough natural abundance to be employed as a

tracer. The tracer was added at fixed concentration to the drinking water and was fed continuously with the diet over 4 months to better mimic dietary intake. Stable isotope tracers do not decay and as such they do not emit radiation and are safe to use in animals and man. Because of their stability, they can be fed over extended periods and samples stored without any time limit, if deemed necessary (35). In addition, stable isotope spiking has permitted determination of tissue iron to determine relative iron uptake. Relative iron uptake of a tissue or organ is more relevant for identifying possible risks of iron accumulation than absolute iron uptake which can be misleading if tissue iron content is low.

3.3 Methods and materials

3.3.1 Animals

Seven male Wistar rats (6 to 8-month-old ex-breeders, body weight 664 ± 33 g) were obtained from a local supplier for laboratory animals. Rats were housed individually under laboratory conditions (12 hrs day and night lighting cycle, 21 ± 1 ℃, 55 ± 5% humidity). All experimental protocols were reviewed and approved by Institutional Animal Care and Use Committee (IACUC) of the National University of Singapore. At the end of the study, rats were anesthetized by intraperitioneal injection of a cocktail of ketamine (Parnell Laboratories PTY. LTD., Alexandria, Australia) and xylazine (Troy Laboratories PTY. LTD., Glendenning, Australia).

In order to answer how dietary iron is distributed between brain and other organs in adult mammals, we provided 6-8 month old ex-breeder male Wistar rats with isotopically-enriched $^{57}FeCl_3$. Male rats were used because they do not experience diestrus blood loss, which may confound iron concentrations (36). The isotope was delivered via the drinking water at an iron concentration of 4 µg/g, which translates into an intake of labeled iron of approximately 100 µg per day and rat. The pH of the drinking water was adjusted to 2.5 to prevent precipitation of iron as per established protocols. Water of low pH is well tolerated by rats as they have no taste receptors for water (37). All rats had *ad libitum* access to the ^{57}Fe-enriched drinking water and conventional rat chow (Teklad 2018S Rodent Diet, Harlan, Indianapolis, USA; iron concentration 200 mg/kg). Drinking water was changed every 3-4 days and bottles were weighed before and after each change to accurately assess stable isotope intake by each rat. Mean amount of enriched ^{57}Fe and natural iron consumed over the course of the study (16 weeks) was 8.90 ± 0.66 mg and 529 ± 16 mg per rat, respectively.

3.3.2 Stable isotope labels

Both isotopic labels were prepared from iron metal (Chemgas, Boulogne, France), isotopically enriched in ^{57}Fe (95.635 ± 0.018 % ^{57}Fe) and ^{58}Fe (99.879 ± 0.027 % ^{58}Fe). The isotopically enriched iron spikes were dissolved in 37% HCl and diluted with water to yield 5 M HCl solutions. The iron isotopic composition of the spike solutions was determined by negative thermal ionization mass spectrometry (NTI-MS) following published procedures (38). The iron concentration of the spike solutions was determined against a commercially

available iron standard solution (Titrisol, Merck, Darmstadt, Germany) by reversed mass spectrometric isotope dilution analysis (38, 39).

For all work involving isotopically enriched labels and blood/tissue samples, principles of inorganic trace analysis were followed so as to minimize the alteration of their iron isotopic composition through contamination with natural iron. All solutions were prepared and handled in polyethylene or Teflon containers pre-cleaned with 10% (v/v) HNO_3. Only analytical grade chemicals were used while nitric acid and hydrochloric acid were further purified by sub-boiling distillation. Samples and solutions were handled in metal free class 10 laminar flow hoods to minimize contamination of samples with natural iron.

3.3.3 Tissue sampling

Animals were sacrificed by hyper-perfusion, i.e. effective removal of blood from tissues by washing of vessels and organs *in situ* with excessive volumes of saline. This was done by opening the abdomen and chest of the anesthetized animals, incision the right atrium and perfusion through the left ventricle at room temperature with heparinized Ringer's solution (5 I.U. heparin/mL, NaCl 0.85%, KCl 0.025%, $CaCl_2$ 0.03%, $NaHCO_3$ 0.02%) using an infusion set and a 19 gauge ¾ inches winged-needle. Perfusion was continued until the effluent became colorless and the liver ochre brown. Used volumes of saline solution (2.5 L to 3 L per rat, 50-60 times the blood volume) were similar or higher than in earlier studies. After hyper-perfusion, whole brain, liver, heart and kidneys were removed and a muscle sample was taken from the upper calf of the hind leg.

Samples were then rinsed with physiologically buffered saline and stored at -20 ℃ until analysis.

3.3.4 Preparation of blood/tissue samples for iron isotopic analysis

For isotopic and elemental analysis, samples were freeze dried and grinded carefully into a fine powder with a ceramic pestle after encasing the samples in two layers of polyethylene zip lock bags to protect them from contamination. A weighed aliquot of the homogenized tissue was transferred into a Teflon vessel together with a known amount of enriched ^{58}Fe label to determine the amount of natural iron in the sample following isotope dilution principles (see below). Samples were mineralized in a microwave digestion system (Ethos 1, Milestone, Sorisole, Italy) using 8 mL conc. HNO_3 (Merck, Darmstadt, Germany) and 2 mL 30% H_2O_2 (Merck, Darmstadt, Germany). Samples were dried down under laminar flow conditions and digested a second time using the same procedures to effectively destroy the organic sample matrix. Isotopic analysis of tissue samples was performed in triplicate.

After mineralization, the solution was dried down and redissolved in 6 M HCl for iron separation by ion-exchange chromatography using the strongly basic ion-exchange resin Dowex AG 1-X8 (200 - 400 mesh, Sigma, St. Louis, USA). For separation, the solution was transferred to the top of a column (8 mm inner diameter) filled with the ion-exchange resin to a height of 40 mm. The column was rinsed with 20 mL 6 M HCl after loading and sample iron was eluted with 10 mL 1 M HNO_3 from the column. After evaporating the iron solution to dryness,

sample iron was redissolved in 6 M HCl and rerun through a second column using the same procedure. The eluate was evaporated to dryness, reconstituted in 0.2 mL 1 M HNO_3 and alkalized by an addition of 1 mL 25% ammonium hydroxide (Merck, Darmstadt, Germany) for iron precipitation. Iron was separated by centrifugation for 45 minutes at 13,000 rpm. The obtained precipitate was washed twice with water and centrifuged each time for 20 minutes at 13,000 rpm. The precipitate was dried in a 70℃ water bath and stored for mass spectrometric analysis in a capped polyethylene vial. With each batch of samples, a known amount of pure ^{58}Fe spike was passed through the entire sample preparation procedure to monitor procedural blanks. Each blood/tissue sample was prepared and isotopically analyzed in triplicate.

3.3.5 Iron analysis of blood

To verify that rats did not become anemic, blood samples were collected at the beginning of the study from the tail artery and the end of the study by cardiac puncture. Concentration of hemoglobin in the rat blood was indirectly determined by measuring the iron concentration of blood using Graphite Furnace Atomic Absorption Spectrometry (GF-AAS). The concentration of hemoglobin in the blood was then calculated based on the concentration of iron, the density of blood (1.06 g/mL) and the iron content of hemoglobin (3.47 mg iron/g). Blood iron concentration was determined in triplicate.

3.3.6 Mass spectrometry

The iron isotopic composition of the isotopic labels and the prepared samples were determined by negative thermal ionization mass spectrometry (NTI-MS)

using FeF_4^- molecular ions and a rhenium double-filament ion source (40). The evaporation filament as well as the ionization filament were coated with BaF_2 to promote the formation of negatively charged ions. Sample iron was loaded as FeF_3 in HF (40%) on top of the BaF_2 layer on the evaporation filament which was then coated with a AgF layer. All mass spectrometric measurements were carried out with a multi-collector thermal ionization mass spectrometer (Triton, Bremen, Germany) equipped with set of Faraday cups for simultaneous ion beam detection. For each individual measurement, 5 data blocks per run and 10 scans per data block were collected. Baseline measurement was performed before each block and the integration time for each scan was 16.777 sec. Precisions for replicate analysis of the same sample were of the order of 0.05% RSD for the $^{57}Fe/^{56}Fe$ ratio for samples and 0.01% for standards after internal normalization to correct for instrumental fractionation in the ion source. Data for samples containing tracer were normalized using an iterative algorithm. First, measured $^{57}Fe/^{56}Fe$ and $^{58}Fe/^{56}Fe$ isotope ratios were converted into amount ratios (in mole/mole) of ^{57}Fe tracer and ^{58}Fe tracer relative to natural iron using algorithms described elsewhere (38, 39). Using the calculated amount ratios of tracer to natural iron in the sample, the $^{54}Fe/^{56}Fe$ isotope ratio of the sample was estimated using the isotopic abundances of ^{54}Fe and ^{56}Fe in the tracers and natural iron. Measured isotope ratios were then normalized to this isotope ratio using an exponential law (41), the amount ratios of tracer to natural iron re-calculated and the $^{54}Fe/^{56}Fe$ isotope ratio in the sample re-estimated for normalization of measured isotope ratios. Iterative

cycles were repeated until estimates of the $^{54}Fe/^{56}Fe$ isotope ratio of the sample differed by less than 10^{-14} between cycles.

3.3.7 Data analysis

Amount of tracer and natural iron in samples was determined after internal normalization of measured data sets following isotope dilution principles as described earlier. The amount of natural iron $n(^{nat}Fe)$ in the sample aliquot was calculated from the calculated $n(^{58}Fe)/n(^{nat}Fe)$ amount ratio and the known amount of added ^{58}Fe spike (in moles) before digestion. The total amount of ^{57}Fe tracer in the sample could then be calculated from the $n(^{57}Fe)/n(^{nat}Fe)$ ratio and the $n(^{nat}Fe)$ in the analyzed sample. Total amount of tracer in the organ was calculated by taking the mass of tissue analyzed and the total mass of the organ/sample into account. Mass of blood was estimated from blood volume *BV* (*BV (mL) = 0.06 (mL/g) × body weight (g)+ 0.77(mL)*) (42) and blood density (1.06 g/ml). Element amounts (in units of moles) were converted into masses (in units of grams) and vice versa using the atomic weights of natural iron and that of the isotopic tracers, respectively.

Isotopic enrichment (*E*) of a tissue sample was calculated as the percentage change of the $^{57}Fe/^{56}Fe$ isotope ratio in the sample compared to natural iron. Transfer rates from diet to tissues (*T*) were calculated as total moles of tracer recovered in the sample/organ relative to total moles of tracer consumed with the drinking water. From the amount of dietary iron consumed and the transfer rate, the amount of non-tracer iron taken up from the diet and transferred into the

different body tissues was calculated. To better assess the magnitude of iron transfer, the amount of iron transferred into each tissue is expressed relative to the amount of total iron in the analyzed tissue.

3.4 Results

No premature deaths were observed among the treated rats. The rats showed a moderate increase in body weight from 664 ± 33 g to 728 ± 51 g over the course of the study, consistent with adult aging. Hemoglobin concentration was 141 ± 10 g Hb/L at the beginning and 140 ± 10 g Hb/L at the end of the study, i.e. within the normal range of 130-170 g/L (43) and with no detectable change over time, indicating that ^{57}Fe provision in drinking water had little effect on gross physiology.

Tracer dosage of approximately 1.75 μmole^{57}Fe per rat per day was found to be sufficient to reliably detect changes in isotopic iron composition of the target tissues (Table 3-1). Tracer doses could be kept low by high precision iron isotope analysis using multi-collector NTI-MS. Limit of quantification (LOQ) for isotopic enrichments was 0.5% based on a minimal necessary shift in the ^{57}Fe/^{56}Fe isotope ratio over its natural value of at least 10 times the standard deviation of replicate measurements. LOQ in this study was found to be limited primarily by available sample iron and ion signal intensities. Variations between individual rats were relatively small as indicated by the low standard deviations obtained for each type of tissue. To compare tracer iron uptake in our study with earlier studies involving tracer injection, we have to estimate the efficiency by which tracer iron was

absorbed in our study. Calculations were based on tracer recovery in blood (Table 3-1) and an incorporation efficiency of about 80% of absorbed tracer iron in red blood cells (44). Our estimated tracer absorption efficiency of 1.9% compares well with data in the literature.

Table 3-1 Iron concentration and iron isotopic enrichment of analyzed tissue samples.

Tissue	*c(Fe)* [µg/g]		*E* [%][a]	$n(^{57}Fe)/n(^{nat}Fe)$ [mol/mol][b]	$n(^{57}Fe)$ [nmol][c]
	Wet weight	Dry weight			
Blood	459 ± 32	-	27.0 ± 3.0	0.00600 ± 0.00066	2314 ± 264
Liver	112 ± 11	439 ± 42	20.1 ± 1.6	0.00445 ± 0.00036	207 ± 38
Kidney	36.1 ± 6.3	349 ± 40	18.2 ± 2.9	0.00404 ± 0.00063	14.3 ± 2.5
Heart	40.7 ± 3.8	224 ± 13	8.50 ± 0.81	0.00188 ± 0.00018	2.80 ± 0.37
Brain	13.50 ± 0.65	59.8 ± 3.9	6.94 ± 0.57	0.00154 ± 0.00013	0.85 ± 0.12
Muscle	-	-	5.32 ± 0.84	0.00118 ± 0.00019	-

[a] Isotopic enrichment *E* is expressed as the relative deviation of the measured from the natural $^{57}Fe/^{56}Fe$ isotopic ratio of 0.023096 ± 0.000072 (45).
[b] Molar ratio of ^{57}Fe tracer to natural iron.
[c] Amount of tracer recovered in blood/organs.

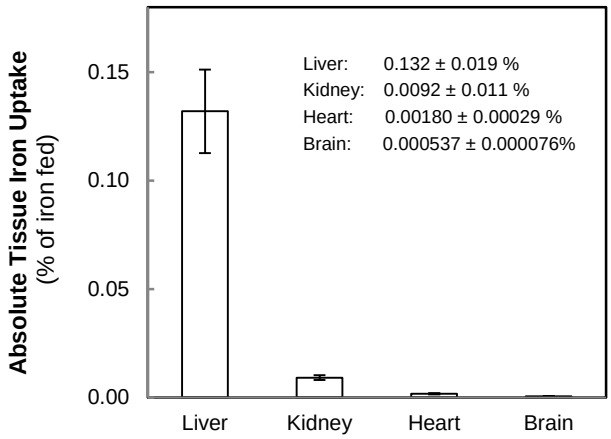

Fig. 3-1 Iron transfer efficiency from diet to organs
Absolute iron uptake is presented as the percentage of tracer recovered in the organ relative to the total amount of tracer iron given in feed (156 ± 12 µmol over 4 months). Values are given as arithmetic means ± SD (n=7 rats; each sample was analyzed in triplicate).

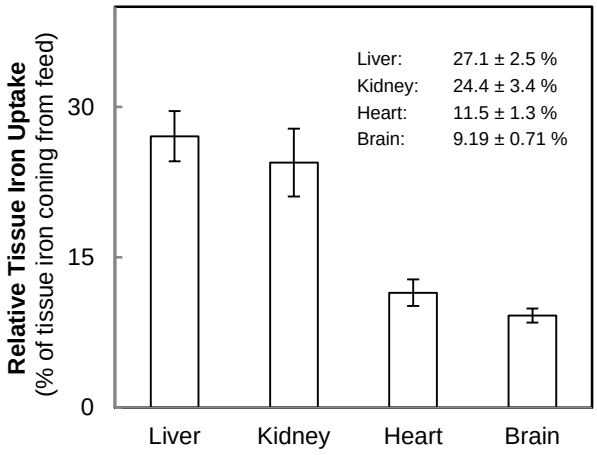

Fig. 3-2 Fraction of iron in the organ coming from feed.
Relative iron uptake was calculated as the amount of iron in the organ that could be traced back to feed relative to total iron content of the organ. Values are given as arithmetic means ± SD (n=7 rats; each sample was analyzed in triplicate).

Isotopic enrichments (*E*), as the percentage change in an isotope ratio relative to its natural value, ranged from 27.0 % for blood down to 5.32 % for muscle in good agreement with expected differences in iron turnover rates (Table 3-1). Blood has the highest turnover rate of all body iron pools due to constant renewal of red blood cells and hemoglobin synthesis. In contrast to blood, iron turnover of muscle tissue is low. Iron in muscle is mainly present as myoglobin for oxygen storage and is only released/replaced when muscle cells are catabolized. Consistent with previous studies (26), efficiency of iron transfer from the feed to the liver (0.132 ± 0.019 %, Fig. 3-1), was about ten times lower than for blood (1.48 ± 0.11%). Iron uptake of heart and kidney was lower by 3 orders of magnitude as compared to blood and even lower for brain (see Fig. 3-1). However, differences between tissues are much smaller when the fraction of iron taken up from the diet is expressed relative to total tissue iron content (see Fig. 3-2). Notably, only 0.00054% of dietary iron intake could be traced in brain but

this amount constitutes approximately 9% of total brain iron taking the low iron content of the organ into account. Thus, our study suggests that iron uptake of mammalian brain even in the mature organ is of similar order of magnitude as for the other tissues under investigation (11.5-27.1 %). This makes brain, in principle, as vulnerable to systemic iron overload and iron accumulation as the other studied organs. An increase in iron content of these tissues is well documented for high iron status or pathologically excessive iron absorption as observed in patients with hereditary hemochromatosis.

3.5 Discussion

In this study we used successfully a stable iron isotope to assess distribution of absorbed iron between organs and the magnitude of iron uptake relative to total iron content of body tissues. Isotopic iron fed to adult rats was broadly distributed among the analyzed tissues at surprisingly similar fractional quantities. This finding challenges the current belief that iron is largely excluded from entering brain by tight regulation of iron entry at the blood-brain barrier (46, 47).

Our current knowledge of the efficiency by which iron is taken up by the brain comes exclusively from merely a dozen animal experiments employing radiotracers. In these experiments, tracer iron uptake of brain was measured in sacrificed animals after administration of a single tracer dose, usually through intravenous or peritoneal injection. Studies were largely conducted in young rats looking at iron as a limiting nutrient for brain development. While such an approach permits to study the effect of growth on brain iron uptake, it is less

suitable to assess the effect of diet on brain iron content during adulthood. Firstly, findings for young animals cannot be extrapolated to adult life. Brain iron uptake drops sharply at an age of 15 to 30 days in rats and declines thereafter at a slower rate up to 5 months (26, 27, 32, 48, 49) and 11 weeks in mice (34). Secondly, the time span between injection and sampling must be long enough to consider that tracer entering brain may not be permanently deposited and possibly subject to export. Accordingly, we yet know little about brain iron turnover as the fraction of iron taken up and leaving brain per unit time. Finally, tracer injection bypasses the intestinal tract as the key regulator of systemic iron uptake. The normal physiological response to a change in dietary iron intake is up-regulation or down-regulation of intestinal iron absorption over time. To take an adaptive response of the body into account, continuous feeding of the tracer over longer periods of time is necessary. In contrast to stable isotopes, such studies are difficult to conduct using radiotracers because of their instability and radiation safety.

Earlier radiotracer studies have shown that only a very small fraction of dietary iron is used by the brain even in the growing organism. In these studies, tracer iron was injected bypassing the intestinal tract. To put our study into perspective, we had to estimate fractional iron absorption from diet in our study for assessing the amount of tracer iron that has entered circulation. Intestinal iron absorption in the rat is age dependent and declines rapidly with age. Ezekiel (1967) reported that intestinal absorption in the rat dropped from 80%-100% at 15 days to 60% at 20 days and 8.7% at 2-3 months (50). Similar observations were made by Forbes

and Reina (1972) (51). Our estimated average absorption rate of about 1.9% at an age of 10-12 months of our rats at sacrifice follows this declining trend. Generally, isotopic enrichment for the organs in our study followed the same trend as reported in earlier studies (26, 28, 34). At an estimated absorption rate of 1.9% and an efficiency of tracer transfer from diet to brain of 0.00054% it can be calculated that about 0.028% of the tracer would have been recovered in brain had it been given via intravenous injection. This recovery is in good agreement with previous data taking the age of our rats (10-12 mo) into account. Prior studies reported a decline of tracer uptake with age in adult animals (26, 27, 32, 48, 52). Recovery of injected tracer iron was 0.055% for 10-wk mice (34) and approximately 0.05% for 63-day old rats (28, 32).

One of the unique advantages of the stable isotope approach described here is the possibility to assess brain iron uptake over extended periods of time relative to total brain iron. Brain iron uptake must always be evaluated relative to total brain iron to assess risks of iron accumulation. This makes an accurate assessment of total brain iron content as important as a reliable estimate of intake. For this reason we have analyzed tissue iron contents by isotope ratio analysis and IDMS. IDMS is widely considered as a reference technique for elemental analysis as all sources of analytical uncertainty can be identified and quantitatively assessed (53-55). Although more tedious, this approach permits a more accurate assessment of iron contents than what can be achieved by conventional elemental analysis using inductively coupled plasma mass spectrometry, optical emission spectroscopy, or

atomic absorption spectrometry as the more widely employed techniques for measuring iron concentration and content. Using these more sophisticated analytical techniques, the determined iron levels in the brain of middle-age rats in the present study (Table 3-1) were in good agreement with concentration ranges reported in earlier studies (26, 27, 32, 56).

The most surprising finding in our study is the observation that iron uptake by brain is significant in normal adult rats. About 9% of brain iron could be traced back to the diet over a period of four months, a time span that compares to 7-10 human years. Most published studies on brain iron uptake have focused on the developing brain and the consequences of iron deficiency due to its critical role in brain development (26, 27, 29, 30, 32, 34, 52, 57). In our study we have chosen rats that were 6-8 months old at study onset, an age at which growth can be considered complete and no significant gain in brain mass and whole body iron should occur. Brain uptake of injected radio-iron was also found to decrease near exponentially with age in earlier studies (26, 27, 29, 32, 48, 52) dropping sharply at approximately 20 days after birth (26, 52). These observations show a variable iron permeability of the blood brain barrier to iron and have let to the suggestion that brain iron uptake is only marginal during adulthood. Information on brain iron turnover is yet very limited due to methodological restrictions arising from the use of radioisotopes and the misconception that a low iron uptake of brain makes iron accumulation unlikely. Earlier studies point to a very slow turnover or even an unidirectional import into brain, i.e. iron taken up by the brain may

remain in brain over the life-time once it has entered brain (26, 52). Linear extrapolation of our data would point to a gain in brain iron during adulthood as high as 50-70% of the amount of iron present in early adulthood due to the naturally low iron content of brain as compared to other tissues. This would be in good agreement with the fundamental study of Hallgren et al. (1958) in humans who analyzed brain iron content of 81 individuals of different age (58). After a sharp rise in brain iron content in the first years of life, iron accumulation appears to slow down but with a steady increase over the remaining lifetime.This could be confirmed in more recent post mortem studies which showed an increase in iron, ferritin and neuromelanin with age in the substantia nigra (SN) of normal human subjects (46, 59). Although not possible yet for reasons of analytical sensitivity, it is possible in principle to trace brain iron uptake down to the different element species and brain regions by continuous feeding of iron stable isotopes. The methods presented here are the first step in this direction. Molecular mechanisms of iron uptake and release of iron from the brain and shuttling within brain are still poorly understood.

3.6 Conclusion

By studying for the first time ever long-term iron uptake by the adult brain in a mammalian model we found that absolute brain iron uptake is small as compared to other tissues but considerable when measured relative to brain iron content. This became possible by using a stable iron isotope for tracing instead of short-living radiotracers and by measuring directly the fraction of iron in brain that originates from diet. Iron accumulation in brain is a still unexplained phenomenon

in the development of AD and PD. Using the developed methods and protocols, it is now possible to explore factors leading to iron accumulation by the brain in adulthood or strategies how to lower brain iron content during ageing, a therapeutic approach already discussed for neurodegenerative disorders (60, 61).

3.7 Bibliography

1. Brookmeyer R, Johnson E, Ziegler-Graham K, & Arrighi HM (2007) Forecasting the global burden of Alzheimer's disease. *Alzheimers Dement* 3(3):186-191.
2. Dorsey ER, *et al.* (2007) Projected number of people with Parkinson disease in the most populous nations, 2005 through 2030. *Neurology* 68(5):384-386.
3. Barnes DE & Yaffe K (2011) The projected effect of risk factor reduction on Alzheimer's disease prevalence. *Lancet Neurol* 10(9):819-828.
4. Kokmen E, Beard CM, OBrien PC, & Kurland LT (1996) Epidemiology of dementia in Rochester, Minnesota. *Mayo Clin Proc* 71(3):275-282.
5. Sekita A, *et al.* (2010) Trends in prevalence of Alzheimer's disease and vascular dementia in a Japanese community: the Hisayama Study. *Acta Psychiat Scand* 122(4):319-325.
6. FAO (2010) *The state of food and agriculture 2009: live stock in the balance* (Bernan Assoc).
7. Crichton RR, Dexter DT, & Ward RJ (2011) Brain iron metabolism and its perturbation in neurological diseases. *Monatsh Chem* 142(4):341-355.
8. Kehrer JP (2000) The Haber-Weiss reaction and mechanisms of toxicity. *Toxicology* 149(1):43-50.
9. Altamura S & Muckenthaler MU (2009) Iron toxicity in diseases of aging: Alzheimer's disease, Parkinson's disease and atherosclerosis. *J Alzheimers Dis* 16(4):879-895.
10. Loef M & Walach H (2011) Copper and iron in Alzheimer's disease: a systematic review and its dietary implications. *Br J Nutr* 107(01):7-19.
11. Jomova K & Valko M (2011) Advances in metal-induced oxidative stress and human disease. *Toxicology* 283(2-3):65-87.
12. Jomova K, Vondrakova D, Lawson M, & Valko M (2010) Metals, oxidative stress and neurodegenerative disorders. *Mol Cell Biochem* 345(1-2):91-104.
13. Nishida Y (2011) The chemical process of oxidative stress by copper(II) and iron(III) ions in several neurodegenerative disorders. *Monatsh Chem* 142(4):375-384.
14. Dixon SJ, *et al.* (2012) Ferroptosis: an iron-dependent form of nonapoptotic cell death. *Cell* 149(5):1060-1072.
15. Borten O, *et al.* (2004) Effects of dietary restriction and metal supplementation on the accumulation of iron-laden glial inclusions in the aging rat hippocampus. *Biogerontology* 5(2):81-88.
16. Wright GL, *et al.* (2010) Metallomic distribution in various regions of the brain as influenced by dietary intakes and their implications. *Procedia Environmental Sciences* 2:149-161.
17. Loef M & Walach H (2012) Copper and iron in Alzheimer's disease: a systematic review and its dietary implications. *Brit J Nutr* 107(1):7-19.

18. Johnson CC, Gorell JM, Rybicki BA, Sanders K, & Peterson EL (1999) Adult nutrient intake as a risk factor for Parkinson's disease. *Int J Epidemiol* 28(6):1102-1109.
19. Powers KM, *et al.* (2003) Parkinson's disease risks associated with dietary iron, manganese, and other nutrient intakes. *Neurology* 60(11):1761-1766.
20. Logroscino G, Gao X, Chen HL, Wing A, & Ascherio A (2008) Dietary iron intake and risk of Parkinson's disease. *Am J Epidemiol* 168(12):1381-1388.
21. Miyake Y, *et al.* (2011) Dietary intake of metals and risk of Parkinson's disease: A case-control study in Japan. *J Neurol Sci* 306(1-2):98-102.
22. Brittenham GM (1994) The red cell cycle. *Iron metabolism in health and disease*, eds Brock JH, Halliday JW, Pippard MJ, & Powell LW (Saunders), pp 31-62.
23. Hotz K, Augsburger H, & Walczyk T (2011) Isotopic signatures of iron in body tissues as a potential biomarker for iron metabolism. *J Anal At Spectrom* 26(7):1347.
24. Dekker MCJ, *et al.* (2003) Mutations in the hemochromatosis gene (HFE), Parkinson's disease and parkinsonism. *Neurosci Lett* 348(2):117-119.
25. Connor JR & Lee SY (2006) HFE mutations and Alzheimer's disease. *J Alzheimers Dis* 10(2-3):267-276.
26. Taylor EM & Morgan EH (1990) Developmental changes in transferrin and iron uptake by the brain in the rat. *Dev Brain Res* 55(1):35-42.
27. Taylor EM, Crowe A, & Morgan EH (1991) Transferrin and iron uptake by the brain: effects of altered iron status. *J Neurochem* 57(5):1584-1592.
28. Crowe A & Morgan EH (1994) Effects of chelators on iron uptake and release by the brain in the rat. *Neurochem Res* 19(1):71-76.
29. Crowe A & Morgan EH (1992) Iron and transferrin uptake by brain and cerebrospinal fluid in the rat. *Brain Res* 592(1-2):8-16.
30. Dwork AJ (1995) Effects of diet and development upon the uptake and distribution of cerebral iron. *J Neurol Sci* 134:45-51.
31. Moos T & Morgan EH (1998) Kinetics and distribution of [Fe-59-I-125]transferrin injected into the ventricular system of the rat. *Brain Res* 790(1-2):115-128.
32. Moos T & Morgan EH (1998) Evidence for low molecular weight, non-transferrin-bound iron in rat brain and cerebrospinal fluid. *J Neurosci Res* 54(4):486-494.
33. Malecki EA, Cook BM, Devenyi AG, Beard JL, & Connor JR (1999) Transferrin is required for normal distribution of Fe-59 and Mn-54 in mouse brain. *J Neurol Sci* 170(2):112-118.
34. Beard JL, Wiesinger JA, Li N, & Connor JR (2005) Brain iron uptake in hypotransferrinemic mice: influence of systemic iron status. *J Neurosci Res* 79(1-2):254-261.
35. Walczyk T (2001) The potential of inorganic mass spectrometry in mineral and trace element nutrition research. *Fresenius J Anal Chem* 370(5):444-453.

36. Forbes A (2009) Iron and parenteral nutrition. *Gastroenterology* 137(5):S47-S54.
37. Hofstetter J, Suckow MA, & Hickman DL (2006) Morphophysiology. *The Laboratory Rat*, eds Suckow MA, Weisbroth SH, & Franklin CL (Academic Press), 2th Ed, pp 93-125.
38. Walczyk T, Davidsson L, Zavaleta N, & Hurrell RF (1997) Stable isotope labels as a tool to determine the iron absorption by Peruvian school children from a breakfast meal. *Fresen J Anal Chem* 359(4-5):445-449.
39. Walczyk T (2012) The use of stable isotope techniques for studying mineral and trace element metabolism in humans. *Isotopic Analysis*, (Wiley-VCH Verlag GmbH & Co. KGaA), pp 435-494.
40. Walczyk T (1997) Iron isotope ratio measurements by negative thermal ionisation mass spectrometry using FeF_4^- molecular ions. *Int J Mass Spectrom Ion Process* 161(1-3):217-227.
41. Russell WA, Papanastassiou DA, & Tombrello TA (1978) Ca isotope fractionation on Earth and other solar system materials. *Geochim Cosmochim Acta* 42(8):1075-1090.
42. Lee HB & Blaufox MD (1985) Blood volume in the rat. *J Nucl Med* 26(1):72-76.
43. Underwood EJ (1977) Iron. *Trace elements in human and animal nutrition*, ed Underwood EJ (Academic Press), 4th Ed, pp 14-15.
44. Reddy MB & Cook JD (1991) Assessment of dietary determinants of nonheme-iron absorption in humans and rats. *Am J Clin Nutr* 54(4):723-728.
45. Taylor PDP, Maeck R, & Debievre P (1992) Determination of the absolute isotopic composition and atomic-weight of a reference sample of natural iron. *Int J Mass Spectrom Ion Process* 121(1-2):111-125.
46. Crichton RR (2009) Brain iron homeostasis and its perturbation in various neurodegenerative diseases. *Iron metabolism: from molecular mechanisms to clinical consequences*, ed Crichton RR (John Wiley & Sons), 3rd Ed, pp 371-372.
47. Rouault TA & Cooperman S (2006) Brain iron metabolism. *Semin Pediatr Neurol* 13(3):142-148.
48. Morgan EH & Moos T (2002) Mechanism and developmental changes in iron transport across the blood-brain barrier. *Dev Neurosci* 24(2-3):106-113.
49. Crowe A & Morgan EH (1996) Iron and copper interact during their uptake and deposition in the brain and other organs of developing rats exposed to dietary excess of the two metals. *J Nutr* 126(1):183-194.
50. Ezekiel E (1967) Intestinal iron absorption by neonates and some factors affecting it. *J Lab Clin Med* 70(1):138-&.
51. Forbes GB & Reina JC (1972) Effect of age on gastrointestinal absorption (Fe, Sr, Pb) in rat. *J Nutr* 102(5):647-652.
52. Dallman PR & Spirito RA (1977) Brain iron in rat: extremely slow turnover in normal rats may explain long-lasting effects of early iron deficiency. *J Nutr* 107(6):1075-1081.

53. Debievre P (1990) Isotope-dilution mass-spectrometry - what can it contribute to accuracy in trace analysis. *Fresen J Anal Chem* 337(7):766-771.
54. Debievre P, Savory J, Lamberty A, & Savory G (1988) Meeting the need for reference measurements. *Fresen Z Anal Chem* 332(6):718-721.
55. Heumann KG (1992) Isotope-dilution mass-spectrometry. *Int J Mass Spectrom Ion Process* 118:575-592.
56. Roskams AJI & Connor JR (1994) Iron, transferrin, and ferritin in the rat brain during development and aging. *J Neurochem* 63(2):709-716.
57. Dwork AJ, *et al.* (1990) An autoradiographic study of the uptake and distribution of iron by the brain of the young rat. *Brain Res* 518(1-2):31-39.
58. Hallgren B & Sourander P (1958) The effect of age on the non-haemin iron in the human brain. *J Neurochem* 3(1):41-51.
59. Zecca L, Youdim MBH, Riederer P, Connor JR, & Crichton RR (2004) Iron, brain ageing and neurodegenerative disorders. *Nat Rev Neurosci* 5(11):863-873.
60. Budimir A (2011) Metal ions, Alzheimer's disease and chelation therapy. *Acta Pharmaceutica* 61(1):1-14.
61. Dexter DT, *et al.* (2011) Clinically available iron chelators induce neuroprotection in the 6-OHDA model of Parkinson's disease after peripheral administration. *J Neural Transm* 118(2):223-231.

Chapter 4

Imbalance of iron influx and efflux results in brain iron accumulation in the healthy adult rat

Jie-Hua Chen[a], Nadia Singh[a], Tay Huimin[a], Thomas Walczyk[a,b]

[a] Department of Chemistry, National University of Singapore, 3 Science Drive 3, Singapore, 117543;
[b] Department of Biochemistry, National University of Singapore, 8 Medical Drive, Singapore, 117597;

Corresponding author: Thomas Walczyk
Department of Chemistry,
3 Science Drive 3,
Singapore, 117543
Tel.: (65) 6516 7986
Fax: (65) 6775 7895
Email: walczyk@nus.edu.sg

4.1 Abstract

Iron accumulation in the brain with age is supposed to be involved in the development of neurodegenerative disorders including Alzheimer's and Parkinson Disease. The question remains, however, whether this accumulation process in the brain is uni-directional without efflux of deposited iron or a bi-directional process in which brain iron exchanges with body iron. The answer to this question may open up new possibilities to slow down brain iron accumulation and, thus, iron induced oxidative stress in the brain as a suspected mechanism of neurodegeneration.

In two separate studies we have fed up to three stable isotope tracers in parallel over 5 months to adult male 6-8 months old wild-type Wistar rats (n=7 per study). Tracers were fed continuously with the drinking water in a staggered design together with diet to assess if iron taken up earlier by the brain is subject to export (Study 1) and to determine iron influx and efflux into brain as well as its half-life in brain, liver, heart, kidneys and blood (Study 2).

In our study we could confirm the hypothesis that iron deposition in brain is bi-directional but unbalanced, i.e. iron influx from diet into brain was higher than iron efflux. The half-life of dietary iron in the adult rat brain was estimated to be about 9 months, which may serve as an indicator for the rather slow turnover rate of dietary iron in the brain. Based on the long half-life of dietary iron in the healthy rat brain, brain iron of the rats in our study can be estimated to increase by

27% from early adulthood (6-8 months of age) to the end of their average life span. It remains to be seen if brain iron accumulation as a possible risk factor for the development of neurodegenerative disorders can be moderated by dietary iron intake.

4.2 Introduction

Iron is the most abundant trace element within the brain. The ease in donating and accepting electrons renders iron an indispensable cofactor for a plethora of enzymatic reactions involved in neurogenesis, brain development and cognition sustenance (1). However, iron is potentially toxic to cells if systemic concentrations of free unbound iron exceed the body's scavenging capabilities. Uncomplexed iron can induce oxidative stress through catalysis of the Fenton and Haber-Weiss reactions which result ultimately in the formation of highly reactive free radicals (2, 3).

Age-related iron deposition within the brain has been observed in all species examined, including mice, rats, monkeys and humans (4-9). Progressively elevated brain iron with age may pose a threat to the brain's oxygen-rich environment by inducing oxidative stress via reactive oxygen species (ROS), ultimately leading to cell death (10-12). Many lines of evidence support now the hypothesis that iron accumulation in the brain with age might be implicated in the pathogenesis of age-related AD/PD with iron induced oxidative stress as the underlying mechanism (13, 14). It has been speculated that iron deposition in the brain could be reflective of dietary iron exposure and an overall accumulation of

iron in the body. Iron accumulation in the body is thus inevitable if iron absorbed from diet overcorrects for habitual losses.

In an earlier study we could demonstrate that stable iron isotopes can be used for tracing iron transfer directly from feed to brain in adult rats (15). In agreement with earlier radiotracers studies we found that less than 0.001% of iron in the diet was transferred to brain. However, due to the low iron content of brain this small amount constituted about 9% of total brain iron. Measurement of relative brain iron uptake became only possible by using stable isotope tracers as they do not decay. Furthermore, stable isotope tracing permits continuous tracer feeding to study brain iron dynamics at the systemic level as opposed to radiotracer protocols in which the tracer is commonly given only once by injection. The key question that remains now is whether brain iron import equals export or if more iron is imported than exported from brain and at which rate. The first scenario would not affect brain iron content in the long-term and tracer influx would reflect brain iron turnover. The second scenario would point to gradual accumulation of iron over time. The answer to this question may open up new possibilities to slow down brain iron accumulation.

In our first study we pioneered long-term feeding of a single tracer to mimic dietary iron influx into brain. In the present study, we have fed up to three stable isotope tracers in parallel to the same rat in a staggered design to assess iron influx/efflux and the half-life of dietary iron in the brain. As in our first study, we

conducted experiments in adult rats. It is reported that the rate of whole brain iron accumulation slows down after the first three decades of life (4) and it is possibly the amount of iron accumulated after that which contributes mainly to the development of the disease.

4.3 Methodology

4.3.1 Study design

The fate of dietary iron was investigated through dual- and triple-isotope feeding schemes. While the dual-isotope feeding scheme provides a qualitative assessment of brain iron balance, the triple-isotope feeding scheme permits to study iron dynamics quantitatively by comparing rates of iron influx and iron efflux and by estimation of the half-life of iron taken up by the brain, respectively.

The dual isotope feeding scheme involves the staggered administration of two different stable iron isotopes, Tracer 1 (T_1; ^{57}Fe) and Tracer 2 (T_2; ^{54}Fe) which are fed continuously over an equal duration of time. Two possible scenarios are illustrated in Fig. 4-1. If there is no export of iron after its deposition into brain, tracer amount ratios in brain must equal that of the feed at the time of sacrifice (see Fig. 4-1A). The more of imported iron is exported from brain, the larger is the difference in the amount ratio of both tracers in brain and feed at the end of the study (see Fig. 4-1B).

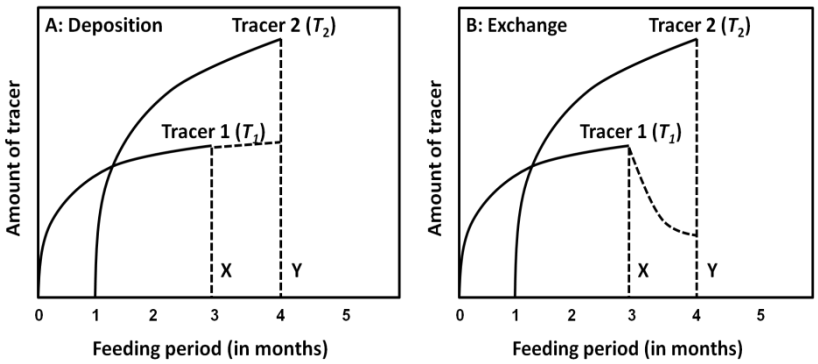

Fig. 4-1 Dual-isotope tracing for studying brain iron import and export
Tracer 1 (T_1) is administered from month 1 to 3 and Tracer 2 (T_2) from month 2 to 4 together with the feed. Vertical lines X and Y indicate the time points when tracer administration was terminated. Dashed lines represent the fate of the tracer thereafter. In **Fig. 4-1A**, iron is deposited in the brain in an uni-directional manner, resulting in the accumulation of both tracer in the brain. Without iron export from brain, the amount ratio of both tracers in brain should be equal to the amount ratio in the consumed feed In **Fig. 4-1B**, iron enters the brain in a bi-directional manner. If iron is exported from brain, the amount of the first tracer in brain will decrease when tracer administration is terminated. The amount ratio of both tracers in the brain is lower than the ratio in the consumed diet.

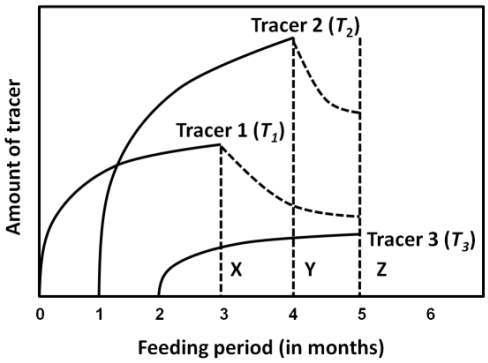

Fig. 4-2 Triple-isotope tracing for modeling kinetics of iron release from brain
The first tracer (T_1) is administered from month 1 to 3, the second tracer (T_2) from month 2 to 4 and the third tracer (T_3) from month 3 to 5. Vertical lines X and Y indicate the time points when tracer administration was terminated. Dashed lines represent the fate of the tracer thereafter. At the time of sacrifice (Z), amount ratios of tracers in brain differ from that of the feed when tracer has been exported from brain. Differences in amount ratios T_1/T_3 *and* T_2/T_3 in brain will be proportional to the rate by which deposited iron tracer is released from brain.

The triple-isotope feeding scheme involves the staggered administration of three different iron isotopes, Tracer 1 (T_1; ^{57}Fe), Tracer 2 (T_2; ^{54}Fe) and Tracer 3 (T_3; ^{58}Fe), respectively, see Fig. 4-2. If iron taken up from diet is exported from brain, tracer amount ratios in brain should be lower than that of the feed. For iron export, the amount ratio of T_1 to T_3 in the brain relative to that in the diet should

be lower than that of T_2 to T_3, since T_1 is administered first, followed by T_2 and lastly T_3. Differences in amount ratios between tracers, i.e. $n(T_1)/n(T_3)$ and $n(T_2)/n(T_3)$ can be used to model kinetics of iron release from brain.

4.3.2 Animals

Eight male Wistar rats (6 to 8-month old, body weight 625 ± 48 g) were obtained from a local supplier (Laboratory Animals Centre, LAC) and housed individually at a temperature of 21 ± 1 °C, with a humidity of 55 ± 5 % and a 12 hour light/dark cycle. Rats were randomly assigned to the two different feeding groups, *DI* (dual-isotope feeding scheme) group (n=3) and *TI* (triple-isotope feeding scheme) group (n=5). The body weight of the rats and the amount of water consumed by the rats were monitored weekly. All experimental protocols were reviewed and approved by Institutional Animal Care and Use Committee (IACUC) of National University of Singapore (NUS).

All rats had *ad libitum* access to a standard rat chow diet (Teklad 2018S Rodent Diet, Harlan, Indianapolis, USA; iron concentration 200 mg/kg) and isotopically enriched drinking water during the course of the study. In the *DI* group, the feeding period lasted for 4 months. The first tracer T_1 (^{57}Fe) was fed during month 1-3 while the second tracer T_2 (^{54}Fe) was fed during month 2-4 via the drinking water (see Fig. 4-1). The average concentrations of ^{54}Fe and ^{57}Fe in the drinking water for the *DI* group was 11.215 ± 0.021 and 5.207 ± 0.045 μg/g respectively. In the *TI* group, the feeding period was extended to 5 months to allow for feeding

of an additional enriched stable iron isotope. As for the *TI* group, all tracers were administered via drinking water. The first tracer T_1 (^{57}Fe) was fed during months 1 to 3, the second tracer T_2 (^{54}Fe) during month 2-4 and the third tracer T_3 (^{58}Fe) from month 3 to 5, respectively (see Fig. 4-2). The average concentrations of ^{54}Fe, ^{57}Fe and ^{58}Fe in the drinking water for *TI* group were, 11.201 $\pm$0.025, 5.216 $\pm$0.030 and 3.004 $\pm$0.016 µg/g, respectively.

In order to maintain dietary iron supply in both groups constant over the course of the study, differences in iron intake induced by differences in tracer concentration in the drinking water were balanced by adding iron of natural isotopic composition to the water. As in our previous study, the pH of the drinking water was maintained at 2.5 in order to ensure no precipitation of iron. Water acidity should not affect water consumption as rats do not have any taste receptors for water (16). Isotopic enriched water was changed every 3-4 days. The masses of the drinking bottles before and after each change of water supply were recorded in order to accurately assess dietary iron tracer intake over the course of the study.

4.3.3 Stable isotope labels

All isotopic labels were prepared from iron metal (Chemgas, France), isotopically enriched in ^{54}Fe (99.873 $\pm$0.010 % ^{54}Fe), ^{57}Fe (95.910 $\pm$0.011 % ^{57}Fe) and ^{58}Fe (99.9109 $\pm$0.0013 % ^{58}Fe). Isotopically enriched iron spikes were dissolved in 37% HCl and diluted with water to yield 5 M HCl solutions. Iron concentrations were determined against a commercially available standard (Titrisol®; $FeCl_3$ in

15% HCl, 1000 mg Fe; Merck). Negative thermal ionization mass spectrometry (N-TIMS) was used to determine the isotopic composition of the spike solutions using the method developed by Walczyk (1997) with modifications (17). The concentrations of iron in the spike solutions were determined by reversed isotope dilution mass spectrometry against the prepared iron standard.

All sample preparation work was performed in a class 10,000 clean room equipped with class 10 fume hoods. Only teflon labware or disposable plastic labware was used. Plastic lab ware was pre-cleaned by soaking in 10% (v/v) HNO_3 (Merck, USA) for 12 hrs and teflon labware by boiling in half-concentrated HNO_3. Acids and reagents used were of analytical-reagent grade. Acids were purified further by sub-boiling distillation before use. Water used throughout the study was ultrapure 18.2 Ω Milli-Q® water (Millipore, Billerica, Massachusetts, USA).

4.3.4 Blood and tissue sampling

Blood samples were collected monthly for hemoglobin concentration and to assess changes in iron isotopic compositions in the rat blood throughout the feeding period. During the study, blood was collected from the tail artery of the rats using 23G needles while they were under light isoflurane anesthesia (Webster Veterinary Patterson Company, USA). Blood samples were obtained via cardiac puncture at the end of the study. Blood samples were collected in EDTA coated vaccutainers and stored at -20 °C before elemental and isotopic analysis.

Tissue sampling followed the procedure as described in Chen et al. (2013) (15). In brief, animals were sacrificed by hyper-perfusion, i.e. effective removal of blood from tissues by washing of vessels and organs *in situ* with excessive volumes of Ringer's solution (NaCl 0.85%, KCl 0.025%, $CaCl_2$ 0.03%, $NaHCO_3$ 0.02%). Heparin (5 I.U. heparin/mL) was added to the solution to prevent blood clotting during the perfusion process. Organs such as heart, kidneys, liver, muscle and brain were harvested and stored at -20°C prior to isotopic analysis.

4.3.5 Iron elemental and isotopic analysis

The collected samples were freeze dried and grinded into fine powders. For *DI* group samples, a weighed aliquot of the homogenized tissue was transferred into a teflon vessel together with a known amount of enriched ^{58}Fe label to determine the amount of natural iron in the sample following isotope dilution principles (see section 4.3.6). The mixture was mineralized in a microwave digestion system (Ethos 1, Milestone, Sorisole, Italy). Tissues collected from the *TI* group were digested directly without addition of an additional tracer for iron quantification. After mineralization, iron in the solution was separated by ion-exchange chromatography using a strongly basic ion-exchange resin (Dowex AG 1-X8; 200 - 400 mesh, Sigma, St. Louis, USA). The eluate obtained was alkalized by addition of 25% ammonium hydroxide (Merck, Darmstadt, Germany) for precipitating sample iron as ferrihydrite. The iron precipitate was stored dry until isotope ratio analysis. The iron isotopic composition of the isotopic labels and the

prepared samples were determined by negative thermal ionization mass spectrometry (NTI-MS) using FeF_4^- molecular ions and a rhenium double-filament ion source with details described earlier (17). Further technical details are described in an earlier publication (15).

Concentration of haemoglobin in the rat blood sample was indirectly determined in triplicate through iron concentration in the blood (15). Iron content of blood samples was analyzed by graphite furnace atomic absorption spectrometry (GF-AAS) (Varian AA240 Zeeman/GTA120, Varian Inc., Palo Alto, CA, USA) by external calibration with an iron standard solution.

4.3.6 Data analysis

The amount ratio of tracers in the brain described were determined following isotope dilution principles using Eqn. (6) (17, 18) based on the abundance of the different isotopes in each enriched isotopic label (***a***) and the measured isotope ratios in the sample (***R***).

In a sample spiked with three iron isotopic labels (enriched ^{54}Fe, ^{57}Fe and ^{58}Fe), the amount of each of iron isotopes ^{54}n, ^{57}n, ^{58}n *and* ^{56}n is determined by the isotopic abundances ***a*** and the amounts (in moles) of each of the tracers in the blend ($n\ (^{nat}Fe)$, $n\ (^{54}Fe)$, $n\ (^{57}Fe)$ and $n\ (^{58}Fe)$). The iron isotopic abundance ^{W}a (W=54, 56, 57 and 58) for both isotopically enriched tracers (*iso,54; iso,57; iso,58*) and natural iron (*nat*) can be obtained from the sum of all measured

isotope abundance ratios $\sum {}^{i}R$ with ${}^{56}a$ as the common denominator. The molar amount of the tracers is related to the measured isotope ratios R_{sample} via the total amount of iron in the sample n (^{tot}Fe) and the abundance ${}^{w}a$ of the isotope in natural iron and the tracers. In sum, the abovementioned relationship can be expressed in a matrix form which can be solved to deliver the molar ratio of a given spike relative to natural iron in the sample.

$$\begin{bmatrix} {}^{54}a_{nat} & {}^{54}a_{iso,54} & {}^{54}a_{iso,57} & {}^{54}a_{iso,58} \\ {}^{57}a_{nat} & {}^{57}a_{iso,54} & {}^{57}a_{iso,57} & {}^{57}a_{iso,58} \\ {}^{58}a_{nat} & {}^{58}a_{iso,54} & {}^{58}a_{iso,57} & {}^{58}a_{iso,58} \\ {}^{56}a_{nat} & {}^{56}a_{iso,54} & {}^{56}a_{iso,56} & {}^{56}a_{iso,56} \end{bmatrix} \begin{bmatrix} \frac{n\left({}^{nat}Fe\right)}{n\left({}^{tot}Fe\right)} \\ \frac{n\left({}^{54}Fe\right)}{n\left({}^{tot}Fe\right)} \\ \frac{n\left({}^{57}Fe\right)}{n\left({}^{tot}Fe\right)} \\ \frac{n\left({}^{58}Fe\right)}{n\left({}^{tot}Fe\right)} \end{bmatrix} = \begin{bmatrix} \frac{{}^{54/56}R_{sample}}{1+\sum {}^{i}R_{sample}} \\ \frac{{}^{57/56}R_{sample}}{1+\sum {}^{i}R_{sample}} \\ \frac{{}^{58/56}R_{sample}}{1+\sum {}^{i}R_{sample}} \\ \frac{{}^{56/56}R_{sample}}{1+\sum {}^{i}R_{sample}} \end{bmatrix} \quad (6)$$

4.3.6.1 Efflux Rate Index

Based on Eqn. (6), the amount ratio of two tracers in a tissue sample with the amount of the last administered tracer as the common denominator, e.g. $n(^{57}Fe)/n(^{54}Fe)$, can be calculated from the molar ratio of the tracers [$n(^{nat}Fe)$, $n(^{54}Fe)$, $n(^{57}Fe)$ and $n(^{58}Fe)$] relative to the total amount of iron in the sample [$n(^{tot}Fe)$]. The calculated amount ratio of tracers in the brain relative to that in the diet was designated as the Efflux Rate Index. The higher the Efflux Rate Index, the less of the tracer taken up by brain was transported out of the brain after termination of tracer administration and the lower is the efflux rate.

4.3.6.2 Tissue iron uptake (*DI* group)

Based on the Eqn. (6), the amount of total iron $n(^{tot}Fe)$ in the sample aliquot in the *DI* group was calculated from the $n(^{58}Fe)/n(^{tot}Fe)$ ratio and the known amount of added ^{58}Fe spike (in moles) before digestion. The total amount of ^{57}Fe tracer in the sample could then be calculated from the $n(^{57}Fe)/n(^{tot}Fe)$ ratio and $n(^{tot}Fe)$ in the analyzed sample. Total amount of ^{54}Fe tracer in the sample could be calculated in the same way as that for the ^{57}Fe tracer. Total amount of tracer in the organ was calculated by taking the mass of tissue analyzed and the total mass of the organ/sample into account. Absolute tissue iron uptake (% of iron fed) was calculated as total moles of tracer recovered in the tissue relative to total moles of tracer consumed.

The amount of iron transferred into each tissue is expressed relative to the amount of total iron in the analyzed tissue as relative tissue iron uptake (% of tissue iron coming from feed). For the *TI* group, all available enriched stable iron isotope tracers had already been used during the feeding and we were not available any more to quantify tissue iron following isotope dilution principles. Iron concentrations were therefore determined by graphite furnace absorption spectrometry (see section 4.3.5) and using standard addition techniques.

4.3.6.3 Evaluation of kinetics of iron efflux (*TI* group)

A single compartment model was used to estimate tracer efflux rates for each individual organ in the *TI* group. The amount of the last administered tracer (T_3; ^{58}Fe) in the organ at sacrifice was set to 100% (Efflux Rate Index of 1.0). Efflux

rate indices for the first administered tracer (T_1; ^{57}Fe) and the second administered tracer (T_2; ^{54}Fe) were expressed relative to the efflux rate index of tracer T_3 and plotted against the time period between termination of tracer administration and sacrifice. The obtained data points were fitted by the Windows version of the SAAM/Consaam software, WinSAAM (Simulation, Analysis and Modelling) to determine tracer efflux rates of iron from the respective organ.

4.3.7 Statistical analysis

Comparisons of absolute/relative tissue iron uptake and iron efflux between different tissues were conducted by performing an independent sample *t*-test for equality of means using SPSS version 20 software (SPSS Inc., Chicago, USA). In all tests, a value of $P \leq 0.05$ was considered statistically significant.

4.4 Results

No premature deaths were observed among the treated rats. The total amount of consumed feed, water and iron isotopes of each feeding group is summarized in Table 4-1**.** The rats showed a moderate increase in body weight in both groups over the course of the study from 643 ± 43 g at the beginning to 692 ± 49 at the end in for the *DI* group and from 613 ± 49 g to 713 ± 61 g for the *TI* group which is consistent with adult aging. The blood hemoglobin concentrations of each rat were within the reported normal range of 130 – 170 g Hb/L (19) at the beginning (161 ± 13 g Hb/L) and end of the studies (159 ± 12 g Hb/L) for the *DI* group and 148 ± 8 g Hb/L and 149 ± 8 g Hb/L for the *TI* group, with minor variations within each study.

Table 4-1 Total amount of consumed feed, water and iron tracers for the *DI* group (4 month of feeding) and the *TI* group (5 month of feeding).

Group	Consumed feed [kg]	Consumed water [L]	Consumed natural iron [mmol]	Consumed iron tracers from water		
				Tracer ^{57}Fe [mmol]	Tracer ^{54}Fe [mmol]	Tracer ^{58}Fe [mmol]
DI	2.93 ±0.15	2.57 ±0.20	10.49 ±0.54	0.350 ±0.030	0.800 ±0.080	-
TI	3.80 ±0.20	3.56 ±0.54	13.61 ±0.70	0.400 ±0.060	0.89 ±0.13	0.220 ±0.033

4.4.1 Tracer analysis of blood samples

The measured amount ratio of tracer to total iron in blood carries information about the bioavailability of tracer iron. For comparison of data obtained for different tracers, amount ratios of tracer to total iron were adjusted for dose to that of the ^{57}Fe tracer for each individual rat using the tracer concentration ratios in the drinking water for normalization. After dose adjustment, the amount ratios of tracer to total iron were comparable for the different iron tracers in blood ($p<0.05$; see Fig. 4-3 and Fig. 4-4). As can be expected, amount ratios of tracer to total iron increased steadily over time until termination of tracer feeding on from which the ratios declined due to blood iron turnover. A trend towards a slower increase in amount ratios of tracer to total iron over time was observed.

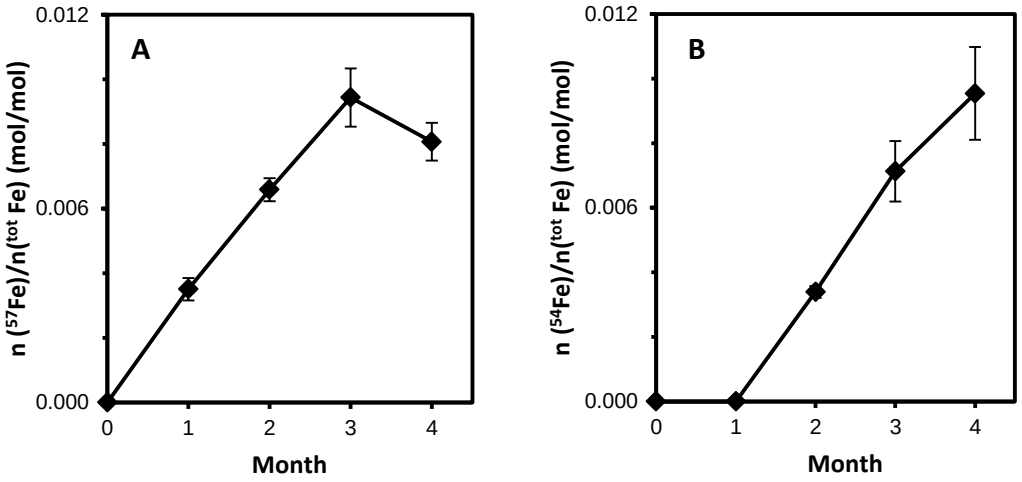

Fig. 4-3 Amount ratios of tracer to total iron (mol/mol) in blood against time for the DI group (n=3 rats).
Feeding of the ^{57}Fe tracer was terminated at the end of month 3. Amount ratios were adjusted to differences in tracer concentration in the diet.

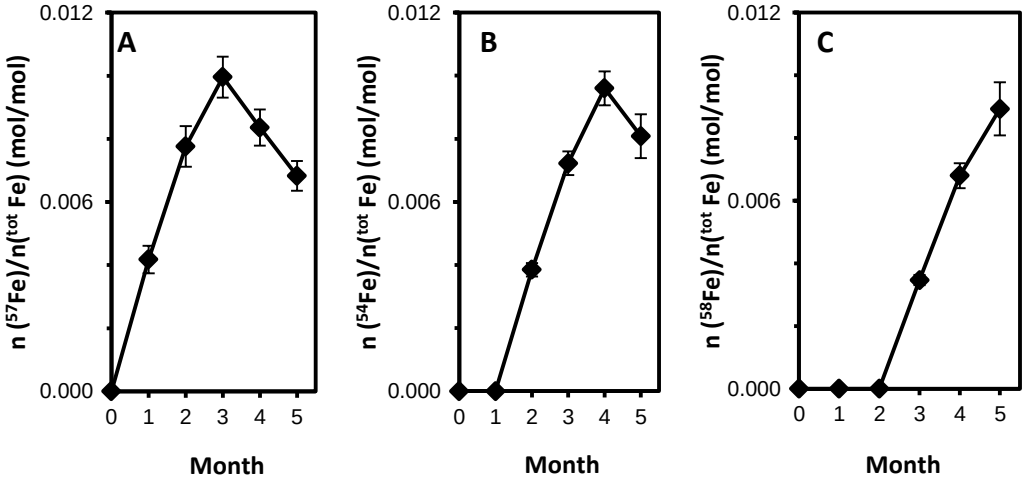

Fig. 4-4 Amount ratios of tracer to total iron (mol/mol) in blood against time for the TI group (n=5 rats)
Feeding of the ^{57}Fe tracer was terminated at the end of month 3 and that of the ^{54}Fe tracer at the end of month 4. Amount ratios were adjusted to differences in tracer concentration in the feed.

4.4.2 Tissue iron uptake for the *DI* group

Fig. 4-5 shows the absolute and relative iron uptake by different tissues in the *DI* group. Absolute iron uptake by different tissues was significantly different from each other and ranged from 0.00062% in brain to 0.102 % in liver in the present

study (see Fig. 4-5A). Fig. 4-5B shows the percentage of tissue iron in rat organs of the *DI* group coming from feed (relative tissue iron uptake)**.** Relative iron uptake of the analyzed tissues was of the same order of magnitude (9.2% - 32.8%) despite the marked differences in absolute iron uptake (0.000621% - 0.102% of the tracer dose). Relative iron uptake of brain was comparable to that of heart (p=0.10) and that of liver was comparable to that of the kidneys (p=0.46) while relative iron uptake of both brain and heart was significantly different from those of liver and kidneys (p<0.05).

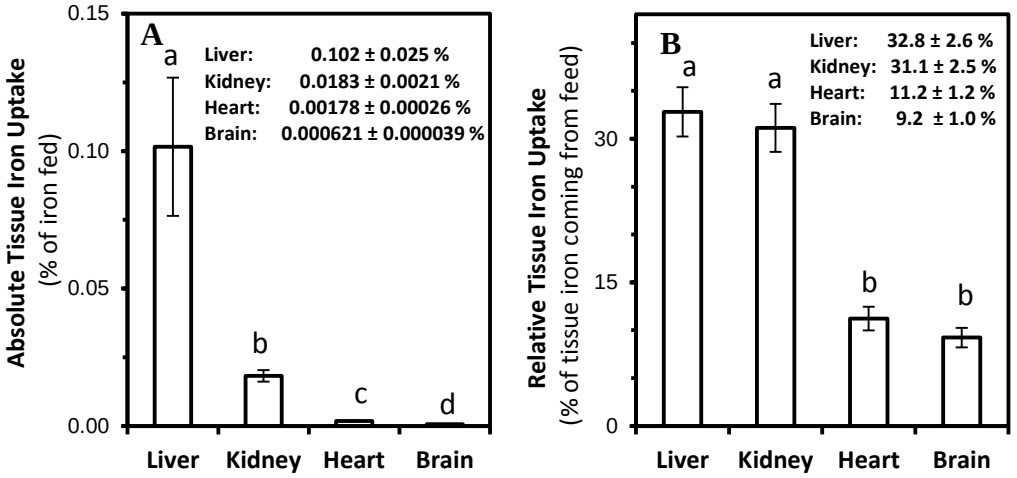

Fig. 4-5 Tissue iron uptake
Fig. 4-5A shows the percentage of dietary iron recovered in rat brains of the *DI* group (n=3 rats). Recoveries were calculated as the amount of ^{54}Fe tracer recovered in the organ relative to total amount of ^{54}Fe tracer given (in %). **Fig. 4-5B** shows the percentage of tissue iron in rat organs of the *DI* group coming from feed**.** Relative tissue iron uptake was calculated as the amount of ^{54}Fe tracer recovered in the organ coming from feed relative to the total amount of iron in the organ (in %). Different lower case letters indicate statistical significant differences between tissues ($p \leq .0.05$). Values are given as arithmetic means ± SD (n=3)

4.4.3 Iron turnover in tissue

4.4.3.1 Qualitative assessment (*DI* group)

Muscle tissues exhibited tracer amount ratios that were the closest to that of the diet, demonstrating the lowest iron turnover rate among all analyzed tissues. After normalization of Efflux Rate Indices to muscle tissue, blood exhibited the highest

turnover rate among major body iron pools (see Fig. 4-6). Efflux Rate Indices were all lower than 1.0 which indicates that more iron was replaced in the studied organs over the observational period than in muscle tissue as the iron pool showing the slowest iron turnover. The Efflux Rate Index of brain of 0.927, was higher than that of the other tissues, showing that iron is exported from brain at a slower rate as compared to other organs. The Efflux Rate Index of brain exhibited no difference with that of heart (p=0.18) whereas the Efflux Rate Index of liver showed no significant difference to those of kidney (p=0.46) and blood (p=0.23) but was significantly lower than that of heart (p<0.05) and brain (p<0.05), respectively.

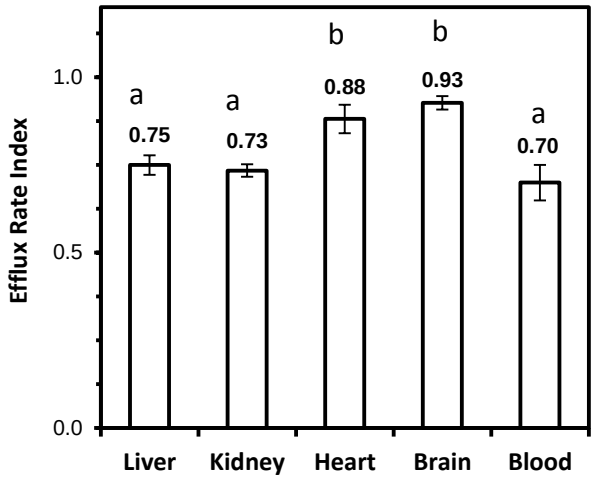

Fig. 4-6 Efflux rate index of different tissues for the DI group (n=3 rats)
The lower the index, the higher the iron efflux rate (see text). Different lower case letters indicate statistical significant differences between tissues ($p \leq .0.05$). Same letter means no statistical difference.

4.4.3.2 Quantitative assessment (*TI* group)

For the triple-isotope feeding scheme, iron turnover of different tissues was quantitatively evaluated by plotting the normalized Efflux Rate Index against time difference between terminations of tracer feeding and sacrifice (see Fig. 4-7).

Dietary iron was found to be released from liver, kidney, heart, brain and blood at different efflux rate. Efflux rates expressed as % of tracer in brain released per month and tracer half-lives in the studied tissues was calculated using a single compartment model (see Table 4-2). Consistent with findings for the *DI* group, brain iron exhibited the lowest efflux rate (8.2 ± 3.1 % tracer per month) among the measured tissues in the *TI* group ($p<0.05$). The half-life of dietary iron taken up by the brain was estimated to be 9.4 ± 3.2 months, the longest half-life among all analyzed tissues ($p<0.05$).

Table 4-2 Efflux rates and half-lives of dietary iron in the rat tissues in *TI* group*

	Liver	Kidney	Heart	Brain	Blood
Efflux rate (% tracer / month)	20.5 ±6.6[a]	19.8 ±6.8[a]	11.5 ±2.1[b]	8.2 ±3.1	37.6 ±9.6[a]
Half-life of dietary iron (month)	3.7 ±1.3[a]	4.2 ±1.9[a]	6.2 ±1.2[b]	9.4 ±3.2	2.0 ±0.6[a]

* The values of efflux rate and half-life of dietary iron in different tissues were compared with those in brain. Lower case indicates statistical difference ($p\leq.0.05$) whereas lower case b means no statistical difference.

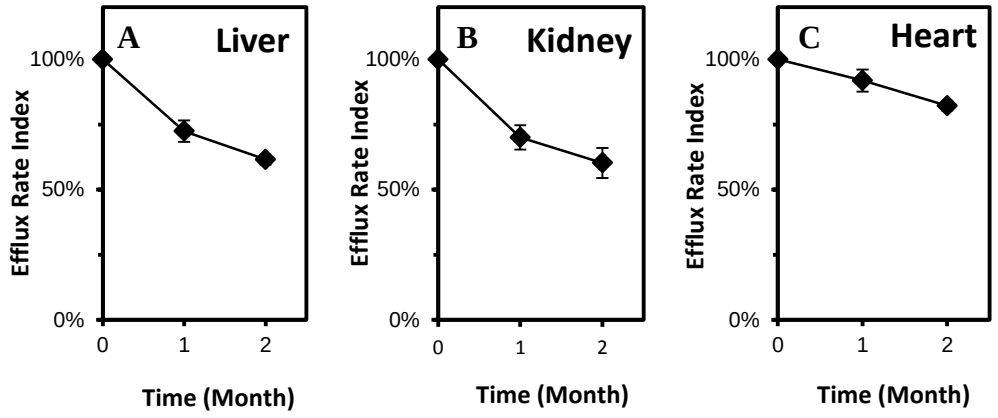

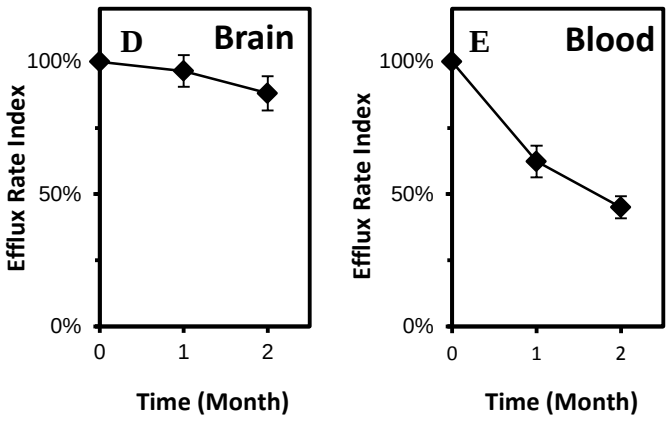

Fig. 4-7 Changes in Efflux Rate Indices over two months in the TI group (n=5 rats)
Efflux Rate Indices at month 1 and 2 were normalized to its value at month 0 (see text).

4.5 Discussion

In the present study we could confirm the major finding of our previous study (15). The fraction of iron in the diet that has been transferred to brain was marginal after 4 months of feeding (0.00062% in this study versus 0.00054% in our earlier study). However, this very small iron amount constituted ca. 9% of brain iron in either study at sacrifice. While this does not challenge the main conclusion from earlier radioisotope experiments that the absolute amount of iron uptake by the brain is very low, it points to brain iron homeostasis and dietary iron intake as key factors in brain iron accumulation as observed in ageing and possibly in the development of AD and PD.

Our studies differ in many ways from earlier radiotracer studies due to the different scope of our experiments. Research interests in the past lied mostly in the developmental stage with limited focus on the effect of dietary iron on brain iron balance as compared to our study (20-25). Because iron uptake by the brain

is age-dependent (26, 27) and the uptake of iron from diet by the brain and its later release is a long term process, it was imperative for us to study brain iron dynamics by feeding tracer continuously to adult and not weaning or young rats. Our studies were conducted in 6-8 mo old rats which correspond to an age of twenty-odd human years at study onset. The pioneering postmortem study by Hallgren and Sourander (1958) demonstrated that the rate of whole brain iron accumulation increases steeply during the first two decades of human life, slows down substantially in the third decade, and reaches a "plateau" or may increase very slowly thereafter (4). The change in iron accumulation rate in the brain suggests a change in brain iron dynamics including brain iron import and export over the course of life. As relatively large amounts of iron are required during the first decade for the developing brain, it is possible that the amount of iron accumulating on from the third decade when brain development can be considered complete, contributes to the development of iron-related neurodegenerative diseases. Similar to humans, iron was found to increase steeply in rat brain early in life but slows down at about the fourth month of life (20, 28-31).

Our understanding of brain iron dynamics is largely based on short-term radiotracer studies. However, due to their instability and because of radiation safety aspects they are less useful for tracing long-term dietary iron uptake by the brain. Long-term feeding of non-decaying stable isotope tracers along with the diet, as in our study, allows not only to study brain iron uptake but also iron efflux

from brain over time. This is essential to assess the effect of interventions on brain iron balance. Furthermore, radiotracers were given only once in earlier studies, usually by injection, which neglects the homeostatic response of the body and possibly brain to changes in dietary iron supply at the systemic level. This is of significance when studying the role of dietary iron in brain iron accumulation.

By feeding iron stable isotopes continuously with the diet we were able to assess brain iron balance relative to total brain iron content which was not possible in earlier radiotracer experiments. Because iron has four stable isotopes that can be used as tracers (^{54}Fe, ^{57}Fe and ^{58}Fe), it is possible to use each rats as its own control when studying brain iron dynamics by staggering tracer administration over time (see Fig. 4-1 and Fig. 4-2). This allows to reduce sample size significantly as compared to earlier radiotracer experiments (20, 21, 28) which used a single tracer for brain iron labeling only. Groups of animals in these studies had to be sacrificed at different time points and compared to each other which requires naturally larger number of animals to control for inter-individual variations.

Iron balance of an organism or organ depends both on iron influx and efflux rate. Iron accumulates inevitably at the moment that influx rates exceed efflux rate with the rate of iron accumulation being determined by their difference. Considerable efforts have been made to understand mechanisms and pathways of brain iron uptake but our understanding here is still limited. Dietary iron was

proposed to be taken up by the brain either across the blood-brain barrier (BBB, main pathway) or the blood-cerebrospinal fluid barrier (BCB, secondary pathway) (32, 33). Many studies suggested that iron uptake across BBB is mainly via transferrin receptor (TfR) mediated endocytosis (34), while the detection of H-ferritin receptors on the BBB led to the suggestion of an additional pathway (34, 35). Expression of DMT1, ferroportin, ceruloplasmin and hephaestin were higher in the choroid plexus in BCB than virtually all other brain regions (36) which points to alternative mechanisms by which iron can enter brain. Our knowledge on iron export is even more limited as it has been studied to a much lower extent. It has been hypothesized that BCB might be responsible for not only brain iron uptake (37) but also iron efflux in the brain owing to its structure and functions (23, 38). Structurally, the tight junctions of the blood-cerebrospinal-fluid barrier are quantitatively leakier than those of the blood brain barrier. This is supported by other rat studies in which radio-labeled iron was injected into the lateral cerebral ventricle to study iron efflux from the CSF to the blood (25, 38, 39).

In agreement with the described mechanisms and previous rodent studies using radioisotope techniques (21-23, 25, 38), our findings support the hypothesis that uptake of iron by the brain is a bi-directional process. Two other studies did not report loss of tracer iron from brain which could be either due to sample size or age of the studied animals (20, 40). Observations by Holmes-Hampton et al. (2012) point to iron incorporation being biphasic as well as age-dependent (27). During the early phase of life, iron influx must exceed efflux significantly to cover the high iron demands of the growing brain. At two years of age, human

brain iron content is ca. 50% of the adult brain, approximately doubles within the following decade and slows down later (41).

Greatly consistent with our earlier study (see Chapter 3) and in good agreement with findings by Bradbury (Number), the rank order of the amount of iron uptake by tissues were blood> liver> kidney> heart> brain (see Fig. 4-5). While we could demonstrate that iron entering the rat brain during adulthood is not deposited permanently, brain iron was found to have the lowest iron turnover among the studied organs. The efflux rate index of brain was 0.927 (see Fig. 4-6) which is statistically higher than that in other tissues, showing that iron in the brain has a turnover rate that is slightly higher than for muscle but the lowest of all other tissues under investigation. This observation is in good agreement with the findings by Dallman and Spirito (1977) who injected radioiron intra-peritoneally into young rats (2-60 days) and monitored radioactivity in the brain for a period of up to 135 days (21). Their results showed that the specific radioactivity of iron in the brain remained at its peak until the end of the observational period, indicating little loss or no loss of brain iron during that period. They therefore concluded that brain iron turnover is at an extremely slow rate based on the assumption that mechanism for brain iron export exist.

In the present study we could estimate the efflux rate of iron from the adult rat brain as 8.2 ± 3.1% per month in the *TI* group. However, this figure must be considered the first gross approximation of the efflux rate of brain iron in a

mammalian organism as only three data points were available per rate for its calculation (see Fig. 4-7). The corresponding half-life of iron tracer in the brain, and thus that of dietary iron taken up by the brain during adulthood, was 9.4 ± 3.2 months. This can be considered relatively long with regard to the short life time of the species of about 3 years (42). As iron turnover rate in rat organs cannot be simply extrapolated to humans based on the ratio of their life spans, the data on iron turnover rate in blood in these two species can be of use to extrapolate findings to human brain. The half life of iron tracer in blood was found to be approximately 83 months in adult men (43) as compared to 2.0 ± 0.6 months for adult rats in the present study. At an average human life time of 75 as compared to 3 years in rats, the half-life of iron in human brain can thus be reasonably estimated to be of the order of decade(s).

In good agreement with our earlier study, dietary iron recovered in the rat brain during early adulthood amounted to ca. 9% of total brain iron after 4 months of tracer feeding. Half of this iron amount will leave brain within one half-life, i.e. 9 months. After 27 months, when the rat reaches its average life span, about 10% of the iron that has accumulated early in adulthood will remain in brain and even more of any iron that has entered brain later in the life of the rat. Assuming that brain iron uptake and its half-life are constant over lifetime, brain iron of the rats in our study can be estimated to increase by 27% in from early adulthood (6-8 months of age) to the end of their average life span (ca. 36 months of age).

4.6 Conclusion

The present study, for the first time ever, revealed that dietary iron enters the brain at an influx rate that is significantly higher than its efflux rate in adult animals. This will automatically lead to brain iron accumulation during adulthood as observed in animals and men. This permits us now to study the effect of dietary iron intake on brain iron accumulation in healthy organisms and in conditions where body iron homeostasis is impaired. Furthermore, the developed methodologies can be used to evaluate treatments and therapies to reduce iron burdens in the brain that are supposed to affect brain health later in life through iron mediated oxidative stress.

4.7 Bibliography

1. Crichton RR, Dexter DT, & Ward RJ (2011) Brain iron metabolism and its perturbation in neurological diseases. *Monatsh Chem* 142(4):341-355.
2. Altamura S & Muckenthaler MU (2009) Iron toxicity in diseases of aging: Alzheimer's disease, Parkinson's disease and atherosclerosis. *J Alzheimers Dis* 16(4):879-895.
3. Kehrer JP (2000) The Haber-Weiss reaction and mechanisms of toxicity. *Toxicology* 149(1):43-50.
4. Hallgren B & Sourander P (1958) The effect of age on the non-haemin iron in the human brain. *J Neurochem* 3(1):41-51.
5. Massie HR, Aiello VR, & Banziger V (1983) Iron accumulation and lipid peroxidation in aging C57bL/6J Mice. *Exp Gerontol* 18(4):277-285.
6. Cook CI & Yu BP (1998) Iron accumulation in aging: modulation by dietary restriction. *Mech Ageing Dev* 102(1):1-13.
7. Maynard CJ, *et al.* (2002) Overexpression of Alzheimer's disease amyloid-beta opposes the age-dependent elevations of brain copper and iron. *J Biol Chem* 277(47):44670-44676.
8. Hardy PA, *et al.* (2005) Correlation of R2 with total iron concentration in the brains of rhesus monkeys. *J Magn Reson Imaging* 21(2):118-127.
9. Hahn P, *et al.* (2009) Age-dependent and gender-specific changes in mouse tissue iron by strain. *Exp Gerontol* 44(9):594-600.
10. Bartzokis G, *et al.* (2011) Gender and iron genes may modify associations between brain iron and memory in healthy aging. *Neuropsychopharmacol* 36(7):1375-1384.
11. Kell DB (2009) Iron behaving badly: inappropriate iron chelation as a major contributor to the aetiology of vascular and other progressive inflammatory and degenerative diseases. *Bmc Med Genomics* 2:2.
12. Zecca L, Youdim MBH, Riederer P, Connor JR, & Crichton RR (2004) Iron, brain ageing and neurodegenerative disorders. *Nat Rev Neurosci* 5(11):863-873.
13. Bush AI (2013) The metal theory of Alzheimer's disease. *J Alzheimers Dis* 33:S277-S281.
14. Kumar H, *et al.* (2012) The Role of Free Radicals in the Aging Brain and Parkinson's Disease: Convergence and Parallelism. *Int J Mol Sci* 13(8):10478-10504.
15. Chen J-H, Shahnavas S, Singh N, Ong W-Y, & Walczyk T (2013) Stable iron isotope tracing reveals significant brain iron uptake in adult rats. *Metallomics* 5(2):167-173.
16. Hofstetter J, Suckow MA, & Hickman DL (2006) Morphophysiology. *The Laboratory Rat*, eds Suckow MA, Weisbroth SH, & Franklin CL (Academic Press), 2th Ed, pp 93-125.
17. Walczyk T (1997) Iron isotope ratio measurements by negative thermal ionisation mass spectrometry using FeF4- molecular ions. *Int J Mass Spectrom Ion Process* 161(1-3):217-227.

18. Walczyk T (2012) The use of stable isotope techniques for studying mineral and trace element metabolism in humans. *Isotopic Analysis*, (Wiley-VCH Verlag GmbH & Co. KGaA), pp 435-494.
19. Underwood EJ (1977) Iron. *Trace elements in human and animal nutrition*, ed Underwood EJ (Academic Press), 4th Ed, pp 14-15.
20. Taylor EM & Morgan EH (1990) Developmental changes in transferrin and iron uptake by the brain in the rat. *Dev Brain Res* 55(1):35-42.
21. Dallman PR & Spirito RA (1977) Brain iron in rat: extremely slow turnover in normal rats may explain long-lasting effects of early iron deficiency. *J Nutr* 107(6):1075-1081.
22. Banks WA, Kastin AJ, Fasold MB, Barrera CM, & Augereau G (1988) Studies of the slow bidirectional transport of iron and transferrin across the blood-brain-barrier. *Brain Res Bull* 21(6):881-885.
23. Bradbury MWB (1997) Transport of iron in the blood-brain-cerebrospinal fluid system. *J Neurochem* 69(2):443-454.
24. Moos T & Morgan EH (1998) Evidence for low molecular weight, non-transferrin-bound iron in rat brain and cerebrospinal fluid. *J Neurosci Res* 54(4):486-494.
25. Moos T, Nielsen TR, Skjorringe T, & Morgan EH (2007) Iron trafficking inside the brain. *J Neurochem* 103(5):1730-1740.
26. Erikson KM, Pinero DJ, Connor JR, & Beard JL (1997) Regional brain iron, ferritin and transferrin concentrations during iron deficiency and iron repletion in developing rats. *J Nutr* 127(10):2030-2038.
27. Holmes-Hampton GP, *et al.* (2012) Changing iron content of the mouse brain during development. *Metallomics* 4(8):761-770.
28. Taylor EM, Crowe A, & Morgan EH (1991) Transferrin and iron uptake by the brain: effects of altered iron status. *J Neurochem* 57(5):1584-1592.
29. Roskams AJI & Connor JR (1994) Iron, transferrin, and ferritin in the rat brain during development and aging. *J Neurochem* 63(2):709-716.
30. Takahashi S, *et al.* (2001) Age-related changes in the concentrations of major and trace elements in the brain of rats and mice. *Biol Trace Elem Res* 80(2):145-158.
31. Tarohda T, Yamamoto M, & Amano R (2004) Regional distribution of manganese, iron, copper, and zinc in the rat brain during development. *Anal Bioanal Chem* 380(2):240-246.
32. Ueda F, Raja KB, Simpson RJ, Trowbridge IS, & Bradbury MWB (1993) Rate of Fe-59 uptake into brain and cerebrospinal-fluid and the influence thereon of antibodies against the transferrin receptor. *J Neurochem* 60(1):106-113.
33. Crowe A & Morgan EH (1992) Iron and transferrin uptake by brain and cerebrospinal fluid in the rat. *Brain Res* 592(1-2):8-16.
34. Crichton RR (2009) Brain iron homeostasis and its perturbation in various neurodegenerative diseases. *Iron metabolism: from molecular mechanisms to clinical consequences*, ed Crichton RR (John Wiley & Sons), 3rd Ed, pp 371-372.

35. Fisher J, *et al.* (2007) Ferritin: a novel mechanism for delivery of iron to the brain and other organs. *Am J Physiol-Cell Ph* 293(2):C641-C649.
36. Rouault TA, Zhang DL, & Jeong SY (2009) Brain iron homeostasis, the choroid plexus, and localization of iron transport proteins. *Metab Brain Dis* 24(4):673-684.
37. Ke Y & Qian ZM (2007) Brain iron metabolism: Neurobiology and neurochemistry. *Prog Neurobiol* 83(3):149-173.
38. Moos T & Morgan EH (1998) Kinetics and distribution of [Fe-59-I-125]transferrin injected into the ventricular system of the rat. *Brain Res* 790(1-2):115-128.
39. Su CK, *et al.* (2010) In vivo monitoring of the transfer kinetics of trace elements in animal brains with hyphenated inductively coupled plasma mass spectrometry techniques. *Mass Spectrom Rev* 29(3):392-424.
40. Lopes TJS, *et al.* (2010) Systems analysis of iron metabolism: the network of iron pools and fluxes. *Bmc Syst Biol* 4.
41. FAO & WHO (2001) Iron. in *Human vitamin and mineral requirements* (FAO;WHO), pp 195-223.
42. Quinn R (2005) Comparing rat's to human's age: How old is my rat in people years? *Nutrition* 21(6):775-777.
43. Finch CA (1959) Body iron exchange in man. *J Clin Invest* 38(2):392-396.

Chapter 5

Changes of brain iron homeostasis in adult rats in response to dietary iron supply

Jie-Hua Chen[a], Bin Li[b], Aik-Xin Neo[b], Nadia Singh[a], Thomas Walczyk[a,b]

[a] Department of Chemistry, National University of Singapore, 3 Science Drive 3, Singapore, 117543;
[b] Department of Biochemistry, National University of Singapore, 8 Medical Drive, Singapore, 117597.

Corresponding author: Thomas Walczyk
Department of Chemistry,
3 Science Drive 3,
Singapore, 117543
Tel.: (65) 6516 7986
Fax: (65) 6775 7895
Email: walczyk@nus.edu.sg

5.1 Abstract

Iron accumulation with age in the brain has been suggested as a contributing factor in the pathogenesis of Alzheimer's disease (AD) and Parkinson's disease (PD) through iron induced oxidative stress. Findings from epidemiological trials regarding possible links between AD/PD and iron nutrition or iron status are conflicting. Animal studies point to dietary iron intake as a determinant of brain iron uptake during growth but no such studies are available for adult mammals. Mechanisms of brain iron homeostasis are supposed to be age dependent due to much higher iron requirements of the growing brain during infancy and childhood.

In the present study, iron was traced from diet to brain using a dual-stable isotope technique in adult male Wistar rats (8 months old) to monitor effects of high dietary iron intake (~2000 mg/kg feed) and low dietary intake (~2 mg/kg feed) versus a control diet (~200 mg/kg feed). Tracers were given continuously with the drinking water over 4 months to the rats (n=7 per group). Changing of dietary intake triggered a normal homeostatic response without inducing changes in blood hemoglobin concentration.

Uptake efficiency of dietary iron by the adult rat brain was found to be determined by the amount of absorbed iron in the intestine and not by dietary intake or body iron stores alone. The low dietary iron regimen resulted in a lower systemic iron influx into the body which could not be compensated by

upregulating dietary iron absorption. Systemic iron influx was also lowered in the high dietary iron regimen due to excessive downregulation of iron absorption in the intestine. In consequence, accumulation of dietary iron in the brain was the highest in the control group. Brain iron uptake appears to be much less regulated in adulthood than during growth. Efficiency of regulatory mechanisms of intestinal iron absorption rather than brain iron homeostasis seems to be the primary determinant of brain iron accumulation during adulthood.

5.2 Introduction

Populations are ageing in the industrialized world and, to a lesser extent, in developing countries. Age-related neurodegenerative diseases, headed by Alzheimer's disease (AD) and Parkinson's disease (PD) in particular, develop on an epidemic scale and are likely to have a significant social and economic impact in the coming decades (1). The exact underlying mechanisms involved in the pathogenesis of AD and PD remain an enigma. Recent studies have shown increased iron accumulation with advancing age at pathoanatomically relevant sites in AD and PD (2-4). The perturbation of brain iron homeostasis has therefore been proposed as a potential mechanism driving the progression of neurodegeneration. Iron's innate ability to accept and donate electrons plays a pivotal role in normal neurogenesis and in a wide spectrum of cellular reactions (5). A disruption in brain iron homeostasis, however, can be potentially detrimental to normal brain function. When in excess, free unbound iron can induce oxidative stress by reducing H_2O_2 to the highly-cytotoxic hydroxyl ($OH^{\bullet}$) radical via Fenton chemistry and Haber-Weiss reaction (6). The resulting reactive

oxygen species (ROS) can damage functional biomolecules including DNA, proteins and lipids at the moment that cellular capacities of oxidative stress defense are exceeded.

In the absence of curative treatments for AD/PD, strategies are needed for prevention or to delay the age of onset. The role of nutrition in neurodegeneration has become a topic of increasing scientific and public interest (7). Prevalence of AD and PD has increased over the past decades when corrected for age (8, 9) pointing to other factors than ageing in the etiology of these diseases. Dietary iron intake is one of them. With rising affluence over the past decades, amounts of bioavailable iron in our diet have increased due to a higher proportion of red meat and iron fortified foods and a growing intake of dietary supplements (10). As iron is vital for life but was difficult to acquire from diet over evolutionary time spans (11), the human body is virtually a closed system for iron with minimal habitual losses (12). If iron absorbed from diet overcorrects for habitual losses, body iron accumulation is inevitable and brain iron accumulation possible.

Several epidemiological studies have suggested that high dietary iron intake may contribute to the risk of developing AD or PD (13-18) while other epidemiological studies showed that higher intake of iron might have a protective effect against AD/PD (19, 20). Animal studies provided a clearer correlation between dietary iron intake and risks of contracting age-related neurodegenerative disorders. Previous rat studies proposed that iron supplementation accelerates the

aging process (21) whereas iron restriction retards it (21, 22). It remains, however, unclear how dietary iron intake affects brain iron homeostasis and brain iron accumulation in the long-term as a possible risk factor for AD/PD development.

Stable isotope techniques have been pioneered by our group to trace iron from the diet into the brain in adult rats by continuous feeding of tracer iron over several months (see Chapter 3 and 4). In the present study, we used the developed methodologies to investigate changes in brain iron homeostasis in response to different levels of dietary iron intake for the first time ever in adult rats and at the systemic level.

5.3 Methodology

5.3.1 Study design

To study changes in iron import and export of brain iron, we have fed two different stable isotope tracers in a staggered design (see Fig. 5-1). Tracer 1 (T_1; ^{57}Fe) as well as Tracer 2 (T_2; ^{54}Fe) were fed continuously over an equal duration of time. Transfer of iron from diet to brain was found to be bi-directional in our previous study in adult rats with rates of iron import exceeding rates of iron export (see Chapter 4). The more of previously imported iron tracer is exported from brain, the bigger is the difference in the amount ratio of both tracers in brain and feed at the end of the study (see Fig. 5-1).

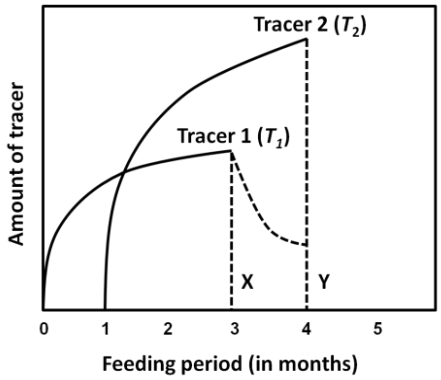

Fig. 5-1 Dual-isotope tracing scheme for studying brain iron import and export in animal models
Tracer 1 (T_1) is administered from month 1 to 3 and Tracer 2 (T_2) from month 2 to 4 together with the feed. Vertical lines X and Y indicate the time points when tracer administration was terminated. Dashed lines represent the fate of the tracer thereafter. The amount of first tracer $n(T_1)_{brain}$ decreases with time when the administration of the tracer is terminated and previously imported tracer is exported from brain. The amount ratio of both tracers $n(T_1)_{brain}$/ $n(T_2)_{brain}$ in the brain is thus lower than that of the consumed diet $n(T_1)_{diet}$ / $n(T_2)_{diet}$ at the time of sacrifice.

5.3.2 Stable isotope labels

Iron stable isotope tracers were prepared from isotopically enriched iron metals (Chemgas, Boulogne, France) which were dissolved in 37% HCl and diluted with water to yield 5 M HCl solutions. The isotopic enrichment was determined as 99.8756% ^{54}Fe for the ^{54}Fe tracer, 97.9266% ^{57}Fe for the ^{57}Fe tracer and 99.9109% ^{58}Fe for the ^{58}Fe tracer. Iron concentration of the tracer solutions was determined against a commercial iron standard solution ($FeCl_3$ in 15% HCl, 1,000 mg Fe, Titrisol®, Merck) by reverse isotope dilution mass spectrometry (23, 24).

5.3.3 Animals

Twenty-one adult male Wistar rats (8 months old, ex-breeders, body weight 638 ± 26g), provided by a local supplier (Department of Comparative Medicine, National University of Singapore), were divided randomly into three groups of 7 animals each and housed individually within the animal holding center at a

temperature of 21 ± 1 ℃ under a 12 h light/dark cycle. The rats had free access to water and food. The body weights of the rats were monitored weekly. All experimental protocols were reviewed and approved by the Institutional Animal Care and Use Committee (IACUC) of the National University of Singapore.

5.3.3.1 Study design

Rats were given three different type of feed which were obtained from a commercial supplier for experimental rodent diets (Harlan Teklad, Indiana, Indianapolis, USA). The low dose (LD) group received an iron-depleted rodent diet (TD.99397). The control (CT) group received an iron-sufficient diet (TD.120353) formulated by the addition of 0.02% carbonyl iron into TD.99397. The high dose (HD) group received an iron-enriched diet (TD.120354) formulated by supplementation of TD.99397 with 2% carbonyl iron. Prior to the commencement of the study, the concentration of natural iron in the feed was verified by Graphite Furnace Atomic Absorption Spectroscopy (GF-AAS). In accordance with the ingredient information provided by the feed supplier, the iron concentration was determined as 1.91 mg/g, 187 mg/g, and 1849 mg/g for LD, CT and HD group, respectively.

Following protocols described in our earlier study (see Chapter 4) the ^{57}Fe and the ^{54}Fe tracer were administered in chloride form via the drinking water for 2 months each following the dual tracer scheme illustrated in Fig. 5-1. The first tracer (^{57}Fe) was fed from Month 1 to 3 and the second tracer (^{54}Fe) from Month 2 to 4. Tracer concentration in the drinking water was adjusted for the different groups

according to iron levels in the feed (see Table 5-1). Tracer concentration in water for LD group was decided to be the same as that in CT group, the dose of which was tested in our earlier study to be sufficient to raise isotopic changes in the rat body (25). The tracer dose was increased to 10 times the tracer dose of the CT group to adjust for the 10 times higher iron concentration in HD feed than that in CT feed. Because of its lower natural abundance, dose requirements for the ^{57}Fe tracer are lower than for the ^{54}Fe tracer. To ensure that iron intake was the same over the course of the study within a given group, resulting differences in tracer iron concentration of the drinking water were compensated by addition of natural iron (see Table 5-1). Amounts of consumed feed and water were recorded.

Table 5-1 Iron composition of the drinking water

The concentration of ^{57}Fe tracer in drinking water for all groups represents the average concentration of ^{57}Fe tracer present in water prepared from Month 1 to 3, while the concentration of ^{54}Fe tracer in drinking water for all groups represents the average concentration of Tracer ^{54}Fe present in water prepared from Month 2 to 4. Natural iron was administered in the water in the first and last month to maintain the same level of dietary iron supply throughout the study.

Group	Feeding period (months)	Concentration of ^{57}Fe tracer (µg/g)	Concentration of ^{54}Fe tracer (µg/g)	Concentration of natural iron (µg/g)	Total iron concentration (µg/g)
LD	1	2.999 ±0.015	-	6.0017 ±0.0078	9.001 ±0.017
	2-3	3.0091 ±0.074	6.0052 ±0.0043	-	9.0143 ±0.0063
	4	-	6.0036 ±0.0017	3.0069 ±0.0079	9.010 ±0.014
CT	1	3.005 ±0.010	-	6.0023 ±0.0084	9.007 ±0.017
	2-3	3.0035 ±0.0040	6.003 ±0.010		9.0063 ±0.0094
	4	-	6.0011 ±0.0037	3.0008 ±0.0089	9.0019 ±0.0094
HD	1	29.991 ±0.043	-	59.998 ±0.020	89.990 ±0.056
	2-3	29.985 ±0.070	59.994 ±0.098		89.979 ±0.089
	4	-	60.032 ±0.050	30.012 ±0.011	90.043 ±0.052

Blood samples were collected prior to the feeding, every four weeks during the course of the study and at the end of the study. For brain and organ harvesting, animals were sacrificed by hyper-perfusion with heparinised Ringer's solution

(25). Tissues such as liver, kidneys, brain and muscle were collected and stored at -20°C prior to isotopic analysis. Haemoglobin level in the rat blood sample was indirectly determined through iron concentration in the blood via GF-AAS.

5.3.4 Iron isotopic analysis

Sample preparation for isotopic analysis followed largely methods described in detail in an earlier publication (25). Tissue samples were freeze-dried prior to sample preparation. The amount of total iron in the sample was determined following isotope dilution principles by adding a known amount of a third iron tracer (^{58}Fe) in solution to a weighed aliquot of the homogenized freeze-dried tissue. The spiked tissue sample was mineralized by microwave digestion and iron in the mineralized sample was then separated from the matrix using anion-exchange chromatography. Separated iron was further purified by precipitation as iron hydroxide by addition of ammonia. The precipitate was stored dry prior to mass spectrometric analysis. Iron isotopic composition of tracers and iron isolated from tissue/blood samples was determined by Negative Thermal Ionization Mass Spectrometry (NTI-MS) employing FeF_4^- molecular ions (25, 26).

5.3.5 Data analysis

Following Isotope Dilution Mass Spectrometry (IDMS) principles (24) (see Chapter 3 and 4), the mole ratio of tracer iron to total iron in tissue at sacrifice ($(n(^{W}Fe_{tissue})/n(^{total}Fe_{tissue})$, W=54 or 57) can be calculated from the iron isotopic composition of the used isotopic tracers and that of iron separated from the tissue/blood samples as obtained by mass spectrometric analysis. The total amount of tissue iron $n(^{total}Fe_{tissue})$ can tbe obtained from the amount ratio

$n(^{58}Fe_{tissue})/n(^{total}Fe_{tissue})$ and $n(^{58}Fe_{tissue})$ which is the known amount of enriched ^{58}Fe tracer $n(^{58}Fe_{tissue})$ that was added into the sample before microwave digestion,

Dietary iron absorption efficiency Fe_{abs} (%) at the intestine was estimated from the mole ratio of ^{54}Fe tracer to total iron $^{54}R_{blood} = n(^{54}Fe_{blood})/n(^{total}Fe_{blood})$ in blood at sacrifice as determined by IDMS, the total amount of iron $n(^{total}Fe_{blood})$ in blood and moles of ^{54}Fe tracer $n(^{54}Fe_{feed})$ consumed through feed, see Eqn. (7).

$$Fe_{abs} = {}^{54}R_{blood} \times n\left({}^{total}Fe_{blood}\right) / n\left({}^{54}Fe_{feed}\right) \quad (7)$$

Incorporation efficiency of tracer iron into erythrocytes (*IE*) in Eqn. (7) was assumed to be about 70% of absorbed iron in normal adult rats; 80% in iron-deficient rats and 60% in iron loaded rats (27). Iron amount (mol) in blood $n(^{total}Fe_{blood})$ was calculated from blood volume V (mL), the concentration of iron in blood $c(^{total}Fe_{blood})$ in g/g, the density of blood (1.06 g/mL) and the standard atomic weight of iron (55.85 g/mol), see Eqn. (8).

$$n\left({}^{total}Fe_{blood}\right) = V \times c\left({}^{total}Fe_{blood}\right) / 55.85 \times 1.06 \quad (8)$$

Blood volume (mL) of the rat was estimated from body weight BW (g) using the equation proposed by Lee and Blaufox (1985) (28), see Eqn. (9).

$$V = 0.06 \times BW + 0.77 \quad (9)$$

Systemic iron influx, as the estimated amount of iron (mol) that has been absorbed from diet over the course of the study, was calculated from the amount

of iron consumed through feed $n(^{total}Fe_{feed})$ and the estimated efficiency Fe_{abs} by which dietary iron has been absorbed.

Absolute Dietary Iron Recovery was calculated as the absolute amount (mol) of dietary iron transferred from diet to a tissue/organ over the three months of ^{54}Fe tracer feeding. With the abovementioned $n(^{total}Fe_{tissue})$ obtained following IDMS principles, the amount of tracers in tissues $n(^{54}Fe_{tissue})$ can thus be calculated from $n(^{54}Fe_{tissue})/n(^{total}Fe_{tissue})$. The absolute amount of dietary iron transferred from diet to tissue can be obtained from the amount ratio of tracer iron in tissue to that in the feed together with the amount of total iron in feed $n(^{total}Fe_{feed})$ in moles consumed over the same period in which the rat has received the ^{54}Fe tracer (3 months), see Eqn. (10).

Absolute Dietary Iron Recovery =

$$n\left(^{total}Fe_{feed}\right)\times\left(n\left(^{54}Fe_{tissue}\right)/n\left(^{54}Fe_{feed}\right)\right) \quad (10)$$

Relative Dietary Iron Recovery (%) in a tissue/organ was calculated by dividing Absolute Dietary Iron Recovery (mol) by the amount of total iron in feed (mol) consumed over the same period in which the rat has received the ^{54}Fe tracer (3 months), which is the same as tracer recovery in tissue, see Eqn. (11).

Relative Dietary Iron Recovery (%)

$$= n\left(^{54}Fe_{tissue}\right)/n\left(^{54}Fe_{feed}\right)$$

$$= \textit{Absolute Dietary Iron Recovery}/n\left(^{total}Fe_{feed}\right) \quad (11)$$

Normalized Dietary Iron Recovery (%) in a tissue/organ was calculated as the ratio of Absolute Dietary Iron Recovery in a tissue (mol) to Systemic Iron Influx (mol), i.e. the fraction of absorbed iron (in contrast to dietary iron) that has been transferred to the organ/tissue.

Iron efflux rates in tissues were assessed by calculation of Efflux Rate Indices. Efflux Rate Index was designated as the amount ratio of both iron tracers in tissues $n(^{57}Fe_{tissue})/n(^{54}Fe_{tissue})$ relative to that in diet based on the dual-isotope feeding scheme. The Efflux Rate Index is inversely correlated with the amount of iron transported out of the tissue per unit time. The lower the Efflux Rate Index, the more of the ^{57}Fe tracer taken up by the tissue was released from the tissue after the administration was stopped.

5.3.6 Statistical analysis

Comparisons among the treatments in each group were conducted by performing an independent sample student t-test for equality of means using SPSS version 20 software (SPSS Inc., Chicago, USA). In all tests, a value of $p \leq 0.05$ was considered statistically significant.

5.4 Results

Rats with different levels of dietary iron treatment exhibited no significant differences in body weight among groups at the end of the study ($p > 0.05$). Body weights of the rats in all groups increased moderately from 638 ± 19 g to 729 ± 20 g over the course of the study.

No significant differences were observed between experimental groups and control group in terms of blood haemoglobin (Hb) levels over the course of the study (p>0.05), indicating that dietary iron availability has little impact on blood Hb levels in adult rats. The average Hb concentrations of rats at the beginning and end of the study were 154 ± 9 g Hb/L and 164 ± 14 g Hb/L for the CT group (p=0.20), 158 ± 20 g Hb/L and 167 ± 8 g Hb/L for the LD group (p=0.33) and 151 ± 8 g Hb/L and 158 ± 7 g Hb/L for the HD group (p=0.09), respectively. All the detected blood Hb levels fall within the reported normal range of 130 – 170 g Hb/L for rats (29)

The total amount of consumed feed, water and iron isotopes of each feeding group is summarized in Table 5-2. Water and feed consumption over the feeding period was similar for all three groups of rats. No anomalies in eating habits were observed at any point of the study showing that the rats adapted well to the environment and the different levels of iron in the feed.

Table 5-2 The summary of the total amount of consumed feed, water and iron tracers of the feeding groups

Group	Consumed feed [g]	Consumed water [g]	Consumed natural iron [mmol]*	Consumed Tracer ^{57}Fe [mmol]	Consumed Tracer ^{54}Fe [mmol]	Total consumed iron [mmol]**
LD	2542 ±166	2212 ±469	0.109 ± 0.019	0.089 ±0.018	0.179 ±0.040	0.352 ±0.060
CT	2494 ±166	1980 ±242	8.43 ±0.56	0.079 ±0.010	0.163 ±0.018	8.67 ±0.59
HD	2630 ±86	1997 ±288	87.88 ±2.84	0.80 ±0.12	1.66 ±0.24	90.3 ±2.9

*****The amount of consumed natural iron constitutes both the amount of natural iron in feed and in drinking water.
** The amount of total consumed iron constitutes the amount of consumed tracers and the amount of natural iron in feed and drinking water.

Fig. 5-2 shows that the estimated intestinal iron absorption efficiencies of rats were influenced significantly by dietary iron intake. The intestinal iron absorption efficiency increased 5-fold in rats receiving the iron-deficient diet and decreased 15-fold in rats receiving the iron-loaded diet as compared to the control group (p<0.01). Differences in the estimated amount of absorbed iron were less attenuated. Systemic iron influx was 5-fold lower in the LD group as compared to the CT group (p<0.01). Despite the much higher amount of iron in the feed, the very low intestinal absorption efficiency observed in the HD group (<1% of dietary iron) resulted in a systemic iron influx that was higher than for the LD group (p<0.01) but still lower than that for the CT group.

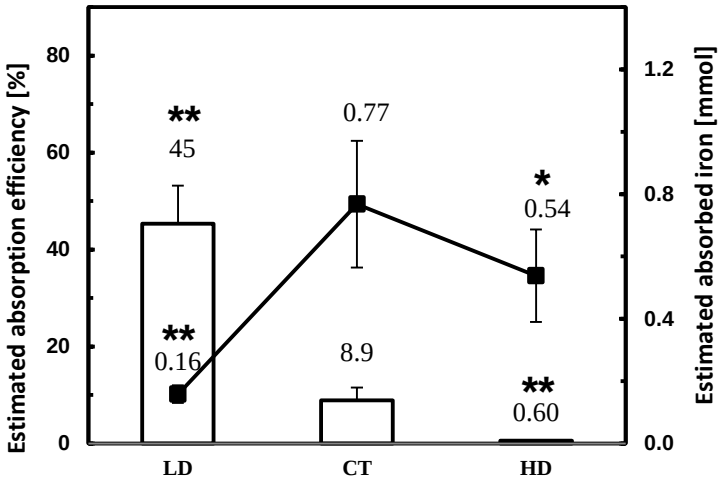

Fig. 5-2 Changes of systemic iron influx in response to different dietary iron levels
The bars represent the estimated iron absorption efficiency at the intestine of three groups (see text). The squares demonstrate the estimated amount of iron absorbed from the diet by the intestine (systemic iron influx). Values are presented as group averages (± SD, n = 7 per group). Statistical differences were identified relative to the CT group [* $p \leq 0.05$; ** $p \leq 0.01$].

Table 5-3 demonstrates systemic changes of tissue/blood iron in response to dietary iron supply with the details of brain shown in Fig. 5-3. Liver, as the

central iron storage organ of the body, showed the highest iron content among all analyzed tissues and exhibited marked differences between groups (p<0.05) whereas no detectable differences were observed in other tissue/blood among groups (p>0.13).

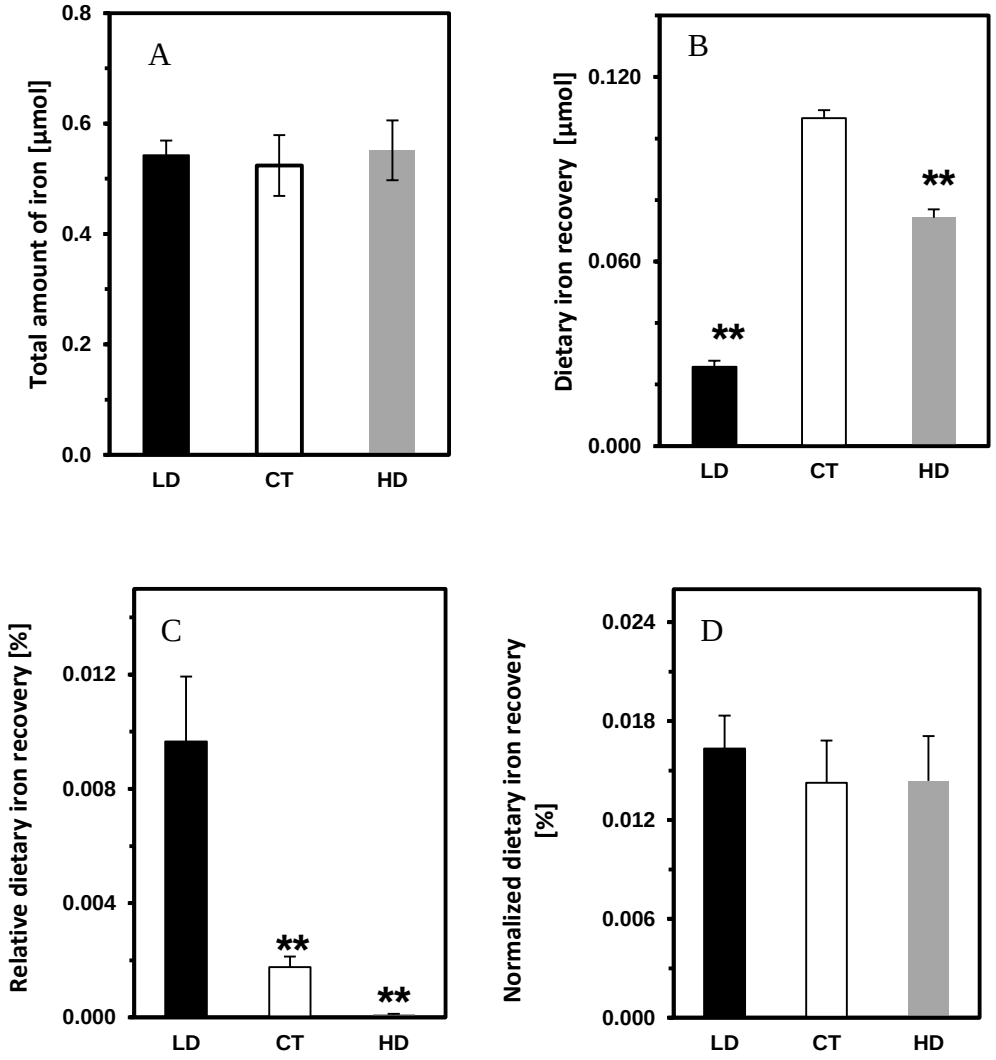

Fig. 5-3 Systemic changes of brain iron in response to dietary iron supply.
Fig.5-3A represents total amount of iron in brain at the end of the study; Fig.5-3B represents the amount of iron recovered from diet in the brain; Fig.5-3C represents the percentage of the amount of iron in the brain recovered from diet relative to that of dietary iron intake; Fig. 5-3D represents the percentage of the amount of iron in the brain recovered from diet relative to that of absorbed dietary iron. Values are presented as group averages (± SD, n = 7 per group). Statistical differences were identified relative to the CT group [* $p \leq 0.05$; ** $p \leq 0.01$]

As shown in Table 5-3, absolute dietary iron recovery was the highest for blood followed by liver as the two main iron compartments in the body. Trends for absolute dietary iron recovery in organs/tissues between groups followed those observed for systemic iron influx. Absolute recovery was lower for all organs in the LD group as compared to the CT group ($p<0.01$) with a less pronounced reduction in the HD group. Only changes in brain and blood reached statistical significance ($p<0.01$) for the HD group with a recovery of dietary iron that was lower compared to the CT group. In contrast, relative dietary iron recovery in tissues/organs followed trends for estimated absorption efficiency. Higher iron absorption efficieny in the intestine resulted in a recovery of dietary iron relative to intake that was higher in all organs in the LD group as compared to the CT group ($p<0.05$). Following this rationale, relative recovery was lower in all organs for the HD group relative to the CT group which is in line with a decrease in iron absorption efficiency for the high iron diet ($p<0.05$). However, when absolute dietary iron recovery by tissues/organs was normalized to systemic iron influx, the amount of absorbed iron available for tissue uptake, differences between LD group and CT goup as well as HD group and CT group became insignificant for all organs/tissues ($p>0.25$). The only exception is liver where normalized dietary iron recovery increased significantly for the HD group ($p<0.01$) and decreased in the LD group ($p<0.05$).

Fig. 5-3A shows that differences in dietary iron intake does not result in a detectable change in total brain iron between all three groups. However, this is

different for the absolute amount of iron transferred from diet to brain which was significantly lower for the LD group ($p<0.01$) as well as for the HD group ($p<0.05$) relative to the CT group, see Fig. 5-3B. Changes in absolute brain iron recovery between groups followed changes in systemic iron influx (Fig. 5-2) remarkably well. Iron recovery from diet in brain relative to dietary iron intake paralelled changes in intestinal iron absorption efficiency (see Fig. 5-3C). However, when being normalized to absorbed iron available for organ uptake (=systemic iron influx), differences became insignificant (see Fig. 5-3D).

Table 5-3 Systemic iron changes in the rat body in response to dietary iron availability

	Tissue/blood	Dietary iron [mmol]	Absorption efficiency [%]	Systemic iron influx [mmol]	Absolute dietary iron recovery [µmol]	Relative dietary iron recovery [%]	Normalized dietary iron recovery [%]	Efflux rate*	Total tissue iron [µmol]
LD	Brain	0.352 ±0.060 (↓↓)**	45.4 ±7.9 (↑↑)	0.158 ±0.028 (↓↓)	0.0258 ±0.0054 (↓↓)	0.0097 ±0.0022 (↑↑)	0.0163 ±0.0020	- (↑↑)	0.542 ±0.027
	Liver				3.5 ±1.3 (↓↓)	1.37 ±0.25 (↑↑)	2.21 ±0.59 (↓)	- (↑↑)	20.2 ±6.4 (↓)
	Kidney				0.77 ±0.54 (↓↓)	0.31 ±0.23 (↑)	0.46 ±0.25	- (↑↑)	5.4 ±2.5
	Heart				0.056 ±0.010 (↓↓)	0.0208 ±0.0033 (↑↑)	0.0355 ±0.0044	- (↑↑)	1.19 ±0.14
	Blood				118 ± 21 (↓↓)	36.3 ±6.3 (↑↑)	-	- (↑↑)	-
CT	Brain	8.67 ±0.59	8.9 ±2.7	0.77 ±0.20	0.107 ±0.019	0.00177 ±0.00037	0.0143 ±0.0026	-	0.524 ±0.055
	Liver				21.3 ±4.0	0.354 ±0.076	2.83 ±0.33	-	33 ±10
	Kidney				2.9 ±1.4	0.047 ±0.019	0.38 ±0.14	-	4.9 ±1.8
	Heart				0.253 ±0.048	0.00418 ±0.00084	0.0344 ±0.0099	-	1.255 ±0.080
	Blood				376 ±97	6.2 ±1.9	-	-	-
HD	Brain	90.3 ±2.9 (↑↑)	0.60 ±0.16 (↓↓)	0.54 ±0.15 (↓)	0.0743 ±0.0074 (↓↓)	0.000114 ±0.000010 (↓↓)	0.0144 ±0.0027	-	0.552 ±0.054
	Liver				24.6 ±2.6	0.0379±0.0045 (↓↓)	4.8 ±1.2 (↑↑)	- (↓)	67 ±15 (↑↑)
	Kidney				2.8 ±1.5	0.0042 ±0.0022 (↓↓)	0.56 ±0.43	-	7.1 ±3.1
	Heart				0.210 ±0.049	0.000323 ±0.000069 (↓↓)	0.0396 ±0.0055	- (↑↑)	1.38 ±0.12
	Blood				232 ±66 (↓↓)	0.36 ±0.10 (↓↓)	-	-	-

*Efflux rates were derived from Efflux Rate Indices.

** Statistical differences were identified relative to the CT group [↓ or ↑ $p \leq 0.05$; ↓↓ or ↑↑ $p \leq 0.01$]

Lowering dietary intake decreased systematically efflux rates ($p<0.01$, see Fig. 5-4) and, thus, led to an increased iron efflux (see Table 5-3) from all organs/tissues in the LD group over time. Observations were less consistent for the HD group. Here, an increased dietary intake decreased systemic iron influx as for the LD group (see Fig. 5-2) which supposedly gave rise to an increased iron efflux from the heart ($p<0.01$) and decreased iron efflux from the liver ($p<0.05$).

Findings for brain show clearly that lowering dietary iron intake over the long-term results in a lower uptake of dietary iron (lower absolute dietary iron recovery) and a lower retention of iron taken up by the brain (higher efflux rate) during adulthood. Both should lower accumulation of iron originating from diet when the rat is ageing. Similar conclusions can be drawn for the HD group in which iron intake was higher but systemic iron influx lower as compared to the CT group. Because absolute uptake of dietary iron by the brain could be lowered without a detectable effect on iron efflux from brain (see Fig. 5-4), we can conclude that brain iron accumulation over time could also be slowed down in the HD group although probably less effectively than in the LD group.

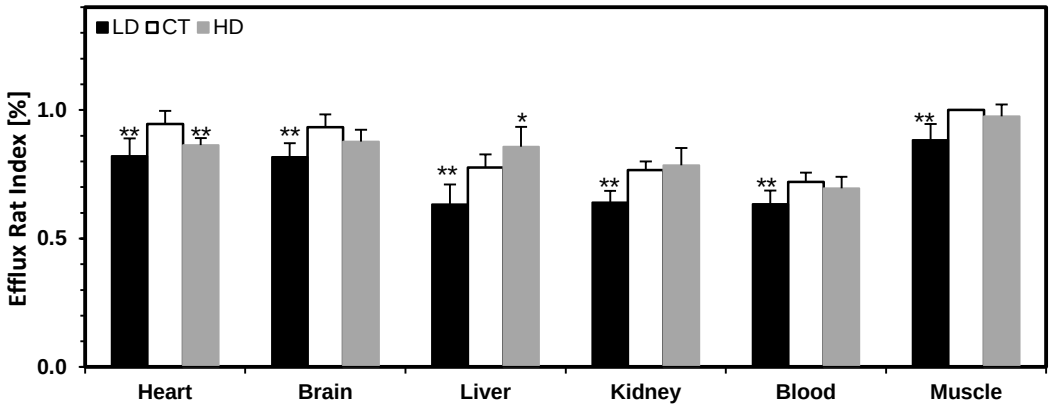

Fig. 5-4 Efflux rate indices of different tissues of the three feeding groups
The lower the index, the higher the iron efflux rate (see text). Values are presented as group averages (± SD, $n = 7$ per group). Statistical differences were identified relative to the CT group [* $p \leq 0.05$; ** $p \leq 0.01$]

5.5 Discussion

Iron homeostasis at the systemic, organ and cellular level involves a machinery of genes for iron transport, storage, export and regulation, each of which presents a possible avenue for systemic malfunction (30). Dietary iron manipulation perturbs iron regulatory systems in the body and may change iron balance if over- or under-corrected. Several epidemiological studies revealed links between dietary iron intake and the risks of developing AD/PD but it is unclear whether association are positive (19, 20) or negative (13-17). The present study demonstrated, for the first time ever, that both low and high dietary iron intake can potentially lower iron transfer from diet to the adult rodent brain.

Methodological concepts we have used in the present study are in many ways unique. Previous rat studies on the effect of dietary iron on brain iron centered mainly on the developmental stage with a research focus on the molecular level, i.e. changes in the expression of iron uptake/export/storage related proteins in

response to change of dietary iron supply in young rats (31, 32). Brain iron homeostasis, however, differs between adult and young rats (33). Rate of brain iron uptake is age-dependent (33). Most brain iron is acquired during the first years of life and slows down until early adulthood on from which brain iron content raises slowly but steadily and possibly reaches a plateau late in life (34). Findings in young animals therefore cannot be extrapolated to adult or old rats. We have therefore decided to do our experiments on fully adult rats at an age of 6-8 month, which correspond to age of 20-30 years in humans (35). Furthermore, we tried to assess brain iron homeostasis at the systemic level, firstly, by feeding and not injecting tracer iron as in earlier experiments and, secondly, by administering isotopes not as a bolus but continuously with the feed. Long-term feeding of tracer iron considers a possible homeostatic response of the organism to changes in dietary iron intake and permits to study both import and export of tracer iron from brain.

Rats in the LD and HD group were given either about ten times less or ten times more iron through diet as compared to the CT group. While still extreme in range as compared to human dietary iron intake, dietary iron levels in our HD group were still much lower than those in some earlier studies where iron intake was increased 100 times or more to toxic levels (36-38) which may result in pathological changes. By feeding different iron levels, we triggered a normal homeostatic response in the rats as intended and expected. In none of the groups we have observed a detectable change in blood hemoglobin concentration over

the four months of the study. This indicates that functional levels of body iron could be maintained in all three groups within statistical limits despite marked differences in dietary iron supply. Instead, liver iron stores were either emptied to provide sufficient iron for erythropoiesis or filled up to store excessively absorbed iron (see Table 5-3). In line with our finding, previous studies demonstrated that adult rats did not develop anemia when provided with 50 times less iron than controls for 2 months (39). In humans, less than 0.03% of body iron is lost and need to be replaced per day (40). With liver iron serving as a buffer, it can take years until changes in functional iron become significant, even for extreme changes in iron influx, similar to the rats in our study.

For most organisms, including rats, iron has been a limiting nutrient over evolutionary time spans. This has made the development of excretionary pathways for iron redundant. Body iron homeostasis in mammals is solely regulated instead by controlling iron absorption in the intestine (41). In the LD group, iron absorption efficiency in the intestine was up-regulated from 9% to 45% while it was down-regulated to less than 1% in the HD group from 9% in the CT group. However, the drop in iron supply exceeded apparently regulatory capacities in the intestine in the LD group. Systemic iron influx into the rat's body dropped (see Fig. 5-2) and liver iron stores had to be emptied for maintaining erythropoiesis (see Table 5-3). Remarkably, changes in iron influx were over-compensated in the HD group. Despite a much higher iron supply through diet, lowering of intestinal iron absorption efficiency in the HD group also lowered

levels of systemic iron influx relative to the CT group. Absorbed iron in the HD group was used primarily for erythropoiesis as recovery of dietary iron in liver was much lower than the change in total liver iron. Liver iron stores were therefore built up mainly from iron released from phagocytosis of senescent red blood cells and not from freshly absorbed iron (42).

Surprisingly, changes in systemic iron influx were paralleled in our study with absolute dietary iron recovery in brain. The lowest recovery of dietary iron in brain was observed for the LD group but the highest recovery was not found in the HD group but the CT group. At the same time total brain iron content did not differ between groups (see Table 5-3). But this observation must be interpreted with care. Changes in brain iron balance over 4 months, which is still short as compared to the 24-36 life span of a rat, are relatively small and to detect them unambiguously would have required much larger sample sizes. This illustrates that measuring incremental changes in iron content of brain as the outcome variable in animal studies inferior to tracer experiments, in particular in studies involving adult rats where changes in brain iron content are much smaller than early in life. Even for small incremental changes in total brain iron, induced relative changes are much larger in tracer studies as test animals are commonly tracer free at study onset.

The observation that recovery of dietary iron in brain parallels systemic iron influx (Fig. 5-3D) was surprising and challenges the common assumption that

brain iron balance is subject to tight homeostatic control in the adult brain. When systemic iron influx is lowered and brain is not a closed system, i.e. brain iron is constantly lost and replaced, brain iron balance can only be maintained by up-regulating brain iron import and/or down-regulating brain iron export to counteract systemic iron depletion. The contrary has been observed in the LD group. Absolute dietary iron recovery in brain dropped (see Fig. 5-3B) and iron efflux increased (see Fig. 5-4) instead when dietary iron and systemic iron influx was restricted. For high iron intake, iron efflux from brain was not measurably affected but absolute dietary iron recovery dropped. This result does not violate the assumption that brain iron homeostasis is controlled, in principle, by body iron status but raises questions about the efficiency by which brain iron balance is maintained by regulation of brain iron import and export.

Our current understanding of brain iron homeostasis as well as its change in response to dietary iron levels is almost entirely based on studies in young rats or mice (31, 32, 36-38, 43-50). These studies investigated rats/mice ranged from ages of 7 days to 90 days with an observational period up to 84 days. In these studies, rats/mice ranging from 7 days to 90 days of age at the beginning were given either an iron-depleted diet or an iron-loaded diet or both for up to 90 days. Iron restriction conclusively lowered total brain iron content in growing animals (<3 months) as compared to controls (36, 47, 48, 50). However, the drop in brain iron content in response to iron-depleted diet was found undetectable when the rats/mice grew older (~6 month) (39). When treated with high level of dietary

iron, brain iron content in young rats/mice increased only when dietary iron reached toxic level (>10,000 ppm in the feed) (36, 46). No such information is available for adult rats and findings in young rodents in earlier studies can hardly be extrapolated and compared to older rats as in our study. In the study conducted by Holmes-Hampton et al. (2012), mice were given ^{57}Fe tracer together with feed of normal iron content from weaning for 58 weeks (33). Their result suggested that brain iron uptake is biphasic, with a higher rate of brain iron uptake/turnover at young age than at old age where iron import seems to be favoured over iron export.

Our present study indicates that brain iron balance is less well regulated in adulthood as compared to infancy and childhood which appears to be a reasonable working hypothesis from a developmental as well as evolutionary perspective. Due to its functional role in brain, brain iron content must parallel brain growth during the first years of life. It is well established that an insufficient dietary iron supply during childhood results in a retarded psychomotoric and intellectual development of the child that can hardly be corrected by providing sufficient iron later in life (51). Because iron has been a limiting nutrient in the evolution of all forms of life, including humans, mechanisms were needed to ensure that sufficient iron is taken up by the brain during growth even in times when dietary iron supply is limited. It has been well established that iron is taken up by the young rodent brain through transferrin receptor (TfR) mediated endocytosis across the blood brain barrier (11, 38), although a few other pathways were also

proposed, e.g. via divalent metal transporter 1 (DMT1) (52). Results obtained from these studies demonstrated that the expression of TfR in the brain was dose-dependent: expression was found to be upregulated in response to low dietary iron to increase brain iron uptake and vice versa (31, 38, 53). This pathway permits not only brain but also other tissues and organs to acquire iron from circulation even if systemic iron supply is low (54). Increase of soluble transferrin receptor concentration in serum is a common observation in iron deprived organisms when liver iron stores are emptied and iron deficiency develops (55, 56). Iron export mechanisms from brain are less well studied but are apparently through turnover of cerebrospinal fluid rather than regulated iron export mechanisms, at least in the growing brain (57). To the best of our knowledge, no studies have been conducted so far to look at the effect of dietary iron deprivation on TfR levels in the brain at different age. Correlations between brain iron uptake and systemic iron influx in older rats, as observed in our study, would point to a limited relevance of actively regulated pathways controlled by iron status making the brain susceptible to diet induced changes in iron balance.

5.6 Conclusion

Our observation that recovery of dietary iron in brain could be lowered both by increasing and decreasing dietary iron intake would be in good agreement with contradictory findings in epidemiological trials which indicated that both low and high dietary intake could lower risks for contracting AD and PD. Our study showed that systemic iron influx rather than iron intake or body iron status alone decides about the rate of iron accumulation in the adult rat brain. Impairments in

body iron homeostasis that fail to maintain systemic iron content over life-time, either by over-compensation or under-compensation of habitual iron losses, may determine brain iron balance and brain damage through iron mediated oxidative stress in the long-run.

5.7 Bibliography

1. Prince M, Prina M, & Guerchet M (2013) World Alzheimer report: Journey of caring-an analysis of long-term care for dementia (Alzheimer's Disease International, London).
2. Bush AI (2013) The metal theory of Alzheimer's disease. *J Alzheimers Dis* 33:S277-S281.
3. Altamura S & Muckenthaler MU (2009) Iron toxicity in diseases of aging: Alzheimer's disease, Parkinson's disease and atherosclerosis. *J Alzheimers Dis* 16(4):879-895.
4. Hare D, Austin C, & Doble P (2012) Quantification strategies for elemental imaging of biological samples using laser ablation-inductively coupled plasma-mass spectrometry. *Analyst* 137(7):1527-1537.
5. Schipper HM (2012) Neurodegeneration with brain iron accumulation - clinical syndromes and neuroimaging. *Biochim Biophys Acta* 1822(3):350-360.
6. Sian-Hulsmann J, Mandel S, Youdim MBH, & Riederer P (2011) The relevance of iron in the pathogenesis of Parkinson's disease. *J Neurochem* 118(6):939-957.
7. Gillette-Guyonnet S, Secher M, & Vellas B (2013) Nutrition and neurodegeneration: epidemiological evidence and challenges for future research. *Brit J Clin Pharmaco* 75(3):738-755.
8. Kokmen E, Beard CM, OBrien PC, & Kurland LT (1996) Epidemiology of dementia in Rochester, Minnesota. *Mayo Clin Proc* 71(3):275-282.
9. Sekita A, *et al.* (2010) Trends in prevalence of Alzheimer's disease and vascular dementia in a Japanese community: the Hisayama Study. *Acta Psychiat Scand* 122(4):319-325.
10. FAO (2010) *The state of food and agriculture 2009: live stock in the balance* (Bernan Assoc).
11. Crichton RR (2009) Brain iron homeostasis and its perturbation in various neurodegenerative diseases. *Iron metabolism: from molecular mechanisms to clinical consequences*, ed Crichton RR (John Wiley & Sons), 3rd Ed, pp 371-372.
12. Hunt JR, Zito CA, & Johnson LK (2009) Body iron excretion by healthy men and women. *Am J Clin Nutr* 89(6):1792-1798.
13. Powers KM, *et al.* (2003) Parkinson's disease risks associated with dietary iron, manganese, and other nutrient intakes. *Neurology* 60(11):1761-1766.
14. Powers KM, *et al.* (2009) Dietary fats, cholesterol and iron as risk factors for Parkinson's disease. *Parkinsonism Relat D* 15(1):47-52.
15. Johnson CC, Gorell JM, Rybicki BA, Sanders K, & Peterson EL (1999) Adult nutrient intake as a risk factor for Parkinson's disease. *Int J Epidemiol* 28(6):1102-1109.
16. Grant WB (1997) Dietary links to Alzheimer's disease. *Alz Dis Rev* 2:42-55.
17. Loef M & Walach H (2012) Copper and iron in Alzheimer's disease: a systematic review and its dietary implications. *Brit J Nutr* 107(1):7-19.

18. Logroscino G, Gao X, Chen HL, Wing A, & Ascherio A (2008) Dietary iron intake and risk of Parkinson's disease. *Am J Epidemiol* 168(12):1381-1388.
19. Miyake Y, *et al.* (2011) Dietary intake of metals and risk of Parkinson's disease: A case-control study in Japan. *J Neurol Sci* 306(1-2):98-102.
20. Ortega RM, *et al.* (1997) Dietary intake and cognitive function in a group of elderly people. *Am J Clin Nutr* 66(4):803-809.
21. Arruda LF, Arruda SF, Campos NA, de Valencia FF, & Siqueira EMD (2013) Dietary iron concentration may influence aging process by altering oxidative stress in tissues of adult rats. *Plos One* 8(4).
22. Shoham S & Youdim MBH (2004) Nutritional iron deprivation attenuates kainate-induced neurotoxicity in rats: Implications for involvement of iron in neurodegeneration. *Ann Ny Acad Sci* 1012:94-114.
23. Walczyk T (2012) The Use of Stable Isotope Techniques for Studying Mineral and Trace Element Metabolism in Humans. *Isotopic Analysis: Fundamentals and Applications Using ICP-MS*, (Wiley-VCH Verlag GmbH & Co. KGaA, Weinheim, Germany.), pp 435-494.
24. Walczyk T, Davidsson L, Zavaleta N, & Hurrell RF (1997) Stable isotope labels as a tool to determine the iron absorption by Peruvian school children from a breakfast meal. *Fresen J Anal Chem* 359(4-5):445-449.
25. Chen J-H, Shahnavas S, Singh N, Ong W-Y, & Walczyk T (2013) Stable iron isotope tracing reveals significant brain iron uptake in adult rats. *Metallomics* 5(2):167-173.
26. Walczyk T (1997) Iron isotope ratio measurements by negative thermal ionisation mass spectrometry using FeF4- molecular ions. *Int J Mass Spectrom Ion Process* 161(1-3):217-227.
27. Vácha J, Znojil V, Holá J, & Dungel J (1982) The internal iron kinetics in mice. *Acta Veterinaria Brno* 51(1):3-22.
28. Lee HB & Blaufox MD (1985) Blood volume in the rat. *J Nucl Med* 26(1):72-76.
29. Underwood EJ (1977) Iron. *Trace elements in human and animal nutrition*, ed Underwood EJ (Academic Press), 4th Ed, pp 14-15.
30. Jellen LC, Beard JL, & Jones BC (2009) Systems genetics analysis of iron regulation in the brain. *Biochimie* 91(10):1255-1259.
31. Moos T (2002) Brain iron homeostasis. *Dan Med Bull* 49(4):279-301.
32. Chen Q, Connor JR, & Beard JL (1995) Brain Iron, transferrin and ferritin concentrations are altered in developing iron-deficient rats. *J Nutr* 125(6):1529-1535.
33. Holmes-Hampton GP, *et al.* (2012) Changing iron content of the mouse brain during development. *Metallomics* 4(8):761-770.
34. Hallgren B & Sourander P (1958) The effect of age on the non-haemin iron in the human brain. *J Neurochem* 3(1):41-51.
35. Quinn R (2005) Comparing rat's to human's age: How old is my rat in people years? *Nutrition* 21(6):775-777.
36. Sobotka TJ, *et al.* (1996) Neurobehavioral dysfunctions associated with dietary iron overload. *Physiol Behav* 59(2):213-219.

37. Qian ZM, *et al.* (2007) Development and iron-dependent expression of hephaestin in different brain regions of rats. *J Cell Biochem* 102(5):1225-1233.
38. Taylor EM, Crowe A, & Morgan EH (1991) Transferrin and iron uptake by the brain: effects of altered iron status. *J Neurochem* 57(5):1584-1592.
39. Williamson AM & Ng KT (1980) Behavioral effects of iron deficiency in the adult rat. *Physiol Behav* 24(3):561-567.
40. Beard JL, Dawson H, & Pinero DJ (1996) Iron metabolism: a comprehensive review. *Nutr Rev* 54(10):295-317.
41. Bothwell TH (1979) *Iron metabolism in man* (Blackwell Scientific Publications ; St. Louis : Distributors USA, Blackwell Mosby Book Distributors).
42. Finch CA, *et al.* (1970) Ferrokinetics in man. *Medicine* 49(1):17-&.
43. Dallman PR & Spirito RA (1977) Brain iron in rat: extremely slow turnover in normal rats may explain long-lasting effects of early iron deficiency. *J Nutr* 107(6):1075-1081.
44. Taylor EM & Morgan EH (1990) Developmental changes in transferrin and iron uptake by the brain in the rat. *Dev Brain Res* 55(1):35-42.
45. Moos T & Morgan EH (1998) Evidence for low molecular weight, non-transferrin-bound iron in rat brain and cerebrospinal fluid. *J Neurosci Res* 54(4):486-494.
46. Ke Y, *et al.* (2005) Age-dependent and iron-independent expression of two mRNA isoforms of divalent metal transporter 1 in rat brain. *Neurobiol Aging* 26(5):739-748.
47. Erikson KM, Pinero DJ, Connor JR, & Beard JL (1997) Regional brain iron, ferritin and transferrin concentrations during iron deficiency and iron repletion in developing rats. *J Nutr* 127(10):2030-2038.
48. Pinero DJ, Li NQ, Connor JR, & Beard JL (2000) Variations in dietary iron alter brain iron metabolism in developing rats. *J Nutr* 130(2):254-263.
49. Monnot AD, Behl M, Ho SN, & Zheng W (2011) Regulation of brain copper homeostasis by the brain barrier systems: Effects of Fe-overload and Fe-deficiency. *Toxicol Appl Pharm* 256(3):249-257.
50. Dallman PR, Siimes MA, & Manies EC (1975) Brain iron: persistent deficiency following short-term iron deprivation in young rat. *Brit J Haematol* 31(2):209-215.
51. Beard J (2003) Iron deficiency alters brain development and functioning. *J Nutr* 133(5):1468s-1472s.
52. Ke Y & Qian ZM (2007) Brain iron metabolism: Neurobiology and neurochemistry. *Prog Neurobiol* 83(3):149-173.
53. Rouault TA & Cooperman S (2006) Brain iron metabolism. *Semin Pediatr Neurol* 13(3):142-148.
54. Cheng Y, Zak O, Alsen P, Harrison SC, & Walz T (2004) Structure of the human transferrin receptor-transferrin complex. *Cell* 116(4):565-576.
55. Punnonen K, Irjala K, & Rajamäki A (1997) Serum transferrin receptor and its ratio to serum ferritin in the diagnosis of iron deficiency. *Blood* 89(3):1052-1057.

56. Mast AE, Blinder MA, Gronowski AM, Chumley C, & Scott MG (1998) Clinical utility of the soluble transferrin receptor and comparison with serum ferritin in several populations. *Clin Chem* 44(1):45-51.
57. Bradbury MWB (1997) Transport of iron in the blood-brain-cerebrospinal fluid system. *J Neurochem* 69(2):443-454.